

RICE UNIVERSITY

**The Effects of Land Use and Human Activities on Carbon Cycling
in Texas Rivers**

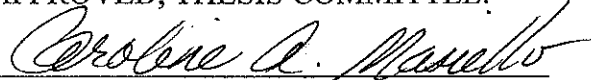
By

Fan-Wei Zeng

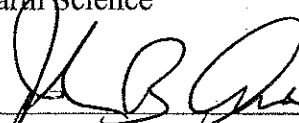
A THESIS SUBMITTED
IN PARTIAL FULFILLMENT OF THE
REQUIREMENTS FOR THE DEGREE

Doctor of Philosophy

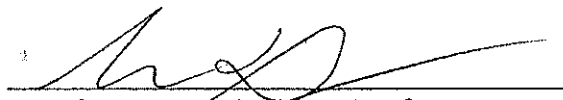
APPROVED, THESIS COMMITTEE:



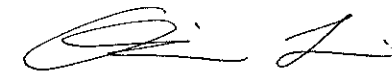
Caroline A. Masiello, Assistant Professor
Earth Science



John B. Anderson, Professor, W. Maurice
Ewing Professorship in Oceanography
Earth Science



Brandon Dugan, Assistant Professor
Earth Science



Qilin Li, Assistant Professor
Civil and Environmental Engineering

HOUSTON, TEXAS
DECEMBER 2010

ABSTRACT

The Effects of Land Use and Human Activities on Carbon Cycling in Texas Rivers

By

Fan-Wei Zeng

I investigated how land use and human activities affect the sources and cycling of carbon (C) in subtropical rivers. Annually rivers receive a large amount of terrestrial C, process a portion of this C and return it to the atmosphere as CO₂. The rest is transported to the ocean. Land use and human activities can affect the sources and fate of terrestrial C in rivers. However, studies on these effects are limited, especially in the humid subtropics.

I combined measurements of the partial pressure of dissolved CO₂ (pCO₂), C isotopes (¹³C and ¹⁴C) and solid-state ¹³C nuclear magnetic resonance (NMR) to study C cycling in three subtropical rivers in Texas, two small rivers (Buffalo Bayou and Spring Creek) and a midsize river (the Brazos).

My pCO₂ data show that small humid subtropical rivers are likely a large source of atmospheric CO₂ in the global C cycle. My measurements on pCO₂, C isotopic and chemical composition of dissolved inorganic C (DIC) and particulate organic C (POC) revealed four types of effects of land use and human activities on river C cycling. First, oyster shells and crushed carbonate minerals used in road construction are being dissolved and slowly drained into Buffalo Bayou and the lower Brazos and may be a source of river CO₂ released to the atmosphere. Second, river damming and nutrient input from urban treated wastewater stimulate algal growth and reduce CO₂ evasion of the

middle Brazos. Third, urban treated wastewater discharge is adding old POC to the middle Brazos and decomposition of the old POC adds to the old riverine DIC pool. Fourth, agricultural activities coupled with high precipitation enhance loss of old organic C (OC) from deep soils to the lower Brazos, and decomposition of the old soil OC contributes to the old CO₂ evaded.

I document for the first time the river C cycling effects of the use of carbonate minerals in construction and the riverine discharge of urban wastewater. Results presented here indicate the need to study disturbed river systems to better constrain the global C budget.

ACKNOWLEDGEMENTS

The work presented in this thesis can not be fulfilled without the efforts of many people along the way. For this, I would like to give warm thanks to all these people for their help over the last five years.

I would like to thank my thesis advisor Dr. Carrie Masiello. Her insight and enthusiasm in research has been inspiring me. Her open-door policy has been providing me with timely help. I sincerely appreciate her guidance, advice, support, and encouragement. I am grateful to our post-doc, now a faculty at Baylor University in Texas, Dr. William Hockaday for training me in many lab techniques and for always being willing to help. I would like to extend a warm thank you to my thesis committee, Dr. John Anderson, Dr. Brandon Dugan, and Dr. Qilin Li, for their suggestions on improving my work. I thank my officemate Morgan Gallagher for her advice, encouragement and helpful comments on my manuscripts. I appreciate Dr. Jeff Baldock's help with my questions about the molecular mixing models. I also want to thank Dr. Emilio Mayorga, Dr. Becca Barnes, Dr. Everett Salas and all the members in our group for their efforts in improving my manuscripts and talks.

Field work is an important part of my research. For this I would like to thank all these people for their help with sample collection: Dr. John Anderson, Dr. Fred Weaver, Dr. Xinfeng Shi, Dr. Yanlu Ma, Dr. William Hockaday, LaQuanti Calligan, Shuaiping Ge, Xuan Guo, Kaijian Liu, Krystle Hodge, Yongbo Zhai, Morgan Gallagher, Li Zhang, Jianping Chen, Yan Chen, Jianping Huang, Yan Zhou, Qinglian Chen, Baoshan Wang, Xinling Wang, Wei Chen, Yuan Li, Yinbin Ma, and Lacey Pyle. Without them, this thesis would never have been possible.

Many thanks to Dr. Tibusay J. Perez, Dr. Simone R. Alin, and Dr. Deirdre Lockwood for their assistance with instrument setup. I would like to also thank Dr. John Southon, Dr. Guaciara dos Santos Winston, Dr. Xiaomei Xu, Will Beaumont, Dr. Ellen R.M. Druffel, Sheila Griffin, Robert Beverly, and Dr. Claudia Czimczik at the W.M. Keck Carbon Cycle Accelerator Mass Spectrometry Laboratory (KCCAMS) at the University of California, Irvine (UCI), and people at the National Ocean Science Accelerator Mass Spectrometry Facility (NOSAMS) at Woods Hole Oceanographic Institution (WHOI), for their assistance with carbon isotope analyses. I also thank the members of Rice University's GIS center, German Diaz, Eva Garza, Jean Niswonger and Kim M. Ricker for their help over the years.

This work was funded by the Texas Water Resources Institute, the U.S. Geological Survey, and the National Institutes for Water Research. It is also aided by the financial support from Hans O. and Suse Jahns, Rice University Mills Bennett Fellowship, a Chevron Fellowship, and BP.

I would particularly like to thank my parents Chunlin Zeng and Jianling Luo for their inspiration and continued support and encouragement. I thank my sister Fanfei Zeng and brothers Fanxin Zeng, Fancong Zeng, Fanshi Zeng and Fanhuan Zeng for always being there. I also thank my boyfriend Yingcheng Liao for his support and encouragement.

This work is dedicated to my grandmother, Yuqiao Chen. Her loving heart will always be close to mine. May she rest in peace.

TABLE OF CONTENTS

ABSTRACT.....	ii
ACKNOWLEDGEMENTS.....	iv
TABLE OF CONTENTS.....	vi
LIST OF TABLES.....	ix
LIST OF FIGURES.....	x
CHAPTER 1: Introduction.....	1
CHAPTER 2: Sources of CO ₂ evasion from two subtropical rivers in North America....	4
Abstract.....	4
2.1 Introduction.....	5
2.2 Study area and methods.....	7
2.2.1 Study area.....	7
2.2.2 Sample collection and analysis.....	11
2.3 Results and discussion.....	12
2.3.1 Daytime riverine pCO ₂ variation.....	12
2.3.2 Effect of rainfall events on riverine pCO ₂	13
2.3.3 Seasonal variation in riverine pCO ₂	18
2.3.4 CO ₂ emission rates of Buffalo Bayou and Spring Creek.....	21
2.3.5 Potential sources of riverine CO ₂ and their carbon isotopic signatures.....	24
2.3.6 Temporal and spatial variation in sources of riverine CO ₂	28
2.3.7 Potential role of anthropogenic carbonate as a source of atmospheric CO ₂	33
2.4 Conclusions.....	34
2.5 Acknowledgements.....	35
CHAPTER 3: Controls on the origin and cycling of riverine dissolved inorganic carbon in the Brazos River, Texas.....	37
Abstract.....	37
3.1 Introduction.....	38
3.2 Study area and methods.....	41
3.2.1 Study area.....	41
3.2.2 Methods.....	44
3.3 Results.....	47
3.3.1 Longitudinal variation in pCO ₂ , concentration and isotope values of DIC.....	47
3.3.2 Black carbon content of riverine POM at site 3 in the lower Brazos..	48
3.4 Discussion.....	52
3.4.1 Isotope values of potential DIC sources in the Brazos River basin....	52

3.4.2 Major controls on riverine DIC in the middle Brazos: damming and urbanization.....	56
3.4.2.1 Enhanced air-water CO ₂ exchange.....	57
3.4.2.2 Respiration of young OM.....	58
3.4.2.3 Algal growth.....	59
3.4.3 Natural and anthropogenic carbonate input to the lower Brazos.....	61
3.4.4 Comparison of Brazos pCO ₂ and DIC with other rivers.....	62
3.4.4.1 Riverine pCO ₂	62
3.4.4.2 Riverine DIC concentration.....	63
3.4.4.3 CO ₂ outgassing and DIC export from the Brazos.....	64
3.5 Conclusions.....	66
3.6 Acknowledgements.....	67

CHAPTER 4: Land use effects on the isotopic and chemical composition of particulate organic carbon in the Brazos River, Texas revealed by carbon isotope and NMR measurements.....	
Abstract.....	68
4.1 Introduction.....	69
4.2 Study area.....	73
4.3 Methods.....	75
4.3.1 Sample collection.....	75
4.3.2 Sample pre-treatment.....	76
4.3.2.1 For C isotope analysis.....	76
4.3.2.2 For NMR analysis.....	77
4.3.3 Sample measurements.....	78
4.3.3.1 C isotope analysis.....	78
4.3.3.2 ¹³ C CP-MAS NMR analysis.....	79
4.3.3.3 Molecular mixing models.....	80
4.3.3.4 Chemical composition of sinking POC.....	81
4.3.3.5 Fraction of sinking POC in total POC.....	81
4.3.3.6 OC recovery of demineralization.....	82
4.3.3.7 Statistic analysis.....	82
4.4 Results.....	82
4.4.1 Concentration and isotopic composition of total and sinking POC... ..	82
4.4.2 C and N concentration of sinking POM.....	87
4.4.3 Selection of the MMMs for sinking POC samples.....	91
4.4.4 Chemical composition of sinking POC.....	95
4.5 Discussion.....	99
4.5.1 Sources and chemical composition of total and sinking POC.....	99
4.5.1.1 Site 1 in the middle Brazos: urban wastewater input and river damming.....	99
4.5.1.2 Site 2 in the middle Brazos: shallow soil input.....	102
4.5.1.3 Sites 3-6 in the lower Brazos: deep erosion of old soil	103
4.5.1.4 Linking total POC data in this study to published DIC data for the Brazos River.....	104
4.5.2 Implications for the marine C cycle.....	105

4.5.2.1 The Brazos River POC export.....	105
4.5.2.2 The Brazos River charcoal export.....	107
4.5.2.3 The Brazos River lignin export.....	109
4.5.2.4 Linking river POC, charcoal and lignin fluxes to water and sediment discharge.....	110
4.6 Conclusions.....	112
4.7 Acknowledgements.....	113
CHAPTER 5: Conclusions.....	114
REFERENCES.....	117

LIST OF TABLES

CHAPTER 2

Table 2-1. Hydrological and lithologic characteristics of Buffalo Bayou and Spring Creek watersheds.....	10
Table 2-2. Measured mean pCO ₂ and calculated mean CO ₂ emission flux.....	15
Table 2-3. Precipitation data for the study period.....	20
Table 2-4. Riverine pCO ₂ values and CO ₂ emission fluxes for world rivers.....	25

CHAPTER 3

Table 3-1. Basin and hydrology information for the Brazos River basin.....	45
Table 3-2. Measured parameters for all sampling sites in the Brazos River.....	49

CHAPTER 4

Table 4-1. Concentration and isotopic signatures of POC and DIC.....	83
Table 4-2. Percentage of sinking POC in total POC.....	88
Table 4-3. %OC, %N, C/N, %Cobs and alkyl/O-alkyl of sinking POM.....	89
Table 4-4. Measured and predicted NMR spectral distributions.....	92
Table 4-5. Percentage of six chemical components in sinking POM.....	93
Table 4-6. Effect of demineralization.....	97
Table 4-7. River POC, charcoal and lignin export.....	111

LIST OF FIGURES

CHAPTER 2

Figure 2-1. Buffalo Bayou watershed and Spring Creek watershed.....	8
Figure 2-2. Daytime variation in riverine pCO ₂	14
Figure 2-3. Effect of rainfall events on riverine pCO ₂	16
Figure 2-4. Seasonal variation in riverine pCO ₂	19
Figure 2-5. $\delta^{13}\text{C}$ versus $\Delta^{14}\text{C}$ of riverine DIC.....	26
Figure 2-6. Seasonal variation in river discharge, concentration of DIC, and $\Delta^{14}\text{C}$ and $\delta^{13}\text{C}$ of DIC.....	29
Figure 2-7. Relationship between DIC concentration and discharge, and DIC mass flow rate and discharge.....	31

CHAPTER 3

Figure 3-1. Surface geologic and land cover maps of the Brazos drainage basin.....	42
Figure 3-2. Longitudinal variations in river water pCO ₂ , DIC concentration, and $\Delta^{14}\text{C}$ and $\delta^{13}\text{C}$ of DIC.....	50
Figure 3-3. CP/MAS ¹³ C NMR spectrum of riverine POM at site 3 in the lower Brazos.....	51
Figure 3-4. $\delta^{13}\text{C}$ versus $\Delta^{14}\text{C}$ of riverine DIC in the Brazos River.....	53

CHAPTER 4

Figure 4-1. Land use and surface geologic map of the Brazos River watershed.....	74
Figure 4-2. Longitudinal variations in the concentration of total POC.....	84
Figure 4-3. Longitudinal variations in $\Delta^{14}\text{C}$ of total and sinking POC.....	86
Figure 4-4. Longitudinal variations in %OC, %N and C/N.....	90
Figure 4-5. CP/MAS ¹³ C NMR spectra of sinking POM.....	94
Figure 4-6. Chemical composition of sinking POC.....	98
Figure 4-7. Correlation between $\Delta^{14}\text{C}$ -DIC and $\Delta^{14}\text{C}$ -POC _{TOT}	106

CHAPTER 1

Introduction

The flux of carbon (C) from land to rivers is estimated to be more than 0.9 Gt yr^{-1} (Cole et al. 2007), comparable to terrestrial net ecosystem productivity ($\pm 2.0 \text{ Gt C yr}^{-1}$, Randerson et al. 2002). This C flux needs to be accounted for in regional and global C budgets to avoid overestimating net land C uptake (Grace and Malhi 2002). Of the terrestrial C delivered to rivers, a fraction is processed and returned to the atmosphere as CO_2 , and the rest is transported to the ocean. Therefore, measurements of river CO_2 evasion and river C export to the ocean are a practical way to calculate the amount of terrestrial C lost to rivers (Cole et al. 2007).

Of the terrestrial organic carbon (OC) that rivers export to the ocean, more than half is completely decomposed in the marine environment, even though it resisted decomposition in the terrestrial environment (Berner 1989; Beusen et al. 2005; Burns et al. 2008; Hedges and Keil 1995; Hedges et al. 1997). The nature of OC is one of the most important controls on the sedimentary fate of organic matter. As such, the nature of riverine OC requires more study to understand the rapid destruction of terrestrial OC in the ocean (Dauwe et al. 1999; Lal 2003).

To date, there are few measurements of river CO_2 evasion, river C export or characterization of riverine C. Data are particularly limited in small to mid-sized rivers. Although individual small rivers may export a trivial mass compared to large rivers, as a group they play an important role in the global C cycle. For example, Rasera et al. (2008) calculated that small rivers in the southwestern Amazon are releasing $0.17 \pm 0.04 \text{ Gt C}$

yr⁻¹ to the atmosphere as CO₂, which is about half the global river CO₂ evasion estimated by Cole and Caraco (2001) and Cole et al. (2007).

Land use and human activities can affect river CO₂ evasion rates and the amount and nature of C rivers export to the ocean by controlling the type of terrestrial C delivered to rivers, the metabolism of terrestrial C in rivers, and the primary production within rivers. Previous studies have shown that agricultural and urban areas can contribute as much as 33% and 17% of river OC load, respectively (Sickman et al. 2010; Sickman et al. 2007). This OC is generally old due to enhanced loss of old organic matter (OM) from deep soil and ¹⁴C-free fossil OM from OM-rich bedrock (e.g. shales), and old OM input from wastewater treatment plant effluent (Griffith et al. 2009; Longworth et al. 2007; Raymond et al. 2004; Sickman et al. 2010; Sickman et al. 2007). River damming can also affect river C cycling, but the results are more complex. On one hand, river damming generally stimulates the growth of phytoplankton, removing CO₂ from the atmosphere (Wang et al. 2007). On the other hand, decomposition of organic matter in the land flooded by damming releases CO₂ and CH₄ (a greenhouse gas with a global warming potential of about 25) to the atmosphere (Abril et al. 2005). However, such studies are limited, and the impact of land use and human activities on the sources and cycling of terrestrial C in rivers is not well understood.

In my thesis I measured the CO₂ emission rate, POC export, and sources and chemical composition of riverine dissolved inorganic carbon (DIC) and POC of two small rivers (Buffalo Bayou and Spring Creek) and one midsized river (the Brazos River) in Texas. I also examined the effects of land use and human activities on C cycling in these rivers. I found high CO₂ emission rates in the two small rivers, showing that small

rivers in humid subtropical areas as a group may be a significant source of atmospheric CO₂, as observed for the tropics by Rasera et al. (2008). I also found that DIC from oyster shells and crushed limestone/dolomite minerals used in road construction is being drained into rivers and may be sustaining part of river CO₂ supersaturation. My results also show that urban treated wastewater input, river damming, and agricultural land use have changed the sources and cycling of C in the rivers I studied. These processes also affect the sources and chemical composition of POC that the Brazos River exports to the Gulf of Mexico.

The thesis has been divided into three parts. Chapter 2 focuses on the amount and sources of CO₂ evasion of Buffalo Bayou and Spring Creek, and how they are affected by urbanization and limestone/dolomite and oyster shells used in road construction. Chapters 3 and 4 concentrate on the sources and metabolism of DIC and POC in the Brazos River, and how they are controlled by urban treated wastewater input, river damming, and agricultural land use.

CHAPTER 2

Sources of CO₂ evasion from two subtropical rivers in North America

Abstract

We directly measured the partial pressure of dissolved CO₂ (pCO₂) in two humid subtropical rivers in coastal Texas, one highly urbanized (Buffalo Bayou) and one relatively undeveloped (Spring Creek), and analyzed carbon isotopic signatures ($\Delta^{14}\text{C}$ and $\delta^{13}\text{C}$) of riverine dissolved inorganic carbon (DIC) to determine carbon sources sustaining river respiration. Both rivers were highly supersaturated with CO₂ at all study sites and on all dates sampled from June 2007 to February 2009. Mean riverine pCO₂ values are $3,052 \pm 1,364$ and $4,702 \pm 1,980$ μatm for Buffalo Bayou and Spring Creek, respectively. Calculated CO₂ emission fluxes per ha of water surface area from these rivers are intermediate between those in tropical and temperate rivers, indicating that globally, humid subtropical rivers may be a significant source of atmospheric CO₂. Carbon isotopic signatures revealed that CO₂ supersaturation is supported by different carbon sources for the two rivers. In the relatively undeveloped river (Spring Creek), young terrestrial organic matter (OM) is the predominant C source fueling river heterotrophic respiration. In the highly urbanized river (Buffalo Bayou), the high concentration of riverine CO₂ is additionally supported by dissolution of CaCO₃ likely from pedogenic carbonate, and crushed limestone/dolomite and oyster shells imbedded in old roads in the watershed. Because urban sources of acidity can include HNO₃ and H₂SO₄, whether the limestone/dolomite and shells used by humans act as a net sink or source of atmospheric CO₂ needs further study.

2.1 Introduction

Annually, a large amount of terrestrial carbon, including soil organic carbon, roots, and aboveground biomass, is transferred from land into river systems. A precise determination of the amount, source and fate of this carbon is critical for regional and global carbon budgets of terrestrial ecosystems (Houghton 2003; Richey et al. 2002).

Terrestrial carbon is exported to river systems through three pathways: 1) as litterfall in the form of particulate organic carbon (POC) carried to rivers by wind and storm water; 2) as soil dissolved organic carbon (DOC) and soil POC exported to rivers; 3) as soil CO₂ from ecosystem respiration in the form of dissolved inorganic carbon (DIC) delivered to rivers by subsurface water flow. Determination of C losses through measurement of individual fluxes of each pathway is difficult because terrestrial carbon is not a point source, but an area source for river systems. A more practical approach is to track the fate of these C sources in river systems. After terrestrial carbon enters rivers, part of it (derived from soil CO₂ and from respiration of terrestrial organic carbon in the water column) is returned to the atmosphere as CO₂ during transit, part of it (some POC) is stored in floodplains and riparian corridors, and the rest is discharged to the oceans as DOC, POC and DIC. Mass balance calculations allow estimation of the rate of carbon losses from terra firma terrestrial environments to rivers by summing up these three fractions of terrestrial carbon (Cole et al. 2007).

CO₂ supersaturation is common in world river systems (Cai and Wang 1998; Cole and Caraco 2001; Mayorga et al. 2005; Raymond et al. 1997, 2000; Richey et al. 2002; Yao et al. 2007). The CO₂ outgassing rate from global rivers has been estimated to be on

the order of 1 Gt C yr^{-1} , comparable to annual river total carbon (organic and inorganic) export to the ocean (Cole and Caraco 2001; Cole et al. 2007; Rasera et al. 2008; Richey et al. 2002). However, there is significant uncertainty in the size of this flux. Conservative estimates from 45 major world rivers suggest that global rivers outgas 0.3 Gt C to the atmosphere annually (Cole and Caraco 2001), while a study in the Amazon suggested that CO_2 evasion flux from the global area covered by humid tropical forests alone is 0.9 Gt C yr^{-1} (Richey et al. 2002).

There are three major reasons for the discrepancy in global river CO_2 flux estimates, all based on data sparsity. First, most (35 out of 45) of the large rivers compiled in Cole and Caraco (2001) are temperate rivers. To better estimate CO_2 evasion flux from global rivers, a more comprehensive survey of rivers in all climate regimes is necessary. To date, studies on CO_2 concentration of subtropical rivers are still very limited. Second, although small rivers are individually trivial CO_2 sources, they are likely to be more supersaturated in CO_2 than large rivers (Finlay 2003), and summed, their bulk CO_2 evasion flux may be significant (Rasera et al. 2008). Third, direct measurements of partial pressure of CO_2 (pCO_2) are very limited. In many previous studies, riverine pCO_2 was calculated from measured pH, alkalinity and temperature, which either overestimated or underestimated the true value of pCO_2 in different case studies (Herczeg et al. 1985; Raymond et al. 1997; Stauffer 1990).

Riverine CO_2 is primarily sustained by CO_2 export from soil by groundwater and *in situ* respiration of terrestrial organic matter (OM) (Cole and Caraco 2001; Finlay 2003; Mayorga et al. 2005). Richey et al. (2002) estimated that degradation of terrestrial OM (in soil or in the water column) contributes about 75% of the CO_2 evasion in the Amazon

River basin. However, large spatial variability exists in the sources and turnover times of this terrestrial organic carbon. In the Hudson River in the northeastern US, respiration of ancient organic carbon (1,000-5,000 years old) in the watershed may be an important source of excess riverine CO₂ (Cole and Caraco 2001), while in Amazonian rivers, less than 5-year-old carbon fixed on land is the dominant labile OM fueling the river respiration (Mayorga et al. 2005). Also, not all riverine CO₂ is derived from decomposition of OM. Addition of bicarbonate (HCO₃⁻) from carbonate dissolution is another possible source of riverine CO₂ as dissolved CO₂ is in chemical equilibrium with bicarbonate in the water.

The natural isotopic compositions ($\Delta^{14}\text{C}$ and $\delta^{13}\text{C}$) of riverine carbon species, including DOC, POC and DIC, are a powerful tool to identify sources and turnover times of riverine C (Mayorga et al. 2005; Raymond and Bauer 2001c; Raymond et al. 2004). Yet, coupled use of dual carbon isotopic signatures is rare, existing only for Amazonian rivers and some temperate rivers in northeast US (Mayorga et al. 2005; Raymond et al. 2004).

In this study, we directly measured pCO₂ and accompanying carbon isotopes (¹³C and ¹⁴C) to better understand the carbon cycling of small subtropical rivers.

2.2 Study area and methods

2.2.1 Study area

We conducted this study from June 2007 to February 2009 in Buffalo Bayou and Spring Creek in southeast Texas. Both rivers flow from west to east and drain into the Gulf of Mexico through Galveston Bay (Fig. 2-1).

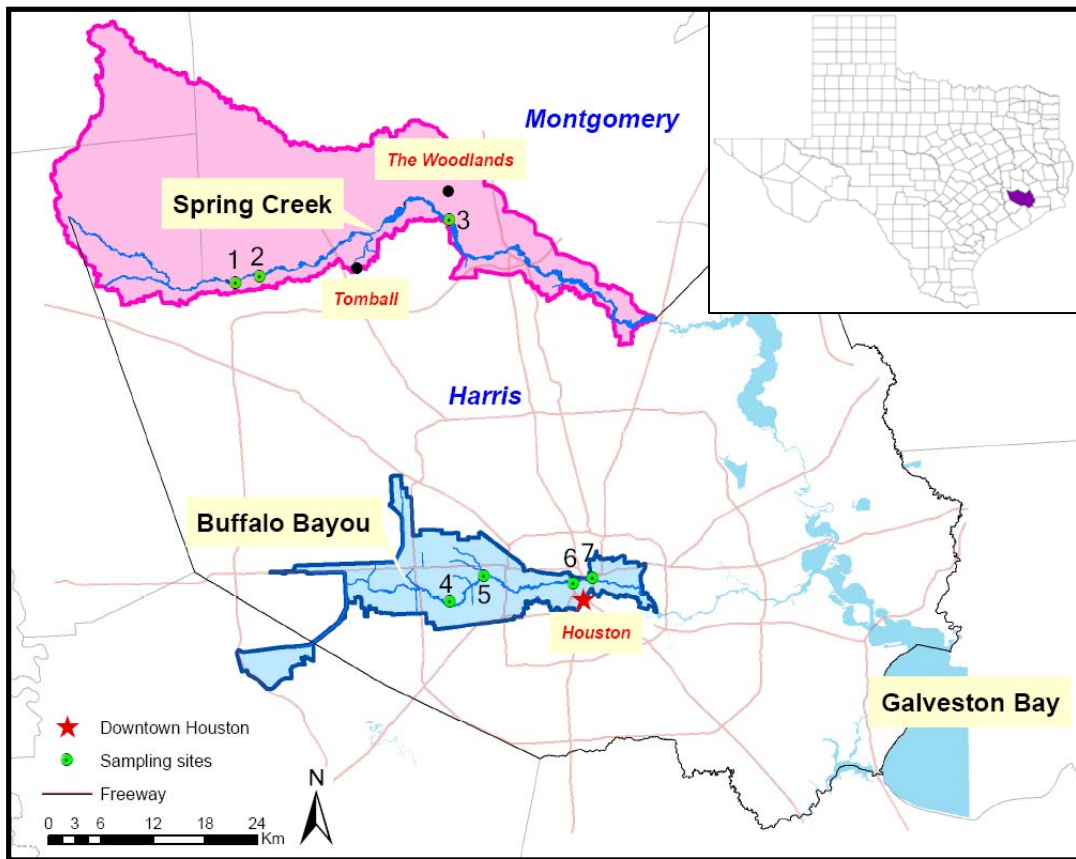


Figure 2-1. Buffalo Bayou watershed and Spring Creek watershed. Both Buffalo Bayou and Spring Creek flow from west to east. The three sampling sites in Spring Creek are Roberts Cemetery (RC, 1), Mueschke (2), and Gosling (3), and the four sampling sites in Buffalo Bayou are South Piney Point (SPP, 4), Father Point (FP, 5), Sabine (6), and McKee (7). The *inset* shows the location of Harris County in Texas.

Buffalo Bayou passes through downtown Houston in Harris County, TX. Its watershed, of which 80% is urbanized, is almost entirely within the City of Houston. Spring Creek flows along the boundary of Texas' Harris and Montgomery Counties. Its watershed is mostly covered by forests, with some agriculture use upstream. The exceptions are the city of the Woodlands (61.8 km²) and the city of Tomball (26.3 km²), both of which are undergoing development.

The majority of the Buffalo Bayou watershed is underlain by the Beaumont Formation, with a minor contribution from the Lissie Formation in the north (Table 2-1, Fisher 1982). The watershed of Spring Creek is underlain mostly by the Willis Formation, and partially by the Lissie Formation and the Beaumont Formation (Table 2-1, Shelby et al. 1992). The Willis Formation covers the upper and middle reach of Spring Creek, while the Lissie and Beaumont Formations cover the lower reach. All three formations were deposited during the Pleistocene (1.8 Ma-11,550 years BP) and are made of clay, silt and sand (Fisher 1982; Shelby et al. 1992).

Carbonate is commonly present in soils in the drainage basin of Buffalo Bayou, but only sparsely found in soils in the Spring Creek watershed (USDA 2009). Possible sources of carbonate are naturally occurring pedogenic carbonate (carbonate formed during soil development) in the Beaumont Formation (Nordt et al. 2006), and crushed limestone/dolomite and oyster shells. Crushed limestone/dolomite has been found in Gulf coast roads (Titi et al. 2003), and shell roads are distributed in a belt extending 80-110 km inland from the coastline of Texas (Doran 1965), just far enough to cover the Buffalo Bayou watershed, but only reaching the Spring Creek watershed near the Gosling site (see Fig. 2-1).

River	Length of Main Stem (km)	Length of Open Streams^a (km)	Watershed Area (km²)	Discharge^b (m³/yr)	Lithology of watershed^c
Buffalo Bayou	51	186	265	3.27×10^8	Beaumont Formation (80%): clay, silt and sand, concretions of calcium carbonate; Lissie Formation (20%): clay, silt and sand, locally calcareous, concretions of calcium carbonate.
Spring Creek	130	178	727	1.02×10^8	Willis Formation (87%): clay, silt and sand, noncalcareous; Lissie Formation (10%) and Beaumont Formation (3%) with same lithology as above.

^a Includes main stem and tributaries; data for length and watershed area are from Harris County Flood Control District: www.hcfcd.org.

^b Discharge data for the South Piney Point station (08073700) in Buffalo Bayou and for the station near Tomball (08068275) in Spring Creek are for hydrological year 2008; data from USGS: www.usgs.gov.

^c Information from Fisher (1982) and Shelby et al. (1992). Numbers in parenthesis are percentages of the watershed.

Table 2-1. Hydrological and lithologic characteristics of Buffalo Bayou and Spring Creek watersheds.

The two rivers are about 32 km apart and share a similar climate. The regional mean annual temperature is about 21°C, and the mean annual precipitation is 100-180 cm, with Spring Creek (122 cm at Tomball) having only a slightly lower annual average precipitation than Buffalo Bayou (Houston: 135 cm) (NOAA 2009b).

We selected seven sampling sites in the study area, four in Buffalo Bayou [S Piney Point (SPP), Father Point (FP), Sabine and McKee] and three in Spring Creek [Roberts Cemetery (RC), Mueschke and Gosling] (Fig. 2-1). All sampling sites are bridges over the rivers. SPP and FP are located in residential areas; Sabine and McKee are in downtown Houston; while the three sites in Spring Creek are located next to private forests. SPP in Buffalo Bayou is additionally a US Geological Survey (USGS) monitoring station (08073700), which allowed us to obtain river discharge data for this site.

2.2.2 Sample collection and analysis

We sampled pCO₂ monthly. To characterize daytime variation in riverine pCO₂, we conducted hourly pCO₂ sampling at the Sabine site in Buffalo Bayou on April 5, 2008 and the Mueschke site in Spring Creek on March 27, 2008 from before sunrise to after sunset (14 h). We also collected hourly pCO₂ samples at these two sites on two rainy days (on June 26, 2008 at Sabine, and on June 21, 2008 at Mueschke) to determine how riverine pCO₂ responds to rainfall events.

For each site we collected three ambient air pCO₂ and three water pCO₂ samples. We took ambient air pCO₂ samples on bridges (2-15 m above the river surface). Since in previous studies ambient air samples were collected closer to the river surface (Raymond

et al. 1997; Yao et al. 2007), we also took air $p\text{CO}_2$ samples <2 m above the river surface where the river bank was accessible. We found no significant difference in CO_2 concentration between air over bridges and air near river surfaces (t test, $p = 0.76$ at 95% confidence level). We took water directly from the upper 30 cm of the river using a submersible pump and collected water $p\text{CO}_2$ samples by headspace equilibration as described in Raymond et al. (1997). All $p\text{CO}_2$ samples were transported to the laboratory and analyzed on an infrared CO_2 analyzer (Li-Cor 7000) in the same day of collection.

We collected DIC samples using 250 mL pre-cleaned (soapy water, deionized water and Milli-Q water) and pre-combusted (500°C for 2 h) bottles. We collected DIC samples prior to collection of water $p\text{CO}_2$ samples to avoid any contamination. To minimize CO_2 exchange between the sample and the air, we overflowed the bottle three times. DIC samples were stored at 0°C from time of collection to poisoning with saturated HgCl_2 solution and sealing with Apiezon-N grease in the lab. Samples were always poisoned within 8 h of collection.

All DIC samples were sent to the National Ocean Sciences Accelerator Mass Spectrometry Facility (NOSAMS) for $\Delta^{14}\text{C}$ and $\delta^{13}\text{C}$ analyses, where samples were processed according to McNichol et al (1994). $\delta^{13}\text{C}$ values were reported, while $^{14}\text{C}/^{12}\text{C}$ ratios were expressed as Fraction Modern (FM). We calculated $\Delta^{14}\text{C}$ values from FM values according to Stuiver and Polach (1977).

2.3 Results and Discussion

2.3.1 Daytime riverine $p\text{CO}_2$ variation

A previous study (Raymond et al. 1997) indicated low diurnal $p\text{CO}_2$ variability in

river waters. Our data are consistent with this study (except on days of rainfall events, see below). We saw little change in riverine $p\text{CO}_2$ values at Sabine (April 5, 2008) in Buffalo Bayou and Mueschke (March 27, 2008) in Spring Creek from predawn (7 a.m.; sunrise 7:30 a.m.) through after sunset (8 p.m.; sunset 7:30 p.m.) (Fig. 2-2). Mean riverine $p\text{CO}_2$ was $3,839 \pm 291 \mu\text{atm}$ at Sabine, and was $4,146 \pm 126 \mu\text{atm}$ at Mueschke. Daytime variations were much smaller than seasonal variations for both sites ($3,157 \pm 1,454 \mu\text{atm}$ for Sabine and $3,660 \pm 706 \mu\text{atm}$ for Mueschke) (Table 2-2). We interpreted the low daytime $p\text{CO}_2$ variability to indicate that $p\text{CO}_2$ samples collected at a specific time of day are generally representative of the average riverine $p\text{CO}_2$ of the day sampled.

2.3.2 *Effect of rainfall events on riverine $p\text{CO}_2$*

Rainfall events control riverine $p\text{CO}_2$ primarily via two concurrent and competitive mechanisms: (1) rainfall events enhance the export of soil CO_2 and soil organic carbon to rivers, which increases riverine $p\text{CO}_2$ (Yao et al. 2007); and (2) rainfall events generally increase river discharge and gas transfer velocity (Ho et al. 1997), both of which lower riverine $p\text{CO}_2$. We saw evidence of both mechanisms, with the dominant mechanism depending on rainfall intensity and watershed impermeability.

On rainy days, daytime variations in riverine $p\text{CO}_2$ were larger, with mean riverine $p\text{CO}_2$ of $2,964 \pm 1,020 \mu\text{atm}$ for Sabine (June 26, 2008) and $3,205 \pm 357 \mu\text{atm}$ for Mueschke (June 21, 2008) (Fig. 2-3a, b). Enhanced river photosynthesis/ respiration processes due to abundant phytoplankton and high water temperatures in summer (Cole et al. 1992) alone can not explain why the $p\text{CO}_2$ fluctuation was higher at Sabine than at Mueschke.

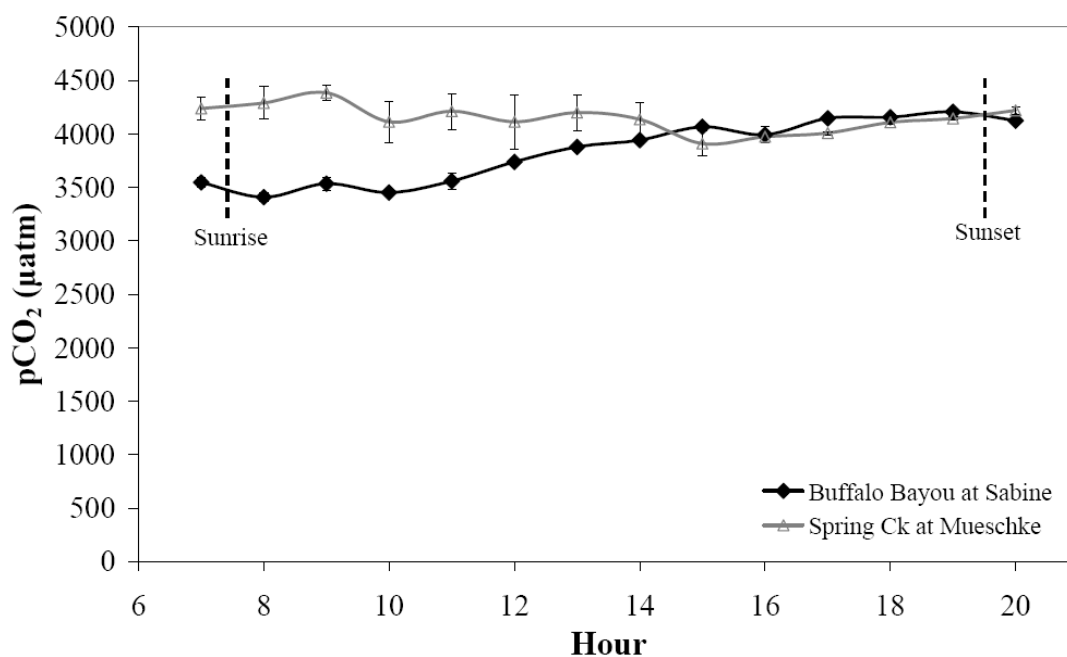


Figure 2-2. Daytime variation in riverine $p\text{CO}_2$ in Buffalo Bayou (Sabine) and Spring Creek (Mueschke) in late March and early April (Sabine 4-5-2008; Mueschke 3-27-2008; Sunrise 7:30 a.m.; Sunset: 7:30 p.m.). Error bar is 1σ on the replicates.

Site	Study period (number of samples)	Width (m)	Depth (m)	pCO _{2,w} (µatm)	pCO _{2,a} (µatm)	CO ₂ emission flux (Mg C ha ⁻¹ y ⁻¹)
<i>Buffalo Bayou</i>						
SPP	08/07 to 02/09 (19)	10 ± 2	1.0-2.0	3,158 ± 1,044	414 ± 69	3.37 ± 1.26
FP	06/07 to 02/09 (20)	10 ± 2	0.5-1.5	3,087 ± 1,610	415 ± 80	3.29 ± 1.94
Sabine	06/07 to 02/09 (20)	20 ± 4	0.8-2.5	3,157 ± 1,454	408 ± 79	3.38 ± 1.77
McKee	06/07 to 02/09 (20)	25 ± 5	1.5-3.0	2,813 ± 1,347	405 ± 78	2.97 ± 1.63
Average				3,052 ± 1,364	411 ± 75	3.25 ± 1.65
<i>Spring Creek</i>						
RC	09/07 to 02/09 (19)	1.5 ± 0.3	0.2-0.6	6,277 ± 2,357	408 ± 64	7.24 ± 2.85
Mueschke	09/07 to 02/09 (19)	3 ± 0.6	0.8-1.2	3,660 ± 706	403 ± 69	4.02 ± 0.82
Gosling	10/07 to 02/09 (16)	10 ± 2	0.5-1.5	4,070 ± 1,285	389 ± 57	4.56 ± 1.57
Average				4,702 ± 1,980	401 ± 63	5.31 ± 2.40

Width is the average width of the river at the site sampled with 20% uncertainty.

Depth is the range of water depth at the site sampled.

pCO_{2,w}: riverine pCO₂; pCO_{2,a}: pCO₂ of air on bridges.

CO₂ emission flux is for per area of water surfaces, not for per area of the basins.

SPP: South Piney Point; FP: Father Point; RC: Roberts Cemetery.

Table 2-2. Measured mean pCO₂ and calculated mean CO₂ emission flux for each study site in Buffalo Bayou and Spring Creek.

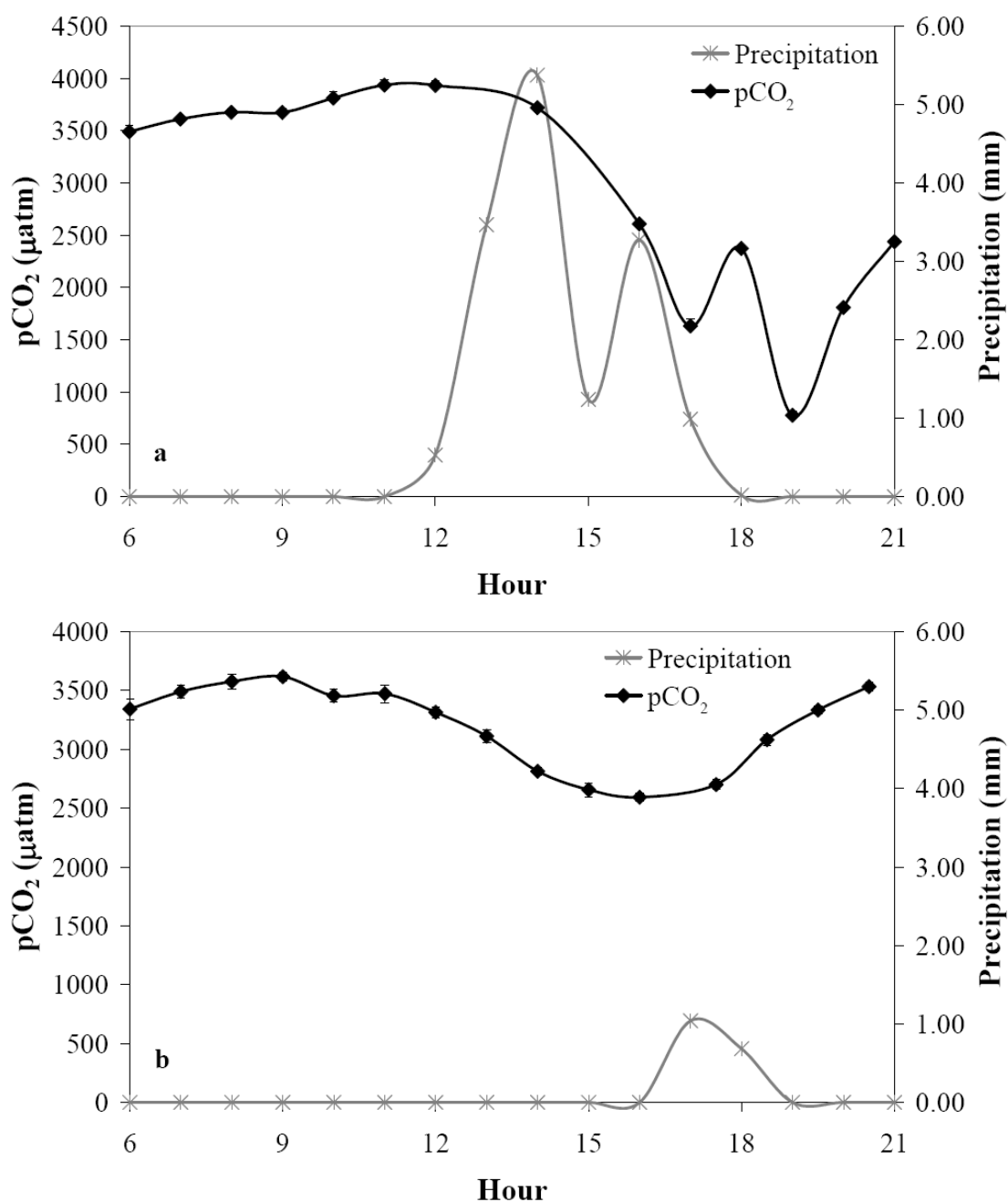


Figure 2-3. Effect of rainfall events on riverine pCO₂ at (a) Sabine in Buffalo Bayou and at (b) Mueschke in Spring Creek (Sabine 6-26-2008; Mueschke 6-21-2008; Sunrise 6:30 a.m.; Sunset: 8:30 p.m.). Hourly precipitation data were obtained from the Spatial Sciences Laboratory at Texas A&M University. Error bar is 1σ on the replicates.

The pronounced changes in riverine $p\text{CO}_2$ at Sabine on June 26, 2008 were likely caused by the intensive rainfall event, which produced about 15 mm (the Spatial Sciences Laboratory at Texas A&M University) of water within 6 h in the Buffalo Bayou watershed (Fig. 2-3a) and significantly raised the water level (river discharge was $1.7 \text{ m}^3/\text{s}$ in the morning and $23.9 \text{ m}^3/\text{s}$ in the late afternoon) (Data from USGS). Similar to others' results (Paquay et al. 2007), we found a negative relationship between riverine $p\text{CO}_2$ and precipitation at Sabine, but with a time lag of about 3 h (Fig. 2-3a). We hypothesize that the 3-h lag was caused by an initial flushing of soil CO_2 by subsurface flow of storm water, which compensated for the dilution effect of nearly CO_2 -free storm water which flowed over urban impervious surfaces (e.g. concrete). As the rain continued, soil CO_2 was flushed out, and hence the storm water dilution effect dominated.

Although there was also a rainfall event at Mueschke on June 21, 2008, we observed a different pattern in riverine $p\text{CO}_2$ (Fig. 2-3b), probably due to much lower precipitation (about 1.72 mm in total, lasted for only 2 h: 5-6 p.m., the Spatial Sciences Laboratory at Texas A&M University) and higher soil permeability in the Spring Creek watershed. There was a continuous decrease in riverine $p\text{CO}_2$ from 11 a.m. to 4 p.m. (Fig. 2-3b). A dilution effect of storm water from upstream can be ruled out because upstream Mueschke rainfall also started at 5 p.m., after the $p\text{CO}_2$ drop (the Spatial Sciences Laboratory at Texas A&M University). Instead, biological uptake of CO_2 through photosynthesis has likely caused the drop in riverine $p\text{CO}_2$. A rise in riverine $p\text{CO}_2$ occurred from the onset of the rainfall event (Fig. 2-3b). This was likely caused by the export of soil CO_2 by rain water. Weaker CO_2 uptake through photosynthesis due to lower sun angle might be an additional reason, but it alone could not explain the rapid $p\text{CO}_2$

increase from 5:30 p.m. to 6:30 p.m., as indicated by the small daytime variation in riverine $p\text{CO}_2$ observed in late March (Fig. 2-2).

2.3.3 Seasonal variation in riverine $p\text{CO}_2$

During the study period, riverine $p\text{CO}_2$ was 2-20 times supersaturated in CO_2 with respect to the atmosphere throughout the year in both rivers (Fig. 2-4). Riverine $p\text{CO}_2$ averaged $3,052 \pm 1,364 \mu\text{atm}$ for Buffalo Bayou and $4,702 \pm 1,980 \mu\text{atm}$ for Spring Creek (Table 2-2). The generally lower riverine $p\text{CO}_2$ values in Buffalo Bayou relative to Spring Creek were likely because of (1) the smaller watershed and larger river discharge (Table 2-1); (2) the buffering effect of carbonate; and (3) less biomass in the urban environment, reducing primary production and respiration associated carbon fluxes in the Buffalo Bayou watershed.

The seasonal patterns in riverine $p\text{CO}_2$ were highly consistent across sites within rivers (Fig. 2-4). This was also observed in Xijiang River in south China by Yao et al. (2007). Consistent with previous studies (Raymond et al. 1997, 2000; Richey et al. 2002; Yao et al. 2007), riverine $p\text{CO}_2$ was generally higher in summer and fall than in winter and spring. Temporal variation in riverine $p\text{CO}_2$ was also much higher in summer and fall than in winter and spring, probably due to more precipitation in summer and fall (Table 2-3, the Spatial Sciences Laboratory at Texas A&M University).

There are two major $p\text{CO}_2$ peaks in our record, one in early August 2007 and a second in late September 2008. The peak in early August 2007 (Fig. 2-4) may be associated with the abundant (253 mm in a month) and evenly distributed precipitation in July 2007 (NOAA 2009b), which allowed the rain water to infiltrate and flush out soil

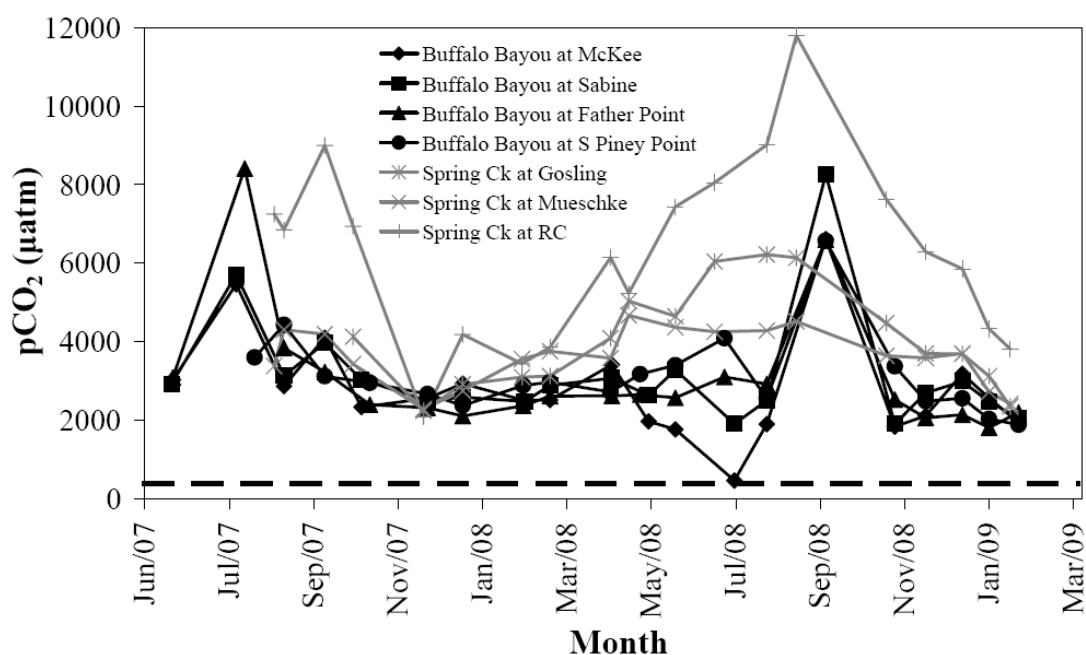


Figure 2-4. Seasonal variation in riverine pCO₂ in Buffalo Bayou and Spring Creek from June 2007 to February 2009. Direct measurement of riverine pCO₂ was made monthly at each study site. Dash line is the measured mean pCO₂ value of the atmosphere (about 410 µatm) at our study sites from June 2007 to February 2009.

Watershed	Summer 07	Fall 07	Winter 07	Spring 08	Summer 08	Fall 08	Winter 08
<i>Buffalo Bayou</i>	311	220	193	121	278	214	74
<i>Spring Creek</i>	200	157	178	161	200	230	55

Spring: March-May; Summer: June-August; Fall: September-November; Winter: December-February. Data obtained from the Spatial Sciences Laboratory at Texas A&M University.

Table 2-3. Precipitation data (in mm) for the study period for the Buffalo Bayou and Spring Creek watersheds.

CO₂ to the river while limiting the dilution effect of rainfall. On September 13-14, 2008, Hurricane Ike, the 3rd most destructive hurricane to ever make landfall in the United States, hit Houston and brought 98 mm of rain (the Spatial Sciences Laboratory at Texas A&M University). The storm water flushed out a large amount of waste water into Buffalo Bayou, making river water dark and fetid. Decomposition of OM from waste water likely led to the pCO₂ peak on September 27, 2008. The lowest riverine pCO₂ value, 476 μ atm, was observed at the McKee site in Buffalo Bayou on July 24, 2008 due to Hurricane Dolly, which produced 63 mm of rain in two days (July 23-24, 2008) (the Spatial Sciences Laboratory at Texas A&M University).

Riverine pCO₂ at Roberts Cemetery in Spring Creek was highly variable. This is likely because river discharge at this site is so low (i.e. shallow water and narrow channel, Table 2-2) that slight changes in river discharge caused large changes in river CO₂ concentration. The much higher riverine pCO₂ values at Roberts Cemetery also likely resulted from the shallow water and narrow channel at this site because: (1) narrow aquatic systems are likely to receive a heavier loading of terrestrial OM per unit discharge from litterfall due to more canopy cover for small streams (Finlay 2003); and (2) sediment processing of OM is strong in shallow aquatic systems (Torgersen and Branco 2008).

2.3.4 CO₂ emission rates of Buffalo Bayou and Spring Creek

Riverine CO₂ evasion rates depend on the CO₂ concentration gradient between the surface water and the overlying air, and the gas exchange coefficient (also known as gas transfer velocity) (Raymond et al. 1997; Wanninkhof 1992):

$$Flux = k_{CO_2} \times (pCO_{2,w} \times K_h - pCO_{2,a} \times K_h) \quad (1)$$

Where K_h is Henry's law constant at a given temperature and salinity; $pCO_{2,w} \times K_h$ and $pCO_{2,a} \times K_h$ are the actual concentration of CO_2 in the surface water and the concentration of CO_2 the water would have if it were in equilibrium with the overlying air, respectively; k_{CO_2} is the gas exchange coefficient for CO_2 at a given temperature for a given type of river. All the CO_2 evasion rates presented in this study are reported per area of water surface, not per area of the basins.

We used two methods to estimate k_{CO_2} for our systems. First, we derived k_{CO_2} from empirical models (Melching and Flores 1999). Second, we estimated k_{CO_2} from the wind speed relationship (Raymond and Cole 2001).

In the first method we calculated the reaeration-rate coefficient (K_2) from the hydraulic characteristics of our river systems using the empirical models in Melching and Flores (1999), and then converted the reaeration-rate coefficient to the gas exchange coefficient for O_2 (k_{O_2} , Hemond and Fechner-Levy 2000), from which we derived k_{CO_2} (Wanninkhof 1992). However, k_{CO_2} values calculated in this way are in a range of 13-26 $cm\ h^{-1}$, much higher than those applied to other river systems (Cai and Wang 1998; Raymond et al. 1997, 2000; Richey et al. 2002; Yao et al. 2007).

To be conservative, we chose to use the k_{CO_2} estimated from the second method, in which k_{CO_2} values were calculated from k_{600} values using the following power function (Jahne et al. 1987):

$$k_{600} / k_{CO_2} = (600 / Sc_{CO_2})^n \quad (2)$$

k_{600} is the gas exchange coefficient for CO₂ at 20°C in freshwater (CO₂ has a Schmidt number of 600 in this condition). k_{600} and n estimated for estuaries in 39 coastal cities in the United States with a mean daily wind speed of $4.6 \pm 0.28 \text{ m s}^{-1}$ (ranging from 3 to 7.7 m s^{-1}) are 3-7 cm h^{-1} and -0.5, respectively (Raymond and Cole 2001). The average wind speed in Houston for the study period, obtained from the same wind speed data resource (NOAA 2009b) as in Raymond and Cole (2001), was 3.4 m s^{-1} (ranging from 0.5 to 9.7 m s^{-1}), so conservatively we applied a k_{600} value of 3 cm h^{-1} and the same n value (-0.5) in the calculation. The Schmidt number for freshwater CO₂ (Sc_{CO_2}) is a function of temperature (t) in °C (Wanninkhof 1992):

$$Sc_{CO_2} = 1911.1 - 118.11 \times t + 3.4527 \times t^2 - 0.04132 \times t^3 \quad (3)$$

Our most conservative calculations (based on k_{CO_2} values estimated from the wind speed relationship) show that average CO₂ emission rates are consistent across sites within rivers, again with the exception of Roberts Cemetery, which has a much higher CO₂ outgassing rate than the other two sites in Spring Creek (Table 2-2). Due to its generally higher riverine pCO₂ values, Spring Creek released CO₂ to the atmosphere at a rate of $5.31 \pm 2.4 \text{ Mg C ha}^{-1} \text{ year}^{-1}$, about 1.5 times that in Buffalo Bayou, $3.25 \pm 1.65 \text{ Mg C ha}^{-1} \text{ year}^{-1}$.

Compared to other rivers in which pCO₂ values or CO₂ evasion fluxes were directly measured, the CO₂ emission rates of Buffalo Bayou and Spring Creek are intermediate

between those of temperate rivers in northeast US and those of Amazonian rivers (Table 2-4). However, it should be emphasized that the k_{CO_2} values we used to estimate CO_2 emission rates are very conservative. If the k_{CO_2} values derived from empirical models and hydraulic characteristics were used, our river systems would have CO_2 emission rates ($24.98 \pm 10.76 \text{ Mg C ha}^{-1} \text{ year}^{-1}$ for Buffalo Bayou and $22.85 \pm 8.85 \text{ Mg C ha}^{-1} \text{ year}^{-1}$ for Spring Creek) higher than those in Amazonian rivers (Table 2-4), as in the case of two other subtropical rivers (Cai and Wang 1998; Yao et al. 2007). Even with the most conservative estimates of k_{CO_2} , results of this study suggest that humid subtropical rivers are releasing CO_2 to the atmosphere at a rate comparable to large humid tropical rivers, and globally they may be a large source of atmospheric CO_2 .

2.3.5 Potential sources of riverine CO_2 and their carbon isotopic signatures

Potential sources of riverine DIC include atmospheric CO_2 , soil CO_2 and *in situ* respiration of terrestrial OM, and dissolution of carbonate. Each of these sources has distinct $\Delta^{14}C$ and $\delta^{13}C$ signatures, allowing individual sources to be visualized separately on a plot of $\delta^{13}C$ vs. $\Delta^{14}C$ (Fig. 2-5). In the next few paragraphs, we will discuss the range of possible $\Delta^{14}C$ and $\delta^{13}C$ signatures of DIC from each potential source.

As river water is in contact with the atmosphere, atmospheric CO_2 exchanges with CO_2 in river water and thus may potentially make up a fraction of riverine DIC. CO_2 in surface air across North America had $\Delta^{14}C$ values of 55-66‰ in 2004 (Hsueh et al. 2007). If we assume that $\Delta^{14}C$ of atmospheric CO_2 has been dropping at a rate of about 6‰ per year (Trumbore et al. 2006), $\Delta^{14}C$ of atmospheric CO_2 in 2007 and 2008 should be in the range of 31-48‰. Since by definition $\Delta^{14}C$ is fractionation corrected, atmosphere-derived

River	Mean pCO ₂ (μatm)	k (cm h ⁻¹)	CO ₂ emission flux (Mg C ha ⁻¹ year ⁻¹)	References
<i>Tropical</i>				
Amazon	4,350 ± 1,900 (mainstem) 5,000 ± 3,300 (major tributaries)	9.58 ± 3.75 (mainstem) 5 ± 2.08 (major tributaries)	8.3 ± 2.4	Richey et al. (2002)
Ji-Parana	-	-	2.27-47.80	Rasera et al. (2008)
<i>Subtropical</i>				
Xijiang River	2,600	8-15	8.3-15.6	Yao et al. (2007)
Satilla River Estuary	-	12.5	18 to >30.6	Cai and Wang (1998)
Buffalo Bayou	3,052 ± 1,364	2.59-4.18	3.25 ± 1.65	This study
Spring Creek	4,702 ± 1,980	2.31-3.78	5.31 ± 2.40	This study
<i>Temperate</i>				
Hudson	1,125 ± 403	1.54-4.1	0.7-1.62	Raymond et al. (1997)
York River Estuary	1,070 ± 867	4.7	0.53-0.75	Raymond et al. (2000)

All the riverine pCO₂ values were directly measured except for the Xijiang River. CO₂ emission fluxes were computed from directly measured riverine pCO₂, or were directly measured where riverine pCO₂ values were not available.

CO₂ emission flux is for per area of water surfaces, not for per area of the basins.

Table 2-4. Riverine pCO₂ values and CO₂ emission fluxes for some world rivers.

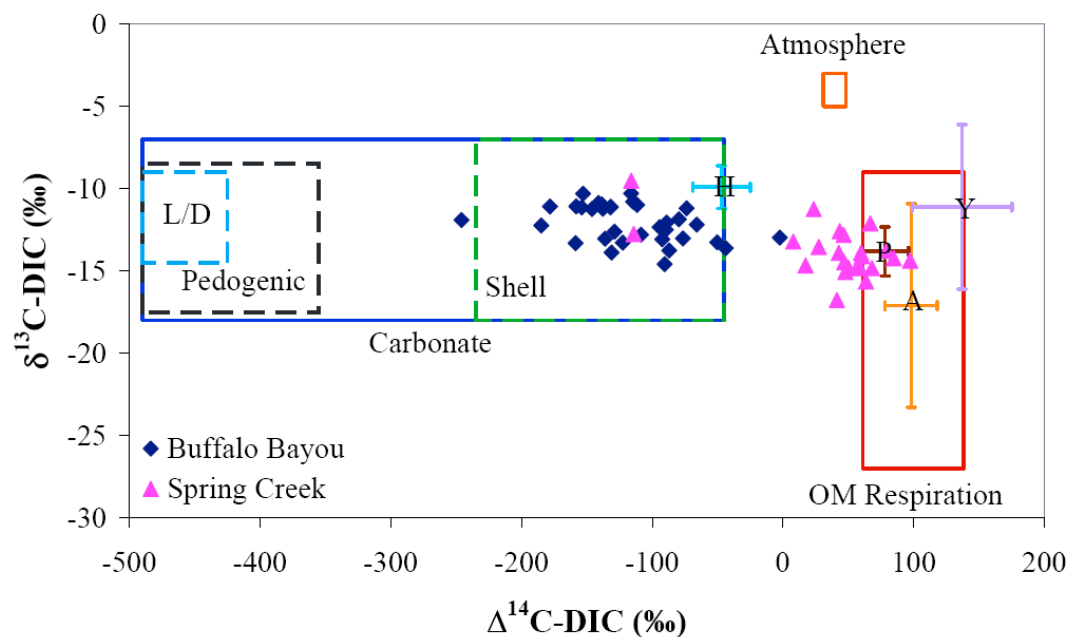


Figure 2-5. $\delta^{13}\text{C}$ versus $\Delta^{14}\text{C}$ of riverine DIC in Buffalo Bayou (diamonds) and Spring Creek (triangles) in comparison with those in Amazonian rivers (A, carbonate free), the Hudson River (H), the Parker River (P), and the York River (Y) (Mayorga et al. 2005; Raymond and Bauer 2001a; Raymond et al. 2004). Also plotted are $\delta^{13}\text{C}$ versus $\Delta^{14}\text{C}$ of DIC from potential sources (in solid boxes): atmospheric CO_2 (Atmosphere), OM respiration, and carbonate dissolution (Carbonate). There are three sources of carbonate in the study watersheds (in dashed boxes): natural pedogenic carbonate (Pedogenic), and anthropogenic use of crushed limestone/dolomite (L/D) and shells (Shell).

DIC should have the same $\Delta^{14}\text{C}$ values as atmospheric CO_2 . For the $\delta^{13}\text{C}$ of DIC from atmospheric CO_2 invasion, we chose the range of -5 to -3‰ from an earlier study (Raymond et al. 2004).

We grouped soil CO_2 and decay of terrestrial OM together as one source, OM respiration (Fig. 2-5). To estimate the age of subtropical soil-respired terrestrial OM, we assumed it was intermediate between that of temperate and tropical soils. Since the mean age of soil respired C in temperate forests is three times of that in tropical forests (Trumbore 2000), we assumed that turnover time of OM in temperate rivers is 15 years, three times of that in Amazonian rivers (<5 years) (Mayorga et al. 2005), unless there is ancient OM respired in rivers as in the Hudson (Cole and Caraco 2001; Raymond et al. 2004). There is no OM-rich shale in the basins of Buffalo Bayou and Spring Creek. Residence time of OM was, therefore, assumed to be in a range of 5-15 years. Based on the average $\Delta^{14}\text{C}$ values of 31-48‰ for atmospheric CO_2 in 2007 and 2008 and the annual decreasing rate of about 6‰, DIC from OM respiration has $\Delta^{14}\text{C}$ values in a range of 61-138‰. The $\delta^{13}\text{C}$ values of DIC derived from soil CO_2 and in-situ OM respiration is determined by the $\delta^{13}\text{C}$ signatures of the OM remineralized, which fall in the range from -34 to -20‰ for other rivers (Masiello and Druffel 2001; Mayorga et al. 2005; Raymond and Bauer 2001b; Raymond et al. 2004; Trumbore et al. 2006). Since there is a 7-11‰ isotopic fractionation (Mook et al. 1974; Zhang et al. 1995) when CO_2 from soil and in-situ OM respiration is dissolved and converted to DIC, riverine DIC from these sources would have $\delta^{13}\text{C}$ values ranging from -27 to -9‰.

Carbon isotopic signatures of DIC from the three types of carbonate in the Buffalo Bayou watershed (pedogenic carbonate, crushed limestone/dolomite and shells), both

individually and as a group, are distinctive from those of DIC from atmospheric CO₂ and OM respiration (Fig. 2-5). Pedogenic carbonate in Texas has $\delta^{13}\text{C}$ values of -6 to +1‰, and $\Delta^{14}\text{C}$ values of -1000 to -860‰ (Nordt et al. 1998; Rightmire 1967; Valastro et al. 1968). Crush limestone/dolomite is radiocarbon dead ($\Delta^{14}\text{C} = -1000\text{‰}$) and has $\delta^{13}\text{C}$ values of ~0‰. The conventional ages of shells in Galveston Bay range from 2,200 to 5,400 years (Kibler 1999), corresponding to $\Delta^{14}\text{C}$ values of -489 to -240‰, and $\delta^{13}\text{C}$ values of shells span a range of -7 to +4‰ (Douglas and Staines-Urias 2007; Gentry et al. 2008; Keller et al. 2002; McConnaughey and Gillikin 2008; Wisshak et al. 2009). When carbonate is dissolved by soil CO₂, DIC produced has $\Delta^{14}\text{C}$ and $\delta^{13}\text{C}$ signatures intermediate between those of carbonate and soil CO₂. Using a $\Delta^{14}\text{C}$ range of +20 to +150‰ (Trumbore 2000; Trumbore et al. 2006) and a $\delta^{13}\text{C}$ range of -29 to -18‰ as in Raymond et al (2004) for soil CO₂, we estimated isotopic signatures of DIC from dissolution of each type of carbonate, as showed in Fig. 2-5.

2.3.6 Temporal and spatial variation in sources of riverine CO₂

Large variation in river discharge (Fig. 2-6a) caused the concentration of riverine DIC in Buffalo Bayou to vary significantly throughout the entire study period (Fig. 2-6b). We found a negative relationship between DIC concentration and river discharge in Buffalo Bayou: DIC concentration was lower when the river had a higher discharge (Fig. 2-7a). A similar observation was reported for a river in Hawaii by Paquay et al (2007). However, at times when river discharge was high, DIC mass flow rates (DIC concentration \times discharge) were higher (Fig. 2-7b). This implies that DIC was added to rivers during rainfall events although the overall concentration of riverine DIC was

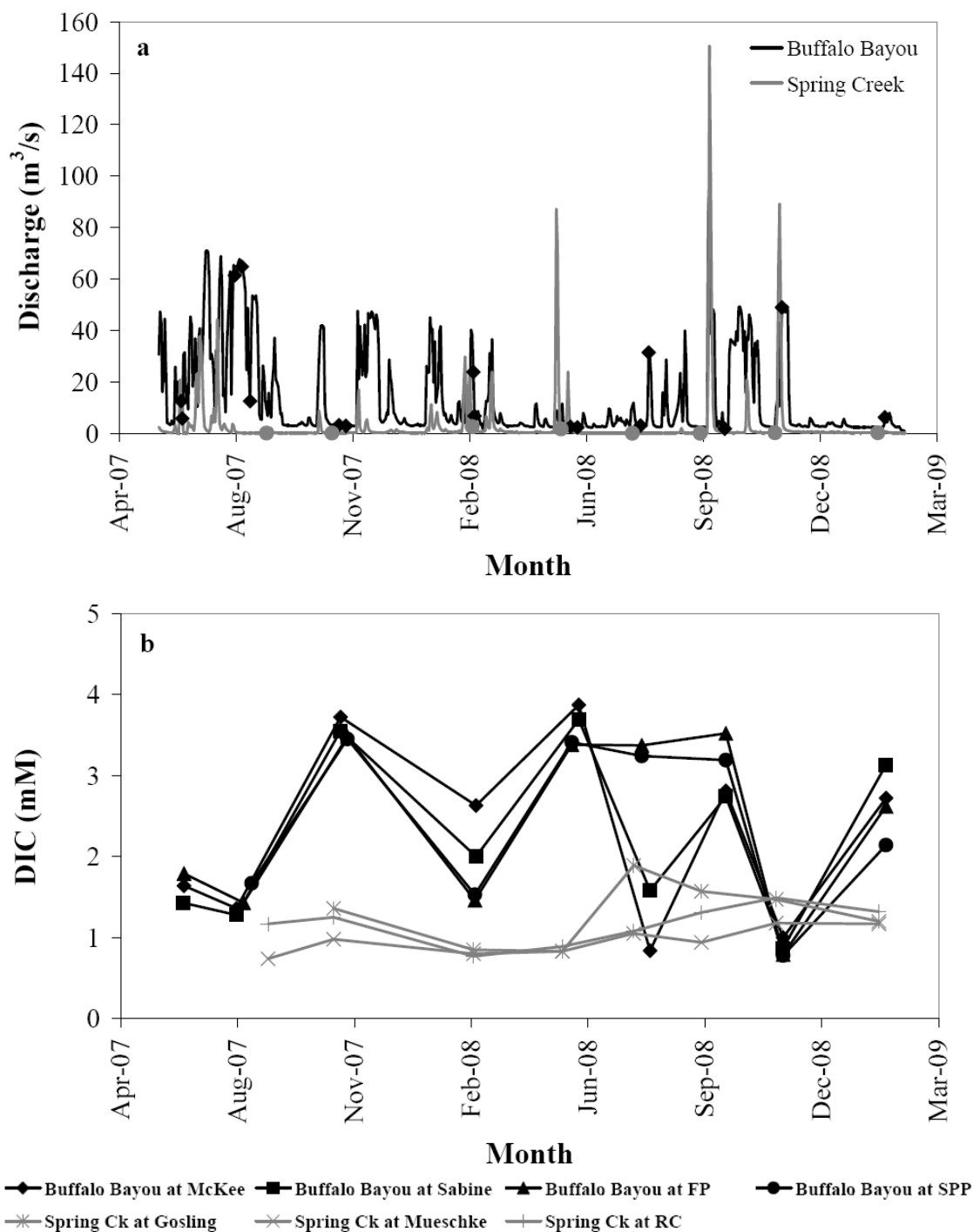


Figure 2-6. Seasonal variation in (a) river discharge and (b) concentration of DIC for Buffalo Bayou and Spring Creek from June 2007 to February 2009. River discharge data were obtained from the USGS for station at SPP (08073700) in Buffalo Bayou and station near Tomball (08068275) in Spring Creek. Diamonds and solid circles are daily discharge for Buffalo Bayou and Spring Creek, respectively, on the days sampled.

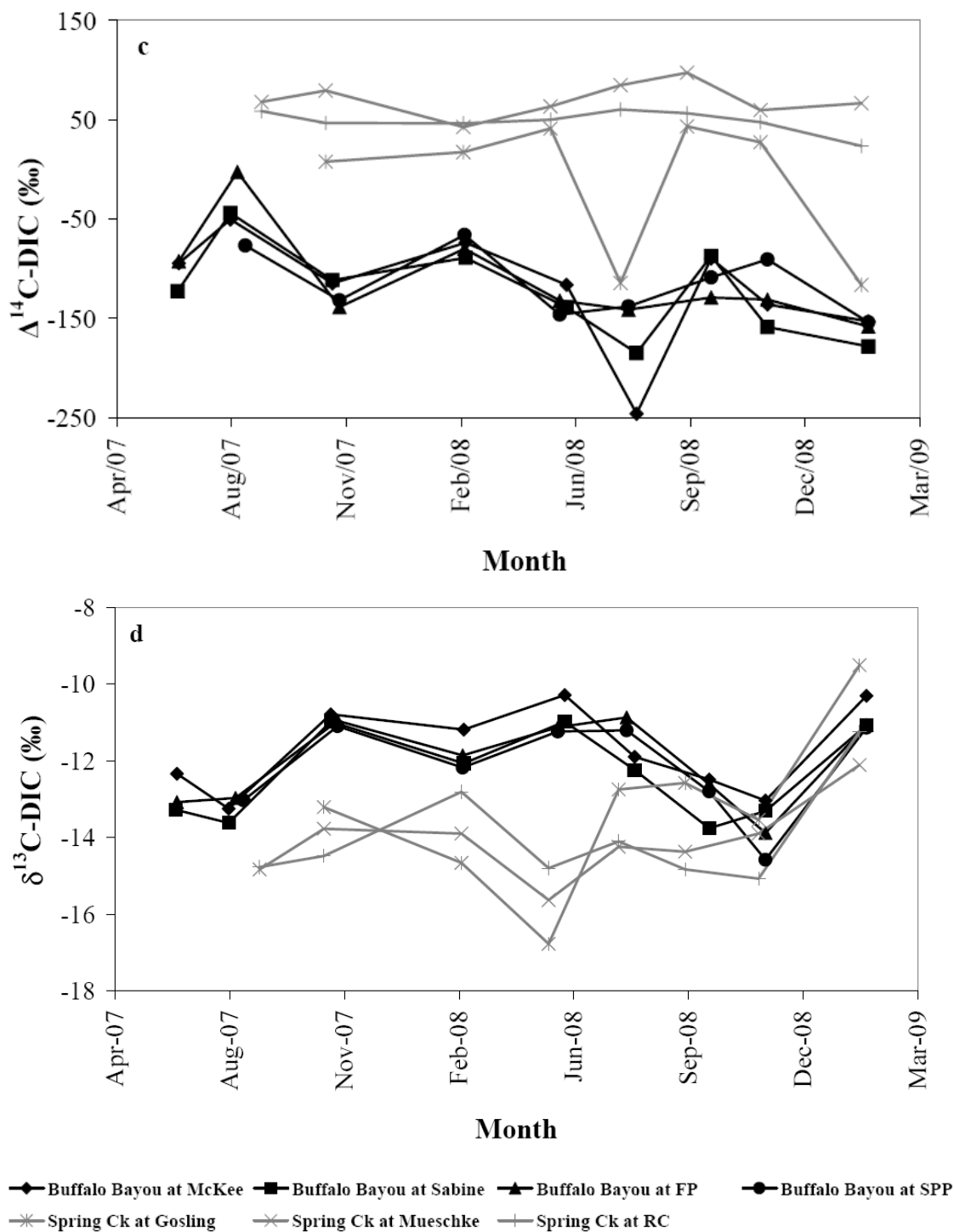


Figure 2-6. Seasonal variation in (c) $\Delta^{14}\text{C}$ of DIC and (d) $\delta^{13}\text{C}$ of DIC for Buffalo Bayou and Spring Creek from June 2007 to February 2009. Error bars on mM DIC, $\Delta^{14}\text{C-DIC}$ and $\delta^{13}\text{C-DIC}$ are smaller than symbols.

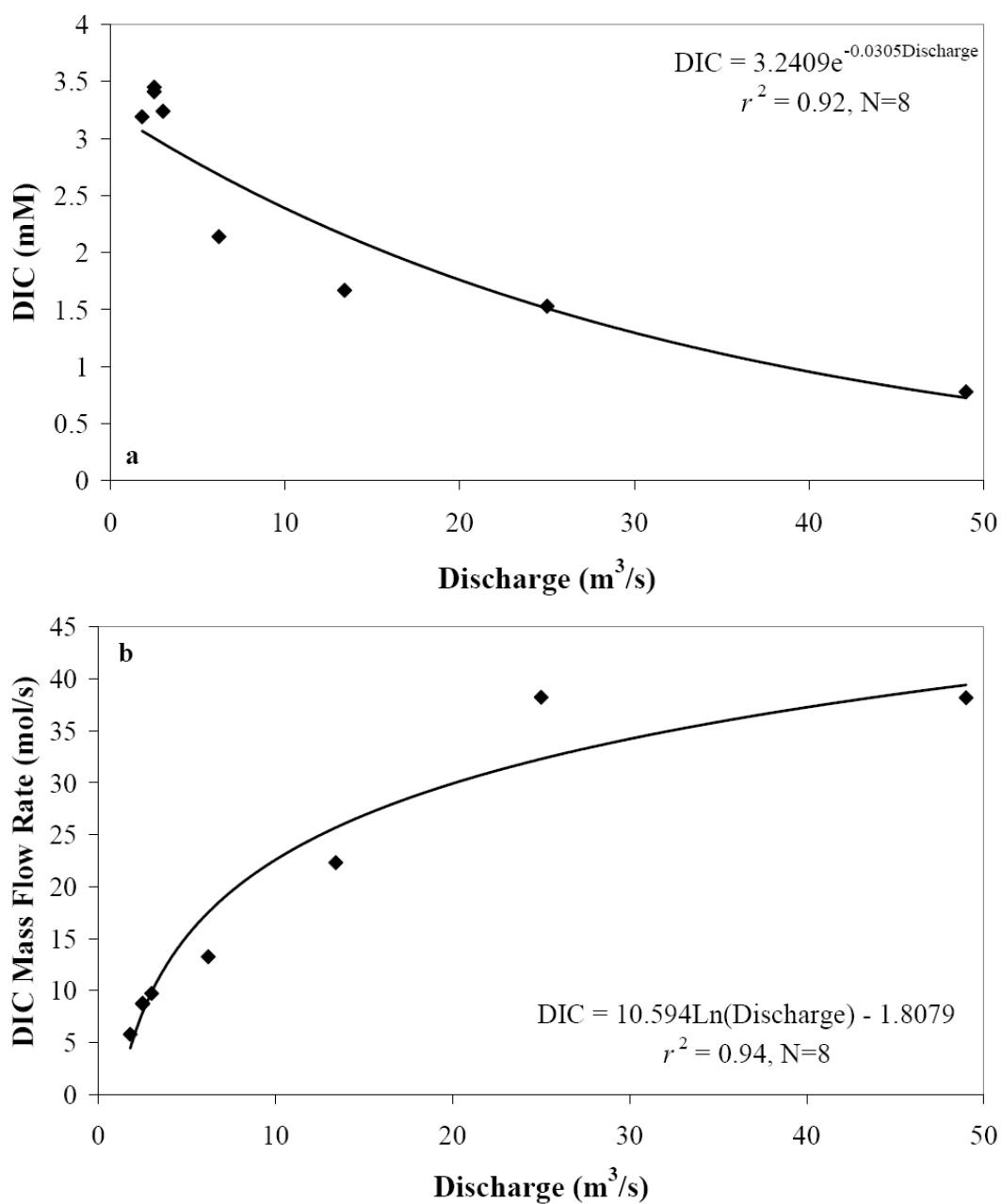


Figure 2-7. Relationship between (a) DIC concentration and discharge, (b) DIC mass flow rate (DIC concentration \times discharge) and discharge, for the SPP site in Buffalo Bayou. Daily discharge data were from the USGS (2009).

diluted. There was no obvious seasonal variation in DIC concentration in Spring Creek, probably due to relatively constant river discharge on all dates sampled (Fig. 2-6a). Concentration of DIC was generally higher in Buffalo Bayou (0.78-3.87 mM, averaging 2.35 ± 1.03 mM) than in Spring Creek (0.74-1.89 mM, averaging 1.14 ± 0.30 mM) (Fig. 2-6b), likely associated with carbonate dissolution in the Buffalo Bayou watershed.

Like riverine $p\text{CO}_2$ for both Buffalo Bayou and Spring Creek, $\Delta^{14}\text{C}$ and $\delta^{13}\text{C}$ values of DIC were generally consistent among sites within the same river (Fig. 2-6c, d), suggesting that sources of DIC were generally similar for different segments of the same river. There was no clear seasonal pattern in $\Delta^{14}\text{C}$ -DIC and $\delta^{13}\text{C}$ -DIC (Fig. 2-6c, d).

DIC in Buffalo Bayou was more depleted in $\Delta^{14}\text{C}$ than in Spring Creek at all times, and was more enriched in $\delta^{13}\text{C}$ than in Spring Creek most of the time (Fig. 2-6c, d). Averaging all sites in each river yields mean $\Delta^{14}\text{C}$ -DIC values of $-117.3 \pm 45.3\text{‰}$ for Buffalo Bayou and $37.3 \pm 52.5\text{‰}$ for Spring Creek. Overall average $\delta^{13}\text{C}$ -DIC for Buffalo Bayou was $-12.1 \pm 1.1\text{‰}$ and for Spring Creek was $-13.8 \pm 1.5\text{‰}$.

Distinctive isotopic compositions of riverine DIC indicate that Buffalo Bayou and Spring Creek have different primary DIC sources. DIC isotopic signatures for Buffalo Bayou are close to those for the Hudson River (Fig. 2-5) in which old DIC was sourced from ancient shale OM and carbonate (Raymond et al. 2004). Since there is no shale OM in our study watersheds, the old DIC in Buffalo Bayou was likely from carbonate dissolution. The much older DIC at Sabine and McKee on July 24, 2008 implies higher input of carbonate to Buffalo Bayou due to Hurricane Dolly.

The carbon isotopic signatures of DIC in Spring Creek resemble those observed in Amazonian rivers, the Parker River, and the York River (Fig. 2-5), in which respiration of

young terrestrial OM support river CO₂ supersaturation (Mayorga et al. 2005; Raymond and Bauer 2001a; Raymond et al. 2000). The riparian zone (100-1000 m from the creek on both sides) along most of the course of Spring Creek is covered by trees. Litterfall production could be very high in such small watersheds (Selva et al. 2007). Direct export of this litterfall, and DOC leached out from this litterfall and eventually delivered to the creek is likely a large source of the relatively young OM sustaining river respiration in Spring Creek. There are two exceptions, both occurred at the Gosling site in Spring Creek, on July 10, 2008 and on February 5, 2009. On these two sampling dates the Gosling site had much older (lower $\Delta^{14}\text{C}$) and significantly more ^{13}C -enriched DIC than the other two sites in Spring Creek, indicating a carbonate input. Without these two data points, average $\Delta^{14}\text{C}$ value of DIC in Spring Creek is +52‰. This is consistent with carbon fixed in 2005 (Hsueh et al. 2007) or in 1956-1957 (Broecker and Walton 1959; Burchuladze et al. 1989), giving a carbon residence time of four or 53 years.

2.3.7 Potential role of anthropogenic carbonate as a source of atmospheric CO₂

Carbonate dissolution is generally regarded as a sink of atmospheric CO₂, because when carbonate is dissolved by soil CO₂, CO₂ is sequestered as bicarbonate ($\text{CaCO}_3 + \text{H}_2\text{O} + \text{CO}_2 \rightarrow \text{Ca}^{2+} + 2\text{HCO}_3^-$). However, carbonate can also be dissolved by stronger environmental acids, like HNO₃ or H₂SO₄ from urban air pollution or fertilizer use, or by soil organic acids from OM decomposition. In the case of these acids, the reaction is $\text{CaCO}_3 + 2\text{H}^+ \rightarrow \text{Ca}^{2+} + \text{H}_2\text{O} + \text{CO}_2$, and this induces a net flux of CO₂ into the atmosphere. The net effect of carbonate dissolution on atmospheric CO₂ concentration, therefore, depends on the sources of acidity driving the dissolution process.

Although results from this study suggest that crushed limestone/dolomite and shells contribute to river CO₂, we can not determine whether this carbonate is a net source or sink of atmospheric CO₂ because the sources of acidity in our watersheds are not well-constrained. Evaluation of the size and direction of anthropogenic carbonate-driven CO₂ fluxes also requires a much finer-scale knowledge of forms of carbonate used, locations of application, amounts applied, and timescales of both human application and dissolution processes.

Despite the difficulties, estimating the role of anthropogenic carbonate as a potential source of atmospheric CO₂ is important for regional and global carbon budgets for two reasons. First, every year crushed limestone/dolomite (shell use is negligible compared to use of crushed limestone/dolomite) is used in large amounts nation-wide. In 2006-2007, about 1.2 Gt of crushed limestone/dolomite was consumed per year in the US (USGS 2007, 2009). Second, strong acids in the environment are capable of dissolving these carbonate minerals and contributing to atmospheric CO₂. One example is the presence of HNO₃ in agricultural soils due to nitrogen fertilizer use, which caused a net 4.4-6.6 Tg CO₂ emission from the use of 20-30 Tg of crushed limestone/dolomite in agricultural land in the US in 2001 (West and McBride 2005). Acid rain is another common environmental source of acidity (Aulenbach et al. 1996; Bricker and Rice 1993; Gatz 1991). To date, attention has been paid only to the 2% of crushed limestone/dolomite used in agriculture, while the fate of the rest 98% used for other purpose remains unknown (USGS 2007; West and McBride 2005) and needs further study.

2.4 Conclusions

pCO₂ measurements indicate that both subtropical rivers we studied are supersaturated with CO₂ relative to the atmosphere throughout the year. Mean riverine pCO₂ values of the two rivers are 7-10 times the CO₂ concentration of the atmosphere, consistent with a recent study conducted in a subtropical river in southern China (Yao et al. 2007). Estimated CO₂ evasion fluxes per unit area of these two rivers are intermediate between those of temperate rivers and Amazonian rivers (Mayorga et al. 2005; Raymond et al. 1997, 2000), implying that humid subtropical rivers may be a large CO₂ source to the atmosphere.

Precipitation is an important control on daytime and seasonal variations in riverine pCO₂ at our sites, probably driving changes in the production and transport of soil CO₂ to rivers. The effect of rainfall events on river CO₂ concentration depends on the intensity of rainfall and watershed impermeability.

Isotopic signatures of riverine DIC suggest that the two subtropical rivers have different carbon sources supporting river CO₂ supersaturation. In Spring Creek, which is relatively undeveloped, river heterotrophic respiration is fueled by relatively young OM (years to decades old), while in Buffalo Bayou, which is 80% urbanized, we observed a significant input of old and relatively ¹³C-enriched DIC. Potential sources of the old DIC are pedogenic carbonate, and anthropogenically added carbonate (crushed limestone/dolomite and shells) used as aggregate in road construction in the drainage basin. Future study is needed to evaluate the role of the carbonate used by humans in the global carbon cycle.

2.5 Acknowledgements

CAM and FWZ acknowledge the support of the Texas Water Resources Institute

through a grant program supported by the U.S. Geological Survey and the National Institutes for Water Research. CAM and FWZ also acknowledge the generous support of Hans O. and Suse Jahns. FWZ is grateful to T.J. Perez, S.R. Alin and D. Lockwood for their assistance with instrument setup and sampling procedure, and Dr. Xinfeng Shi, Dr. Yanlu Ma, Dr. William Hockaday, Shuaiping Ge, Kaijian Liu, Yongbo Zhai, LaQuanti Calligan, Krystle Hodge, Li Zhang, Jianping Chen, Yan Chen, Jianping Huang, Xuan Guo, Yan Zhou, Qinglian Chen, Wei Chen, Baoshan Wang, Xinling Wang, and Lacey Pyle for their assistance in sample collection. An early draft of this paper benefited from Emilio Mayorga's input.

CHAPTER 3

Controls on the origin and cycling of riverine dissolved inorganic carbon in the Brazos River, Texas

Abstract

Rivers draining watersheds including carbonate bedrock or organic matter (OM)-rich sedimentary rocks frequently have ^{14}C -depleted dissolved inorganic carbon (DIC) relative to rivers draining carbonate- and OM- free watersheds, due to dissolution of carbonate and/or decomposition of ancient OM. However, our results from a subtropical river, the Brazos River in Texas, USA, show that in this watershed human activities appear to dominate basin lithology in controlling the origin and metabolism of DIC. The middle Brazos flows through limestone and coal-bearing bedrock, but DIC isotope data suggest no limestone dissolution or respiration of ancient OM, and instead reflect efficient air-water CO_2 exchange, degradation of relatively young OM and photosynthesis in the river as a result of river damming and urban treated wastewater input. The lower Brazos drains only small areas of carbonate and coal-bearing bedrock, but DIC isotope data suggest the strong influence of carbonate dissolution, with a potentially minor contribution from decomposition of old soil organic matter (SOM). Oyster shells and crushed carbonate minerals used in road construction are likely sources of carbonate in the lower Brazos, in addition to natural marl and pedogenic carbonate. Additionally, the generally low pCO_2 and high DIC concentration in the Brazos River lead to a low CO_2 outgassing : DIC export ratio, distinguishing the Brazos River from other rivers.

3.1 Introduction

Conservative estimates show that globally, rivers receive at least 1 Gt C year⁻¹ (in both organic and inorganic forms) from land (Cole et al. 2007; Meybeck 1993), equivalent to half of the net oceanic uptake of anthropogenic CO₂ (Sarmiento and Sundquist 1992). Of the terrestrial carbon transported by river systems, at least 0.35 Gt year⁻¹ is released to the atmosphere as CO₂, and about 0.7 Gt year⁻¹ is exported to the ocean (Cole et al. 2007).

One important control on the source and fate of terrestrial carbon in river systems is basin lithology, as reflected in the isotope values of riverine dissolved inorganic carbon (DIC = dissolved CO₂ + HCO₃⁻ + CO₃²⁻). Black shales rich in organic matter (OM) in the northeast US provide rivers with very old organic carbon, and decomposition of this ancient terrestrial organic carbon may have contributed to the low $\Delta^{14}\text{C}$ values of the DIC (-69 to -6‰) and to evasion of CO₂ from the northeast US rivers (Cole and Caraco 2001; Raymond et al. 2004). In watersheds composed of carbonate rocks (e.g. limestone and dolomite), dissolution of carbonate is generally an important source of riverine DIC (Chakrapani and Veizer 2005; Helie et al. 2002; Kanduc et al. 2007b; Karim and Veizer 2000; Lambs et al. 2009; Zhang et al. 2009). Even in the Tana River in Kenya, in which river particulate organic carbon (POC) is significantly decomposed during transit, the dissolution of carbonate and silicate in the watershed still dominates OM respiration as the major source of river DIC (Bouillon et al. 2009).

Human activities, such as river damming and urban development, are another control on river carbon cycling. Wachniew (2006) found that rapid decomposition of labile OM from effluents of two wastewater plants lowered $\delta^{13}\text{C}$ values of DIC in the Vistula River

in Poland by about 1‰. Enrichment of ^{13}C in the DIC pool due to enhanced air-water CO_2 exchange in reservoirs also affects river carbon isotope values (Brunet et al. 2005; Wachniew 2006). Increased DIC export from urban watersheds as a result of increased chemical weathering, CO_2 production, and wastewater input has additionally been observed (Barnes and Raymond 2009).

Studies assessing the effects of lithology versus human activities on river carbon cycling are few, and these studies have generally found that the influence of lithology is more important than that of human activities. For example, although carbonates compose only ~5% of the bedrock geology of the watershed in the densely populated Lagan River basin in Northern Ireland, they were a more important source of river DIC than wastewater discharged from industries and urban-rural areas (Barth et al. 2003). In the Vistula River in Poland which receives high loads of pollutants from its watershed and drains a watershed mostly composed of carbonate bedrocks, $\delta^{13}\text{C}$ values of DIC suggest a predominant influence of carbonate rock dissolution (Wachniew 2006). Similarly, lithology showed a dominant control on carbon geochemistry in a mountainous tributary of the Zhujiang (Pearl River) in southeast China, although impacts of agricultural, urban, and river damming activities were also observed (Zhang et al. 2009).

Our first objective in this study was to determine the relative influence of basin lithology and human activities on carbon cycling in the Brazos River, a subtropical river in Texas. The Brazos River is the longest river (2060 km) in Texas. It runs through large areas of carbonate bedrock in its middle reach, which has minor outcrops of coal-bearing bedrock. Several cities are developing along this middle reach of the Brazos River, and the river main stem is dammed in two of these cities. These characteristics make the

Brazos River an excellent field site to study the effects of basin lithology and human activities on the sources and carbon isotope values ($\delta^{13}\text{C}$ and $\Delta^{14}\text{C}$) of riverine DIC.

The second objective of this study was to determine the fraction of the inorganic carbon in the Brazos River that is exported to the ocean. Cole et al. (2007) estimated that about $0.23 \text{ Pg year}^{-1}$ of terrestrial carbon is lost from rivers to the atmosphere through CO_2 outgassing, and about the same amount of terrestrially derived inorganic carbon ($0.26 \text{ Pg year}^{-1}$) is exported to the ocean, suggesting that the CO_2 outgassing : DIC export ratio of global rivers is about 1:1. However, tropical rivers tend to outgas substantially more CO_2 to the atmosphere relative to the inorganic carbon they deliver to the ocean. For example, in the Amazon River system, the amount of terrestrial carbon returned to the atmosphere each year is more than ten times the total carbon (organic and inorganic) the river exports to the ocean (CO_2 outgassing : DIC export > 10:1) (Richey et al. 2002). Similarly, the Nyong River in Cameroon releases CO_2 to the atmosphere at a rate four times that of DIC export to the Gulf of Guinea (CO_2 outgassing : DIC export = 4:1) (Brunet et al. 2009). If river CO_2 evasion and DIC export are equal ($0.23\text{-}0.26 \text{ Pg year}^{-1}$) on a global scale, then some rivers must export more inorganic carbon to the ocean than they release as CO_2 (i.e. CO_2 outgassing : DIC export < 1:1). One example is the Ottawa River, of which CO_2 evasion is about 30% of DIC export by the river (CO_2 outgassing : DIC export = 0.3:1) (Telmer and Veizer 1999). Therefore, the second objective of this study was to quantify the CO_2 outgassing and DIC export fluxes, and the CO_2 outgassing : DIC export ratio of the Brazos River.

We measured concentration and carbon isotopes ($\delta^{13}\text{C}$ and $\Delta^{14}\text{C}$) of DIC as well as pCO_2 to demonstrate that the Brazos River differs from previously studied rivers in that

(1) human activities appear to have overprinted the natural isotope values of DIC in the Brazos River derived from basin lithology, and (2) the Brazos River degasses much less CO₂ to the atmosphere than it delivers DIC to the ocean.

3.2 Study area and methods

3.2.1 Study area

The Brazos River begins at the juncture of the Salt Fork and the Double Mountain Fork, which merge at 33°16'N, 100°0.5'W, about 110 km upstream of Seymour, TX. It then flows 1,344 km across Texas in a southeasterly direction, and drains into the Gulf of Mexico at 28° 52.5' N, 95° 22.5' W, 3 km south of Freeport in Brazoria County, TX (Fig. 3-1a). Of the 116,000 km² Brazos River basin, 107,520 km² are in Texas. The relief of the Brazos River basin is generally low, with a channel gradient of no more than 0.67 m per kilometer (Stricklin 1961). Besides the Salt and Double Mountain forks, the Brazos has five other principal tributaries: the Clear Fork, the Bosques River, the Little River, Yegua Creek and the Navasota River (Fig. 3-1a).

The climate in the middle and lower Brazos varies from temperate to subtropical. During the entire study period (March 2007 to July 2009), mean annual precipitation was 990 mm in Granbury, TX (middle Brazos, 32°26.5'N, 97°47.5'W) and 1,050 mm in Freeport, and mean annual temperature was 16°C in Granbury and 21°C in Freeport (NOAA 2009a). Daily discharge variations were consistent along the Brazos River, with high river discharges in the spring and summer of 2007 and 2008, and spring and fall of 2009 (data from USGS).

The lithology of the Brazos River basin varies along the river (Fig. 3-1a). In the

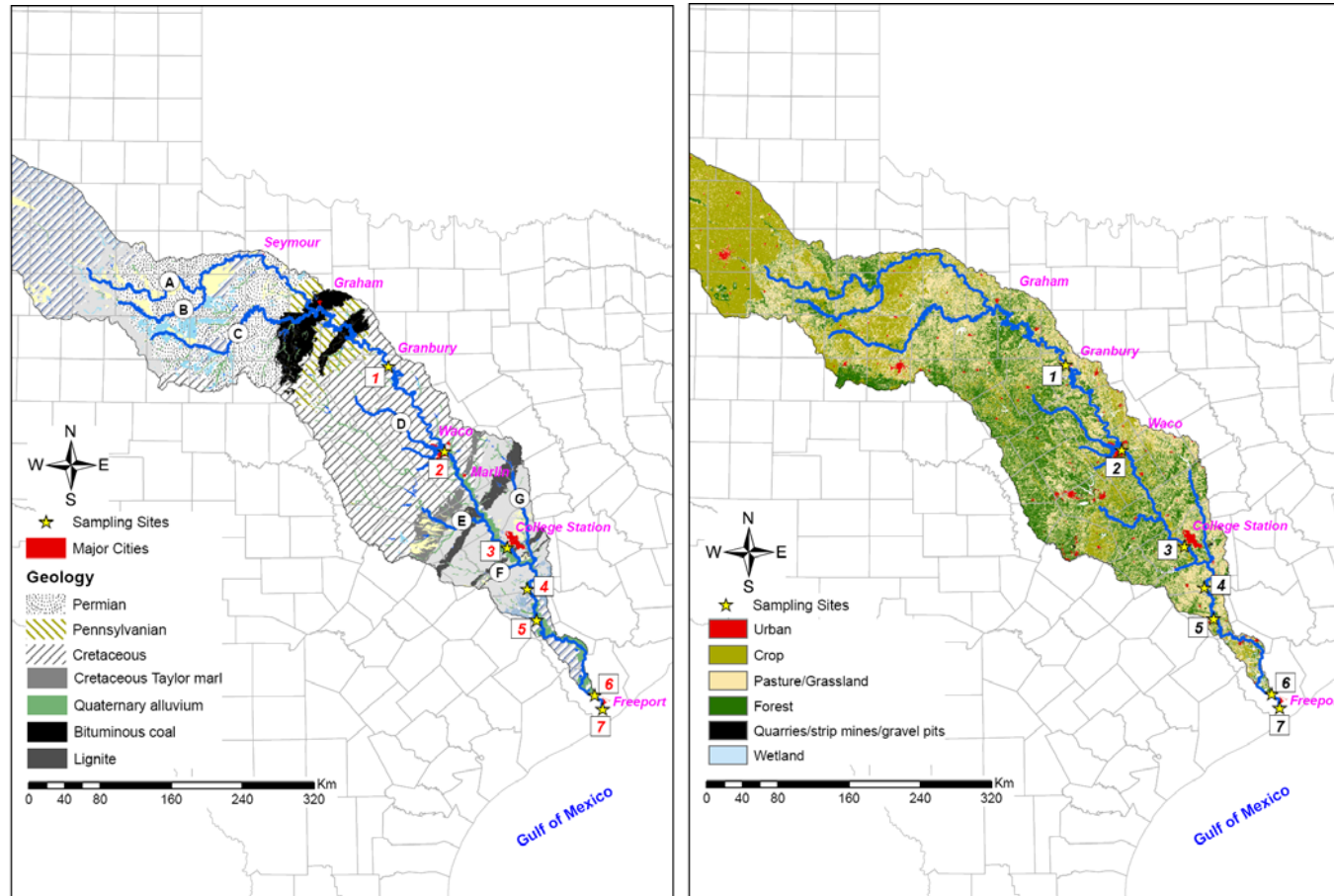


Figure 3-1. (a) Surface geologic map of the Brazos drainage basin made according to digital maps by Stoesser et al (2005) and Tewalt et al (2008). Compositions of strata are: Permian age - red beds, with a large fraction of sand; Pennsylvanian age - red beds and limestone; Cretaceous age - limestone (Stricklin 1961). The seven tributaries of the Brazos (letters in circles) are Salt Fork (A), Double Mountain Fork (B), Clear Fork (C), Bosques River (D), Little River (E), Yegua Creek (F), and Navasota River (G). Cities are labeled in pink. There are 7 sampling sites numbered in the boxes. Sites 1 and 2 are dammed several kilometers downstream. Dams cannot be seen because they are masked by sampling site symbols (yellow stars). (b) Land cover map of the Brazos drainage basin made according to the digital map by National Center for Earth Resources Observation and Science and U.S. Geological Survey (2005).

upper Brazos (upstream from Graham, TX), the bedrock is primarily composed of highly erodible Pennsylvanian (upper Carboniferous, 318-299 Ma BP) and Permian (299-251 Ma BP) red beds, with a large fraction of sand (Stricklin 1961). The middle Brazos (Graham to Waco, TX) is underlain by resistant Pennsylvanian and Cretaceous (145.5-65.5 Ma BP) limestone and red beds (Moore and Plummer 1922; Stricklin 1961). Bituminous coal is present in the Middle-Upper Pennsylvanian Strawn, Canyon, and Cisco groups (Hackley et al. 2009; Moore and Plummer 1922). In the lower Brazos (downstream from Waco), the predominant bedrock is Eocene (56-34 Ma BP), Miocene (23-5.3 Ma BP) and Pleistocene (2.6 Ma to 11.7 Ka BP) sand, silt and clay deposits (Cronin et al. 1963; Stricklin 1961). The channel floor and walls of the lower Brazos are alluvium (green color in Fig. 3-1a) formed in the Pleistocene and Holocene (11.7 Ka BP to present) (Phillips 2007; Stricklin 1961). This alluvium consists of aluminosilicate gravel, sand, clay and silt (Shah et al. 2007). The presence of old carbon in the drainage basin bedrock is very limited in the lower Brazos compared to the middle Brazos (Fig. 3-1a), but includes (1) carbonate existing as Cretaceous Taylor marl (99.6-65.5 Ma BP) about 40 km downstream Waco, TX in a belt 160 km long and 56 km wide parallel to the coast (Cronin et al. 1963); (2) lignite in the Tertiary Wilcox and Jackson groups (Ruppert et al. 2002); (3) pedogenic carbonate in the Beaumont Formation in the coastal region of Texas (Nordt et al. 2006); and (4) oyster shells and crushed carbonate minerals used in road construction in US Gulf coast (Doran 1965; Titi et al. 2003). Although these small sources of old carbon are numerous, they are scattered and account for only a small portion of regional lithology.

The predominant land use in the entire Brazos watershed is agriculture (Phillips 2007)

(Fig. 3-1b). Within the middle and lower Brazos watershed, forests and pasture dominate the northern region from 80 kilometers upstream of Graham to Waco, while grassland and row-crop agriculture dominate downstream of Waco. Both sides of the land adjacent to the lower Brazos from Waco to College Station, TX are dominated by cropland, with little or no riparian borders. As the Brazos flows toward the Gulf of Mexico, it runs through or near several cities (Fig. 3-1b). The total population in the entire Brazos drainage basin is about 3.5 million (Phillips 2007). The Brazos is dammed in several places, and all three major dams are located north of Waco.

We collected samples at seven sites in the main stem of the middle and lower Brazos (Fig. 3-1a). The two sites (1 and 2) in the middle Brazos are located where the Brazos flows through urban areas, Granbury and Waco (Table 3-1). The main stem of the Brazos is dammed several kilometers downstream these sites, forming Lake Granbury in Granbury and a town-lake in Waco. The river is wide and flows slowly at both sites 1 and 2 (Table 3-1). The five sites in the lower Brazos are located in rural areas. From north to south, they are at FM 60 about 10 km southwest of College Station (site 3), at US 290 (site 4), at FM 1458 (site 5), about 20 km upstream from the mouth (site 6), and the mouth (site 7) (Fig. 3-1a and 3-1b; Table 3-1). We sampled sites 1-5 on bridges over the Brazos River and sites 6 and 7 using a boat.

3.2.2 Methods

This study was conducted between March 2007 and July 2009. At each site, we measured surface water temperature and pH in situ using a YSI pH10 pH/Temperature meter. On July 23, 2009, we also measured dissolved oxygen content (DO) of surface

Site number	Site location	Distance from the site to the mouth (km)	Catchment area upstream sites (km ²)	Elevation (m)	City adjacent	City area (km ²)	Population (in 2007)	Distance upstream of the nearest dam (km) (year dam completed)	Width of the river (m)		Annual mean discharge (m ³ /s) (period)
									Upstream of dam	Downstream of dam	
1	In Granbury (32°26.5'N, 97°46'W)	460	65,350	191.9	Granbury	15.9	8,029	12 (1969)	400	80	29.3 (1970-2008)
2	In Waco (31°33.7'N, 97°07.7'W)	344	75,671	106.5	Waco	247.4	122,222	4 (1970)	100	50	62.2 (1971-2008)
3	At FM 60 * (30°33.5'N, 96°25.5'W)	230	99,965	57.7	-	-	-	-		70	149.9 (1994-2008)
4	At US 290 * (30°07.7'N, 96°11.2'W)	160	112,333	32.9	-	-	-	-		100	198.7 (1939-2008)
5	At FM 1458 * (29°48.5'N, 96°05.7'W)	125	113,903	20.7	-	-	-	-		140	206.2 (1939-2008)
6	Near the mouth (29°1.5'N, 95°27.7'W)	20	116,068	14.9	-	-	-	-		120	240.4 (1968-2008)
7	At the mouth (28°52.7'N, 95°22.8'W)	0		0.9	-	-	-	-		200	

Sites in the middle Brazos: sites 1 and 2, in Granbury and Waco, respectively. Sites in the lower Brazos: sites 3-7.

Sites 1-5 were sampled on bridges crossing the Brazos River. Sites 6 and 7 were sampled using a boat.

Discharge, catchment and elevation data were obtained from US Geological Survey. For site 1: average of data from stations 08090800 and 08091000; for site 2: station 08096500; for site 3: station 08108700 (about 15 km upstream of site 3); for site 4: station 08111500; for site 5: average of data from stations 08111500 and 08114000; for sites 6 and 7: station 08116650 (about 30 km upstream of site 6).

*: Numbers are the names of roads or highways.

Table 3-1. Basin and hydrology information for the Brazos River basin.

water in situ at sites 1 and 2 using an HI 9828 multimeter from Hanna Instruments. All the water pCO₂ and DIC samples were taken directly from the middle part of river cross-sections at depths between 10 and 30 cm from bridges using a submersible pump (SHURflo 9325-043-101).

For each site we collected three ambient air pCO₂ and three water pCO₂ samples. We took ambient air CO₂ samples on bridges, and collected river water pCO₂ samples by headspace equilibration as described in Raymond et al. (1997). All pCO₂ samples were transported to the laboratory and analyzed using an infrared CO₂ analyzer (Li-Cor 7000) on the same day they were collected, using a set of 349, 1500, 3000, and 10,100 µatm CO₂ gas standards (Scott Specialty Gases).

We collected DIC samples using 250 ml pre-cleaned (soapy water, deionized water and Milli-Q water) and pre-combusted (500°C for 2 h) bottles. To minimize CO₂ exchange between the sample and the air, we overflowed the bottle from the bottom three times. DIC samples were stored at 0°C from time of collection to poisoning with saturated HgCl₂ solution and sealing with Apiezon-N grease in the lab. All DIC samples were sent to the National Ocean Sciences Accelerator Mass Spectrometry Facility (NOSAMS) for analysis of DIC concentration and isotopic composition ($\Delta^{14}\text{C}$ and $\delta^{13}\text{C}$). There, DIC samples were acidified using 85% H₃PO₄ and then sparged with high-purity N₂ gas (99.99%) (McNichol et al. 1994). The evolved CO₂ was collected cryogenically using liquid nitrogen traps (-190°C) on a vacuum line (McNichol et al. 1994). Small aliquots (10%) of the CO₂ gas were analyzed on an isotope ratio mass spectrometer VG PRISM or VG OPTIMA for $\delta^{13}\text{C}$. Larger aliquots (20%) of the CO₂ gas were reduced to a graphite target, which was finally analyzed by accelerator mass spectrometry (AMS) to

determine $\Delta^{14}\text{C}$ (McNichol et al. 1994).

To explore the possible contribution of old organic carbon from coal weathering to the Brazos River's DIC pools, we analyzed the black carbon content of riverine particulate organic matter (POM) at site 3, which is downstream from most of the lignite deposits (Fig. 3-1a). We made this measurement using cross-polarization and magic angle spinning (CP/MAS) solid-state ^{13}C NMR (nuclear magnetic resonance) and a molecular mixing model. We collected about 120 l of river water, which was stored in a refrigerator overnight to let the particles settle. We then removed the top clear water and used a centrifuge to collect sediment from the bottom water. Finally we dried the sediment using a freeze dryer. We conducted the NMR experiments on Rice University's 200 MHz Bruker Avance spectrometer, equipped with a 4 mm magic angle spinning (MAS) probe. We acquired CP spectra with a 1 ms contact time, at 5 kHz MAS frequency, and 2 s recycle delay. For each experiment, we collected 40,000 acquisitions (scans). We then processed and deconvoluted the NMR spectrum with the parameters and molecular mixing model described by Baldock et al (2004). The molecular mixing model generates an estimate of black carbon content, among other properties.

We applied Student's t -test to examine if there is significant difference in river pCO_2 , DIC concentration, $\delta^{13}\text{C}$ and $\Delta^{14}\text{C}$ of DIC between the middle and lower Brazos. p values equal to or less than 0.05 suggest that the difference is significant, and p values less than 0.01 suggest that the difference is very significant.

3.3 Results

3.3.1 Longitudinal variation in pCO_2 , concentration and isotope values of DIC

Measured concentration of atmospheric CO₂ at all study sites averaged 424 ± 43 μatm (Table 3-2). Riverine pCO₂ values in the Brazos were generally low. Average pCO₂ was 760 ± 243 μatm in the middle Brazos and was $1,174 \pm 418$ μatm in the lower Brazos (Table 3-2, Fig. 3-2a), showing no significant difference ($p = 0.0564$) between the middle and lower Brazos. Riverine pCO₂ values at sites 6 and 7 were about three times the atmospheric pCO₂, slightly lower than those at sites 4 and 5 (4-5 times the atmospheric pCO₂) probably due to mixing of high-pCO₂ river water with low-pCO₂ ocean water in the Gulf of Mexico (Green et al. 2006; Lohrenz and Cai 2006).

The concentration of DIC was consistent along the Brazos ($p = 0.9732$), averaging 2.8 ± 0.4 mM in the middle Brazos and 2.8 ± 0.9 mM in the lower Brazos (Table 3-2, Fig. 3-2b). However, the $\Delta^{14}\text{C}$ ($p < 0.0001$) and $\delta^{13}\text{C}$ ($p = 0.0011$) values of DIC differed significantly between the middle and lower Brazos (Table 3-2, Fig. 3-2c and 3-2d). Average $\Delta^{14}\text{C}$ values of DIC in the middle and lower Brazos were $+85 \pm 77\text{‰}$ and $-151 \pm 52\text{‰}$, respectively, and average $\delta^{13}\text{C}$ values of DIC in the middle and lower Brazos were $-5.2 \pm 1.4\text{‰}$ and $-8.9 \pm 1.6\text{‰}$, respectively (Table 3-2). Temporal variations in these parameters were minor relative to longitudinal variations (Table 3-2). The statistically significant differences in carbon isotope values between the middle and lower Brazos suggest distinctive, regional sources and metabolism patterns of DIC.

3.3.2 Black carbon content of riverine POM at site 3 in the lower Brazos

Black carbon is detected within the NMR peak occurring between 110 and 145 ppm. This peak is small relative to other peaks in the spectrum of riverine POM at site 3 (Fig. 3-3). Because aromatic carbon within lignin is also detected between 110 and 145 ppm, it

Site number	Date sampled	pH	T (°C)	DO (mg L ⁻¹)	pCO _{2,a} (µatm)	pCO _{2,w} ^a (µatm)	DIC ^b (mM)	Δ ¹⁴ C-DIC ^{*c} (‰)	δ ¹³ C-DIC ^{*d} (‰)
<i>The middle Brazos</i>									
1	3/5/2009	8.08	15.6	-	361	439	3.0	+10	-4.2
	7/23/2009	8.55	27.3	3.36	415	966	2.3	-10	-3.5
	Mean ± SD	8.32 ± 0.33	21.5 ± 8.3	-	388 ± 38	703 ± 373	2.6 ± 0.5	0 ± 14	-3.9 ± 0.5
2	1/6/2008	8.65	12.6	-	443	858	3.5	+73	-7.5
	7/3/2008	7.92	27.5	-	447	805	2.8	+162	-5.9
	10/30/2008	7.70	18.7	-	389	483	2.8	+96	-5.7
	7/23/2009	8.69	28.9	5.47	389	1007	2.6	+179	-4.6
	Mean ± SD	8.24 ± 0.50	21.9 ± 7.7	-	417 ± 32	788 ± 221	2.9 ± 0.4	+128 ± 51	-5.9 ± 1.2
1-2	Mean ± SD	8.27 ± 0.42	21.8 ± 7.0	-	407 ± 34	760 ± 243	2.8 ± 0.4	+85 ± 77	-5.2 ± 1.4
<i>The lower Brazos</i>									
3	3/5/2009	8.01	21.1	-	363	435	4.2	-84	-6.8
4	3/25/2007	8.22	22.8	-	456	1351	2.4	-135	-9.4
	6/13/2007	-	-	-	480	1770	4.1	-220	-6.6
	Mean ± SD	8.22	22.8	-	468 ± 17	1561 ± 296	3.3 ± 1.2	-177 ± 60	-8.0 ± 1.9
5	3/25/2007	8.24	22.7	-	468	1451	2.5	-141	-9.2
6	11/28/2007	8.32	16.6	-	451	1120	2.3	-194	-9.9
	11/19/2008	7.83	17.4	-	379	1029	2.0	-192	-10.6
	Mean ± SD	8.08 ± 0.35	17.0 ± 0.60	-	415 ± 51	1075 ± 64	2.2 ± 0.3	-193 ± 1.5	-10.3 ± 0.6
7	11/28/2007	7.94	15.8	-	466	1060	2.2	-94	-9.9
3-7	Mean ± SD	8.09 ± 0.19	19.4 ± 3.2	-	438 ± 47	1174 ± 418	2.8 ± 0.9	-151 ± 52	-8.9 ± 1.6

Sites 3, 5, and 7 were measured only once during the study period. We applied Student's *t*-test to examine if there is significant difference between the middle Brazos (sites 1 and 2) and the lower Brazos (sites 3-7) in the parameters.

* means that the difference is significant.

^a *p*=0.0564, ^b *p*=0.9732, ^c *p*<0.0001, ^d *p*=0.0011.

Table 3-2. Measured parameters for all sampling sites in the Brazos River.

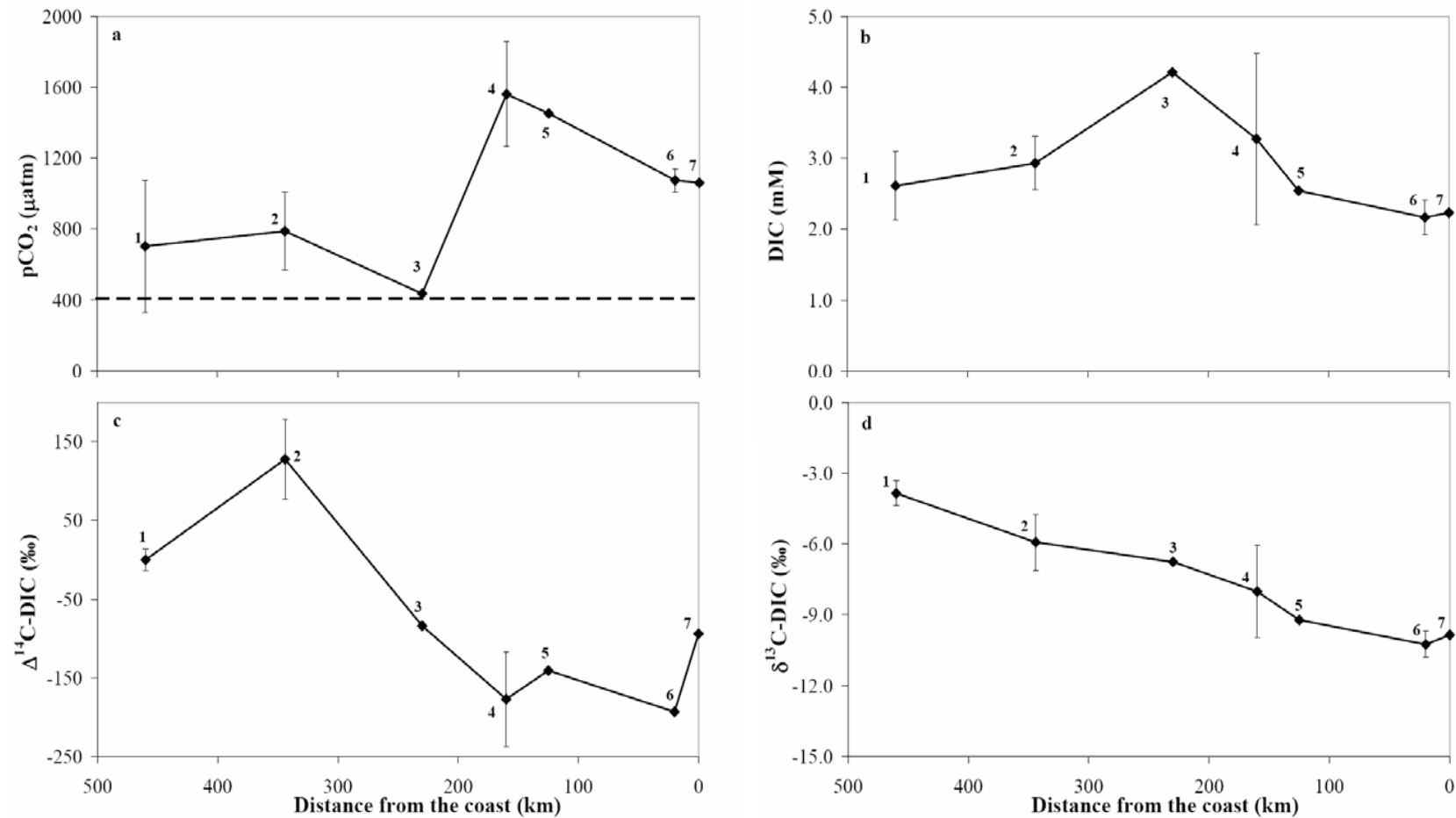


Figure 3-2. Longitudinal variations in river water pCO₂ (a), DIC concentration (b), Δ¹⁴C of DIC (c) and δ¹³C of DIC (d) in the middle and lower Brazos. Dash line in (a) is the measured mean pCO₂ value of the atmosphere (428 μatm) at the study sites. Numbers on the figures are study site numbers (Table 3-1). Vertical bars represent the standard deviation of all the data for the site.

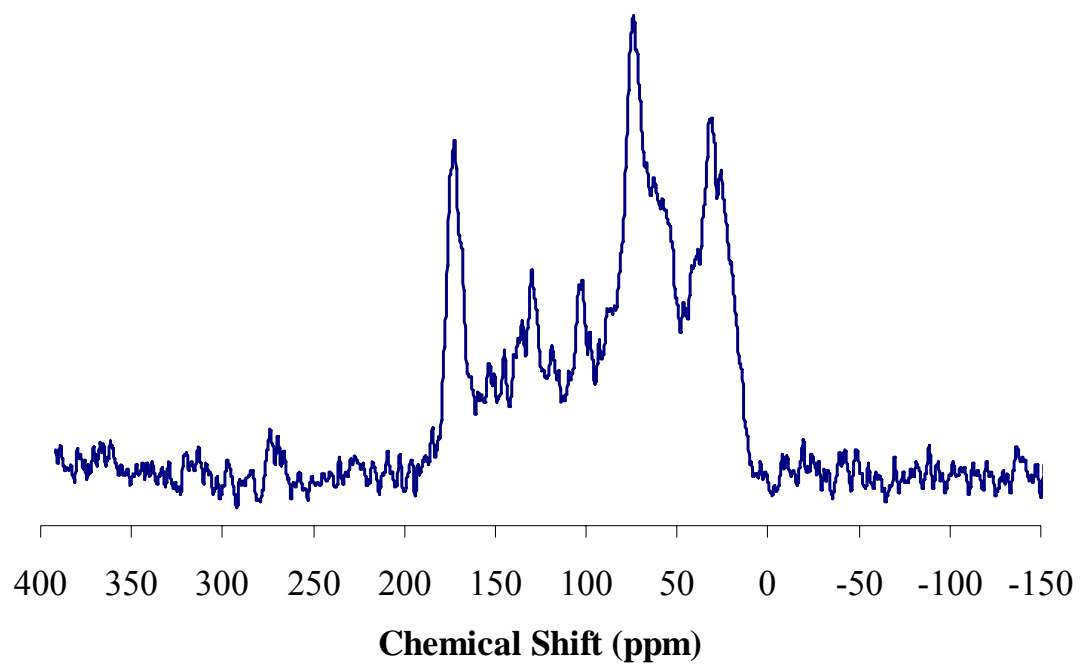


Figure 3-3. CP/MAS ^{13}C NMR spectrum of riverine POM at site 3 in the lower Brazos.

is necessary to use a molecular mixing model to determine the black carbon concentration. Using the molecular mixing model of Baldock et al (2004), we calculated black carbon to be 3.8% of the riverine POM. Since NMR-measured black carbon identifies both coal-derived black carbon and soil-derived charcoal black carbon as one pool, our final measurement of 3.8% is an upper estimate for coal input to river POM, allowing us to conclude that lignite contributed to no more than 3.8% of POM in the Brazos.

3.4 Discussion

3.4.1 Isotope values of potential DIC sources in the Brazos River basin

We investigated the origins of riverine DIC using a plot of $\delta^{13}\text{C}$ versus $\Delta^{14}\text{C}$ for our samples and potential DIC sources (Raymond et al. 2004; Zeng and Masiello 2010) which include atmospheric CO_2 invasion, OM respiration (young and old), and dissolution of carbonate (Fig. 3-4). There are three potential sources of carbonate in the Brazos watershed: (1) natural carbonate rocks (Pennsylvanian and Cretaceous limestone in the middle Brazos and Cretaceous Taylor marl in the lower Brazos), (2) natural pedogenic carbonate in the lower Brazos, and (3) anthropogenic carbonate minerals (oyster shells and crushed limestone used in road construction) in the lower Brazos. Each potential DIC source has a characteristic range of carbon isotope ratios (Fig. 3-4), which we outline below.

Atmospheric CO_2 invasion is one potential source of DIC. The $\Delta^{14}\text{C}$ values of atmospheric CO_2 were +55 to +66‰ in 2004 (Hsueh et al. 2007), and have been dropping at a rate of 6‰ per year (Trumbore et al. 2006), implying that for 2007-2008 DIC from

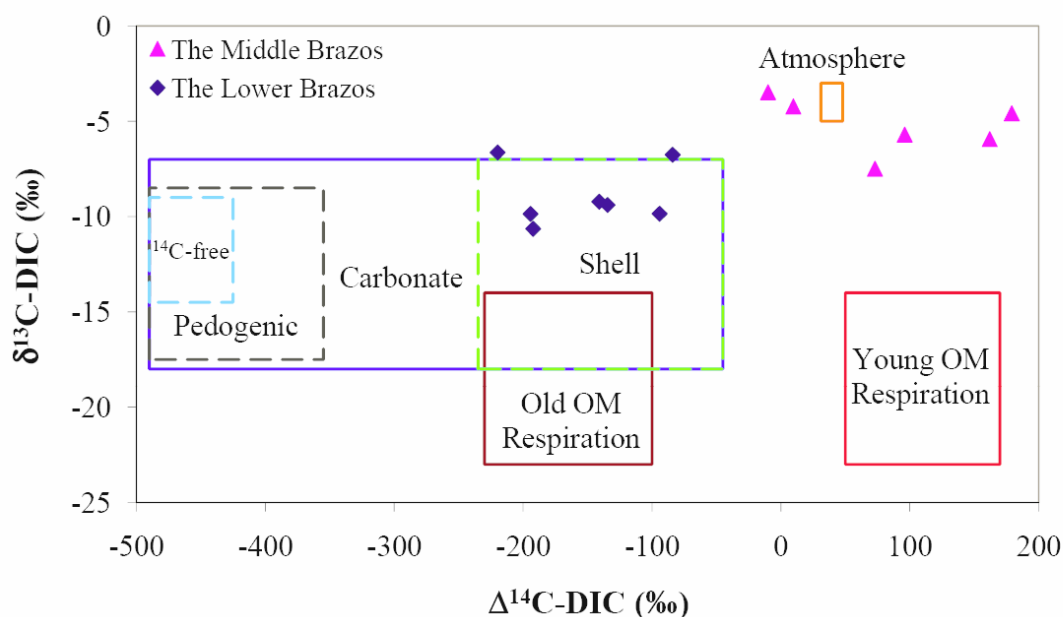


Figure 3-4. $\delta^{13}\text{C}$ versus $\Delta^{14}\text{C}$ of riverine DIC in the middle (pink triangles) and lower (blue diamonds) Brazos. Also plotted are $\delta^{13}\text{C}$ versus $\Delta^{14}\text{C}$ of potential DIC sources (in solid boxes): atmospheric CO_2 (orange), young OM respiration (red), old OM respiration (brown) and carbonate dissolution (blue). There are four possible sources of carbonate in the study watershed (in dashed boxes): natural sedimentary carbonate minerals and crushed carbonate minerals (blue), natural pedogenic carbonate (black), and oyster shells (green). Carbon isotope values of each source are discussed in detail in the text.

atmospheric CO₂ invasion had $\Delta^{14}\text{C}$ values of +31 to +48‰ and $\delta^{13}\text{C}$ values of -5 to -3‰ (Raymond et al. 2004).

A second potential source of DIC is CO₂ derived from respiration of terrestrial OM. $\delta^{13}\text{C}$ values of DIC from terrestrial OM respiration are typically in the range -23 to -14‰, after correction for fractionation (Barth et al. 2003; Mook et al. 1974; Raymond et al. 2004; Zhang et al. 1995), and $\Delta^{14}\text{C}$ values of DIC from OM respiration are +50 to +170‰ for young OM and -230 to -100‰ for old OM (Raymond et al. 2004). A recent study (Griffith et al. 2009) found that OM in municipal wastewater treatment plant effluent had a mean radiocarbon age of about $1,600 \pm 500$ years ($\Delta^{14}\text{C} = -180 \pm 50$ ‰). Thus, DIC from the respiration of municipal waste falls within old OM respiration in Fig. 3-4.

The final DIC source is carbonate dissolution. Isotope values of DIC produced by carbonate dissolution vary depending both on the source of carbonate and on the dissolving acid. Soil CO₂ is generally the dominant source of acidity that dissolves carbonate in river systems (Garrels and Mackenzie 1971; Karim and Veizer 2000). Dissolution of different types of carbonate by soil CO₂ produces DIC with isotope values intermediate between the carbonate and soil CO₂, which for soil CO₂ are $\Delta^{14}\text{C} = +20$ to +150‰ and $\delta^{13}\text{C} = -29$ to -18‰ (Raymond et al. 2004; Trumbore 2000; Trumbore et al. 2006). The dissolution of carbonate rocks and crushed limestone ($\Delta^{14}\text{C} = -1000$ ‰, $\delta^{13}\text{C} = \sim 0$ ‰) by soil CO₂ produces DIC with $\Delta^{14}\text{C}$ values of -490 to -425‰ and $\delta^{13}\text{C}$ values of -14.5 to -9‰. Pedogenic carbonate in Texas has $\Delta^{14}\text{C}$ values of -1000 to -860‰, and $\delta^{13}\text{C}$ values of -6 to +1‰ (Nordt et al. 1998; Rightmire 1967; Valastro et al. 1968). Therefore, the DIC sourced from pedogenic carbonate and soil CO₂ has $\Delta^{14}\text{C}$ values of -490 to

-355‰ and $\delta^{13}\text{C}$ values of -17.5 to -8.5‰. The $\Delta^{14}\text{C}$ and $\delta^{13}\text{C}$ values of shell carbonates have been measured in many studies (Douglas and Staines-Urias 2007; Gentry et al. 2008; Keller et al. 2002; McConnaughey and Gillikin 2008; Wisshak et al. 2009). Combining data from all these studies, we estimate shell carbonate $\Delta^{14}\text{C} = -489$ to -240 ‰ and $\delta^{13}\text{C} = -7$ to $+4$ ‰. The dissolution of shell carbonate by soil CO_2 generates DIC with $\Delta^{14}\text{C}$ values of -235 to -45 ‰ and $\delta^{13}\text{C}$ values of -18 to -7 ‰.

The broad ranges of isotopic values for every potential DIC source precluded identifying the amount of DIC derived from each source. For example, carbonate $\Delta^{14}\text{C}$ values could range from -490 ‰ to -45 ‰; respirable OM $\Delta^{14}\text{C}$ values could range from -230 ‰ to $+170$ ‰, and atmospheric CO_2 $\Delta^{14}\text{C}$ values could range from $+31$ to $+48$ ‰. There are also large ranges of values for the $\delta^{13}\text{C}$ of each source. The range of $\Delta^{14}\text{C}$ values for carbonates alone, holding all other potential contributors' $\Delta^{14}\text{C}$ and $\delta^{13}\text{C}$ values constant, is enough to cause the potential carbonate contribution to vary between 32 and 94% of DIC in the lower Brazos. Isotopic data do allow us to say conclusively what the major sources of DIC are likely to be, but we cannot assign specific fractions to each source.

Assuming that basin lithology is the dominant control on the source and cycling of riverine DIC in the Brazos River as in other river systems (Helie et al. 2002; Kanduc et al. 2007b; Raymond et al. 2004), we expected to see a clear longitudinal trend in carbon isotope values of riverine DIC. In the middle Brazos, DIC should be highly depleted in ^{14}C relative to the atmosphere resulting from dissolution of large areas of carbonate bedrock and perhaps respiration of ancient OM from bituminous coal erosion. In the lower Brazos, due to the limited sources of old carbon, we expected DIC with a higher

$\Delta^{14}\text{C}$ value compared to DIC in the middle Brazos. Our observation that DIC in the middle Brazos was generally enriched in ^{14}C relative to the lower Brazos was opposite to predictions based upon lithology. This suggests a dominant influence of human activities on carbon cycling in the Brazos River.

3.4.2 Major controls on riverine DIC in the middle Brazos: damming and urbanization

The $\Delta^{14}\text{C}$ values of DIC in the middle Brazos ($+85 \pm 77\text{‰}$) suggest that the Pennsylvanian and Cretaceous limestone and bituminous coal contribute little or no carbon to riverine DIC (Fig. 3-4), although they outcrop in large areas in the middle Brazos. The relatively low $\Delta^{14}\text{C}$ -DIC values at site 1 ($+10\text{‰}$ and -10‰) could be due to a very minor input of these ancient carbonate rocks. They could also be due to decomposition of old OM from treated urban wastewater. However, either case suggests that carbonate dissolution is not the predominant source of DIC at site 1. The average $\Delta^{14}\text{C}$ -DIC value of $+128 \pm 51\text{‰}$ at site 2 rules out a carbonate input, and instead likely reflects an 8- to 50-year residence time of carbon in drainage basin ecosystems (Burchuladze et al. 1989; Hsueh et al. 2007; Trumbore et al. 2006).

The concurrently high $\Delta^{14}\text{C}$ -DIC and $\delta^{13}\text{C}$ -DIC values and low pCO_2 values in the middle Brazos are likely due to damming and urbanization of the Brazos River in Granbury and Waco. The low pCO_2 values that we observed in the middle Brazos were consistent with observations in dammed, urbanized Chinese rivers. In China, river damming activities and increasing eutrophy driven by urban growth have reduced dissolved CO_2 concentrations in the Changjiang River, the largest river in China (Wang et al. 2007). Iwata et al (2007) also observed that streams draining more urbanized

watersheds were less heterotrophic (meaning with lower dissolved CO₂ concentrations) than streams in intensively farmed watersheds. Damming and urbanization control the geochemistry of river water by: (1) enhancing exchange between riverine DIC and atmospheric CO₂, (2) leading to respiration of relatively young OM in river sediments above the dams, and (3) stimulating surface algal production. The influence of each mechanism is discussed below.

3.4.2.1 Enhanced air-water CO₂ exchange

Damming of rivers creates reservoirs that have large surface areas and relatively long hydraulic residence times, both of which enhance exchange of gas between river water and the atmosphere. At sites 1 and 2 the river is 2-5 times its original width (Table 3-1). Extensive air-water exchange reduces the concentration gradient of dissolved gases between river water and the atmosphere, and draws riverine pCO₂ values closer to that of the atmospheric CO₂ (for sites 1 and 2, average water pCO₂ = 760 ± 243 µatm, average ambient air pCO₂ = 407 ± 34 µatm).

Extensive air-water exchange also resulted in relatively high $\Delta^{14}\text{C}$ and $\delta^{13}\text{C}$ values of riverine DIC. Atmospheric CO₂ has $\Delta^{14}\text{C}$ values of +31 to +48‰ in 2007-2008 (Hsueh et al. 2007; Trumbore et al. 2006) and a $\delta^{13}\text{C}$ value of -8‰ (Levin et al. 1987). The invasion of atmospheric CO₂, therefore, shifted both $\Delta^{14}\text{C}$ and $\delta^{13}\text{C}$ values of riverine DIC to heavier values. Since dissolved CO₂ is more ¹³C-depleted relative to other DIC components (i.e. HCO₃⁻ and CO₃²⁻) (Alin et al. 2008; Mook et al. 1974), removal of dissolved CO₂ through outgassing could increase $\delta^{13}\text{C}$ values of DIC in the water. Our pCO₂ and DIC isotope data in the middle Brazos are consistent with the results of

previous studies (Brunet et al. 2005; Finlay 2003; Zhang et al. 2009), in which high $\delta^{13}\text{C}$ values of DIC (up to -1.8‰) and lower concentrations of dissolved CO_2 were attributed to efficient air-water exchange in large rivers and impoundment due to dam construction.

3.4.2.2 Respiration of young OM

The $\Delta^{14}\text{C}$ -DIC values of $+73$ to $+179\text{‰}$ at site 2 can only be explained by decomposition of relatively young OM, because neither atmospheric CO_2 invasion nor carbonate dissolution could produce DIC with values this high (Fig. 3-4). Northern hemisphere atmospheric ^{14}C values spiked at $\sim 900\text{‰}$ between 1962 and 1963, at the peak of atmospheric nuclear weapons testing (Burchuladze et al. 1989). Since the late 1960s, the bomb spike has mixed into the oceans and terrestrial biosphere, leading to a drop in the atmosphere's ^{14}C value (Burchuladze et al. 1989). Because of the spiked shape of the atmosphere's ^{14}C value since 1950, environmental ^{14}C values $>0\text{‰}$ do not correspond to unique carbon residence times. Instead, each ^{14}C value corresponds to two possible carbon residence times, one on each side of the bomb spike. The $\Delta^{14}\text{C}$ -DIC values (approx. $+170\text{‰}$) in July 2008 and July 2009 suggest that the OM decomposed was either ~ 20 or ~ 50 years old (Burchuladze et al. 1989), while the $\Delta^{14}\text{C}$ -DIC values (approx. $+85\text{‰}$) in January and October of 2008 correspond to OM 8-10 or ~ 50 years old (Hsueh et al. 2007; Trumbore et al. 2006). The longer ^{14}C -derived residence times in this ecosystem are unlikely, given the region's high temperature and precipitation. The Amazon, draining a similarly warm, wet climate, has a carbon residence time of ~ 5 years (Mayorga et al. 2005), making the 8-10 and 20 year residence time interpretations of our ^{14}C data most likely.

If the +170‰ $\Delta^{14}\text{C}$ value reflects about a 20 year residence time, and the +85‰ $\Delta^{14}\text{C}$ value reflects an 8-10 year residence time at our site 2 (Waco), then the Brazos respire older OM in the summer and younger OM in the winter. Respiration of older OM in summer may be a result of more intensive heterotrophic microbial activity or a shift in microbial community stimulated by warmer water (Table 3-2) (Boer et al. 2009). Alternatively, crops are typically harvested and replanted in May and June in this part of the US. Increased soil mobility after crop harvest in summer could have led to loss of old soil organic matter (SOM) to the river.

The respiration of OM at site 2 may involve methanogenesis, which can highly enrich ^{13}C in the DIC pool. It has been reported that OM in bottom sediments of lakes can be respired by anaerobic bacteria via methanogenesis, producing highly ^{13}C -depleted methane (CH_4) and ^{13}C -enriched CO_2 relative to the OM source (Gu et al. 2004; Stiller and Magaritz 1974; Stiller et al. 1985; Wachniew and Rozanski 1997). Lake Apopka in central Florida (about 7.5 mg L^{-1}) (Gu et al. 2004) has $\delta^{13}\text{C}$ -DIC values as high as +6 to +8‰ due to methanogenesis of sedimentary OM. Compared to the DO content of Lake Apopka, measured DO contents in the surface water at sites 1 and 2 (averaging $4.4 \pm 1.5 \text{ mg L}^{-1}$, Table 3-2) were lower, suggesting that methanogenesis of OM may have occurred and provided ^{13}C -heavy CO_2 to the water column. However, without CH_4 measurements in the water column, this hypothesis cannot be confirmed.

3.4.2.3 Algal growth

CO_2 uptake by algae can also lead to ^{13}C enrichment of DIC. In algal photosynthesis, dissolved CO_2 is preferentially used because of lower energetic costs of dissolved CO_2

acquisition relative to HCO_3^- (Burkhardt et al. 2001; Rotatore et al. 1995). Like removal of dissolved CO_2 through outgassing, CO_2 uptake by algal photosynthesis causes a reduction of dissolved CO_2 concentrations, and increases $\delta^{13}\text{C}$ -DIC values. For example, in a study conducted in the Dead Sea (Oren et al. 1995), $\delta^{13}\text{C}$ -DIC values as high as +5.1‰ were driven by a *Dunaliella* bloom, while $\delta^{13}\text{C}$ -DIC values were 8.5‰ lighter before the bloom.

Chlorophyll *a* concentration in Lake Granbury (site 1) can reach $90\ \mu\text{g l}^{-1}$ in March (Roelke et al. 2007), comparable to levels published for a eutrophic lake in central Florida ($96\ \mu\text{g l}^{-1}$) (Gu et al. 2004), suggesting intensive algal photosynthetic activity in Lake Granbury. The growth of algae is favored by nutrient enrichment. Total phosphorus was about $50\ \mu\text{g l}^{-1}$ in Lake Granbury (BRA 2009), within the range of mesotrophic conditions (moderately nutrient enriched, total phosphorus ranging from 25 to $75\ \mu\text{g l}^{-1}$) (EPA 2001). Most of the lake nutrients are from wastewater treatment plants and on-site sewage facilities near the Granbury site (Riebschleager and Karthikeyan 2008).

The river water passing through Waco is partially from Lake Waco, a reservoir constructed in the Bosque River (Fig. 3-1a) about ten river kilometers before the Bosque River merges with the Brazos River at a point only three river kilometers upstream of our sampling site in Waco. Lake Waco has been classified to be mesotrophic or eutrophic in different time periods primarily due to the input of nutrients from dairy waste and forage fields in the Lake Waco-Bosque River watershed (McFarland et al. 2001; McFarland and Hauck 2001). Enhanced algal growth in Lake Waco is confirmed by increased chlorophyll *a* concentration (Jones 2009; McFarland et al. 2001).

3.4.3 Natural and anthropogenic carbonate input to the lower Brazos

DIC in the lower Brazos was strongly influenced by old carbon (Fig. 3-4), although ancient carbon sources, carbonate and lignite outcrops, are very limited in the lower Brazos. The black carbon content from NMR analysis was 3.8% of the riverine POM at site 3, of which a fraction is from the Vertisol soils drained in this region. These soils have been shown to be rich in charcoal (Skjemstad et al. 2002), leading us to conclude that lignite is much less than 3.8% of the riverine POM. Longworth et al (2007) observed young dissolved organic matter (DOM) in watersheds draining OM-rich shale, suggesting little or no contribution of shale organic carbon to riverine DOM. Assuming that contributions of lignite black carbon to the DOM pool are also negligible in the lower Brazos River, we conclude that lignite decomposition has a trivial impact on ^{14}C content of riverine DIC. Soil erosion due to agricultural practices in the lower Brazos could have caused loss of old SOM to the river as described in other studies (Krusche et al. 2002; Longworth et al. 2007; Raymond et al. 2004) and decomposition of this old OM may be a source of old riverine DIC. However, this process is less important compared to carbonate dissolution in driving the carbon isotope values of DIC, as indicated by the relatively high $\delta^{13}\text{C}$ values of DIC (Fig. 3-4).

Possible carbonate sources in the lower Brazos include naturally occurring Cretaceous Taylor marl and pedogenic carbonate, and oyster shells and crushed carbonate minerals used in road construction (Doran 1965; Titi et al. 2003; Zeng and Masiello 2010). Taylor marl consists of highly calcareous clay or clay marl, which is a loose mixture of clay (65-35%) and calcium carbonate (35-65%) (Matson and Hopkins 1917). This soft bedrock material is susceptible to erosion and could have added to the riverine

DIC pool.

Pedogenic carbonate present in the Vertisols of the Beaumont Formation in coastal Texas is another source of carbonate (Nordt et al. 2006). Pedogenic carbonate is generally formed in arid and semi-arid areas. However, Vertisols in the Beaumont Formation of the east Texas Gulf coast preserve pedogenic carbonate despite the high rainfall (>1,000 mm per year), due to their high clay content and shrink-swell properties (Nordt et al. 2006).

Oyster shells and crushed carbonate minerals are a significant regional anthropogenic source of soil carbonate. Oyster shells were widely used in the US Gulf coast as aggregate for the construction of roads and parking lots through the mid-20th century (Doran 1965). In the 1960s, shell roads could be found in a belt about 100 km wide along the Texas coast (Doran 1965), and their remnants are ubiquitous in coastal Texas urban environments. Crushed limestone has also been used in Gulf coast roads (Titi et al. 2003). In Buffalo Bayou, one of the rivers draining Houston about 50 km east of the lower Brazos, dissolution of shell and crushed limestone/dolomite imbedded in old city roads has contributed to the river's old DIC ($\Delta^{14}\text{C} = -117 \pm 45\%$) (Zeng and Masiello 2010). Our isotope data show that shells and crushed carbonate minerals are also likely an important source of DIC in the lower Brazos, as illustrated by Fig. 3-4.

3.4.4 Comparison of Brazos $p\text{CO}_2$ and DIC with other rivers

3.4.4.1 Riverine $p\text{CO}_2$

Measured $p\text{CO}_2$ values in the middle and lower Brazos ranged from 435 μatm to 1,770 μatm , with an average (\pm SD) of 983 ± 397 μatm during the study period (March 2007 to July 2009). Compared to other subtropical rivers, $p\text{CO}_2$ values in the Brazos were

much lower than those of the Xijiang River in southeast China (about 2,600 μatm , Yao et al. 2007), the Satilla and Altamaha rivers in the coastal region of Georgia (4,000-8,500 μatm , Cai and Wang 1998), and Buffalo Bayou and Spring Creek in Harris County, TX (3,000-4,200 μatm , Zeng and Masiello 2010).

The low pCO_2 values in the Brazos River are probably due to the combined effects of lower precipitation, an important control on river pCO_2 (Yao et al. 2007; Zeng and Masiello 2010), larger river size, and damming and urbanization as discussed above. The annual mean temperature in the middle and lower Brazos was 16.5-21.3 °C for the study period, similar to that in the Xijiang River (14-22 °C, Yao et al. 2007) and that in the Satilla and Altamaha river basins in 1995 (about 21 °C, NOAA). However, annual mean precipitation in the study area for the study period, 898-1,050 mm, is much lower than that in the Xijiang River basin (1,451 mm, China Meteorological Data Sharing Service System), the Satilla and Altamaha river basins (1,580 mm in 1995, NOAA), and the Buffalo Bayou and Spring Creek watersheds (1,220 to 1,350 mm, NOAA). Also, large rivers in general are less supersaturated in CO_2 compared to smaller streams under similar climate conditions (Finlay 2003).

3.4.4.2 Riverine DIC concentration

The DIC concentration in the Brazos River, 2.8 ± 0.7 mM, far exceeded the average value of world rivers (0.9 mM, Livingstone 1963). It is an order of magnitude higher than some northeast US rivers (Raymond et al. 2004), and higher than those in some rivers in the Coast Range of northern California (Finlay 2003).

High DIC concentrations have also been observed in the St. Lawrence River (0.5-5

mM, Helie et al. 2002), the Sava River (2.9 ± 1.0 mM, Kanduc et al. 2007a), three major US rivers (Ohio, upper Mississippi, and Missouri, 1-5 mM, Raymond and Oh 2007), and Buffalo Bayou (2.4 ± 1.0 mM) (Zeng and Masiello 2010). Most of these high DIC concentrations are associated with carbonate input to the river systems, and sources of carbonate include bedrock, oyster shells and crushed limestone used in road construction and as agricultural soil amendments. Dissolution of limestone and dolomite accounts for up to 26% of DIC in the Sava River (Kanduc et al. 2007a), and agricultural liming contributed 17% of DIC in the Ohio River (Oh and Raymond 2006). Similarly, $\Delta^{14}\text{C}$ and $\delta^{13}\text{C}$ values of DIC in the lower Brazos suggest that although lithologic sources of carbonate are minor, anthropogenic and possibly pedogenic carbonates are a significant source of DIC.

For the middle Brazos, the high DIC concentration was not due to dissolution of carbonate bedrock, but instead due to urbanization. It has been observed that wastewater treatment plant effluent contributes up to 22% of the total DIC in the Hockanum River, Connecticut (Barnes and Raymond 2009). Weathering of bedrock material exposed to the surface due to urban soil disturbance, and dissolution of urban concrete are two other mechanisms for the high DIC concentration in urbanized watersheds (Baker et al. 2008).

3.4.4.3 CO₂ outgassing and DIC export from the Brazos

We used pCO₂, DIC concentration and river discharge data (obtained from the USGS) to calculate the fluxes of CO₂ outgassing and DIC export from the Brazos in a preliminary attempt to estimate the Brazos River basin as a C source to the atmosphere and the ocean.

CO₂ outgassing is calculated using the following equation (modified from Raymond et al. 1997):

$$Outgas = k_{CO_2} \times (pCO_{2,w} \times K_h - pCO_{2,a} \times K_h) \times A$$

Where K_h is Henry's law constant at a given temperature and salinity; $pCO_{2,w}$ and $pCO_{2,a}$ are the partial pressure of CO₂ in surface water and the overlying air, respectively; k_{CO_2} is the gas exchange coefficient for CO₂ at a given temperature for a given type of river; and A is the area of water surface.

Measured mean $pCO_{2,w}$ and $pCO_{2,a}$ values for the Brazos were 983 μ atm and 424 μ atm, respectively. The average temperature was 20.6°C, so K_h was 0.0383 mol l⁻¹ atm⁻¹ (Stumm and Morgan 1996). We chose a commonly used range of k_{CO_2} values, 2.5-5 cm h⁻¹ (Raymond et al. 1997; Richey et al. 2002; Zeng and Masiello 2010), in our calculation. Using a water surface area (A) of 565.79 km² for the Brazos River (including the river itself and the three main reservoirs along the main stem river channel, BRA 2010b), we calculated CO₂ outgassing rate from the Brazos River to be 0.03 to 0.06 Tg C year⁻¹.

DIC export from the Brazos River to the Gulf of Mexico is the product of average DIC concentration and average river discharge at the river mouth. Average DIC concentration at the Brazos mouth was 2.8 ± 0.7 mM. River discharge data were obtained from a US Geological Survey station (08116650) located about 50 km upstream of the river mouth. Annual mean river discharge for 2007-2008 at this station was 349 m³ s⁻¹. Our estimated rate of river DIC export to the Gulf of Mexico is 0.37 ± 0.09 Tg C year⁻¹. Since the discharge at the river mouth should be higher than at the 50 km upstream USGS

station, the estimated DIC export here is a conservative value.

The CO₂ outgassing : DIC export ratio of the Brazos River is, therefore, about 0.1:1. This value is not only lower than those of tropical rivers, but also lower than that of northern rivers such as the Ottawa River (Brunet et al. 2009; Richey et al. 2002; Telmer and Veizer 1999). The low CO₂ outgassing : DIC export ratio implies that of the total DIC in the Brazos River, about 90% is exported to Gulf of Mexico, while only about 10% is released to the atmosphere. It is possible that this very low CO₂ outgassing : DIC export ratio is also a result of human activities, with pCO₂ driven down by damming and urban treated wastewater input and DIC driven up by carbonate dissolution.

3.5 Conclusions

Our results show that human activities (i.e. damming and urbanization) dominate geology as a control on the origin and cycling of DIC in the Brazos River. Although limestone bedrock underlies a large area of the middle Brazos River watershed, this limestone does not influence riverine DIC, as shown by the radiocarbon values ($+85 \pm 77\text{‰}$) of riverine DIC in the middle Brazos. Neither does the coal-bearing bedrock present in the watershed. $\Delta^{14}\text{C}$ ($+85 \pm 77\text{‰}$) and $\delta^{13}\text{C}$ ($-5.2 \pm 1.4\text{‰}$) values of DIC in the middle Brazos are likely due to extensive air-water CO₂ exchange, respiration of decades old OM in river sediments, and algal growth, all of which are driven by a combination of damming and wastewater input from urban areas. In contrast, $\Delta^{14}\text{C}$ ($-151 \pm 52\text{‰}$) and $\delta^{13}\text{C}$ ($-8.9 \pm 1.6\text{‰}$) values of DIC in the lower Brazos suggest input of carbonate-sourced DIC to the lower Brazos, despite the absence of carbonate bedrock in the lower Brazos watershed. Oyster shells and crushed limestone used as aggregate in road construction in

the Gulf coast areas are two likely sources of carbonate, in addition to naturally occurring marl and pedogenic carbonate in the lower Brazos.

The $p\text{CO}_2$ values in the Brazos River were generally lower than other subtropical rivers, while the DIC concentration in the Brazos River is relatively high compared to many other rivers. As a result, the amount of DIC the Brazos River releases to the atmosphere as CO_2 gas is much smaller than the amount of DIC it delivers to the ocean.

3.6 Acknowledgements

CAM and FWZ acknowledge the support of the Texas Water Resources Institute, the U.S. Geological Survey, and the National Institutes for Water Research. CAM and FWZ also acknowledge the generous support of Hans O. and Suse Jahns. FWZ is grateful to T.J. Perez, S.R. Alin and D. Lockwood for their assistance with instrument setup and sampling procedures, and John B. Anderson, Fred M. Weaver, Xinfeng Shi, LaQuanti Calligan, Kaijian Liu, Krystle Hodge, Yongbo Zhai, and Morgan Gallagher for their assistance in sample collection.

CHAPTER 4

Land use effects on the isotopic and chemical composition of particulate organic carbon in the Brazos River, Texas revealed by carbon isotope and NMR measurements

Abstract

Characterization of riverine organic carbon (OC), which is primarily from terrestrial ecosystems, is important to understand the fate of terrestrial organic matter (OM) in rivers and the ocean. In this study, we combined carbon (C) isotope (^{13}C and ^{14}C) and solid-state ^{13}C NMR measurements to constrain the sources and chemical composition of bulk particulate organic carbon (total POC) and the operationally defined high-density fraction of particulate organic carbon (sinking POC) in the lower and middle Brazos River in Texas, USA. Our results suggest that, in the middle Brazos, land use is the major control on the sources and chemical composition of riverine POC; while in the lower Brazos, lithology and climate are two additional controls. In the middle Brazos, total POC ($\Delta^{14}\text{C} = +10 \pm 69\text{‰}$, $\delta^{13}\text{C} = -31.6 \pm 2.3\text{‰}$) was a mixture of old and young C. The majority the old C was likely from wastewater treatment plant (WWTP) effluent, while the young C was from phytoplankton and shallow soil OC. Phytoplankton comprised more of sinking POC ($\Delta^{14}\text{C} = +22 \pm 36\text{‰}$, $\delta^{13}\text{C} = -27.0 \pm 0.7\text{‰}$) than total POC. In the lower Brazos, old OM from erosion of deep soil (including modern soils and paleosols) was the major source of total POC ($\Delta^{14}\text{C} = -355 \pm 155\text{‰}$, $\delta^{13}\text{C} = -29.1 \pm 2.6\text{‰}$). High soil erosion rates were caused by the soft river banks and bed, agricultural land use, and high precipitation. Young C4 plant-derived soil OM comprised more of sinking POC ($\Delta^{14}\text{C} = -82 \pm 18\text{‰}$, $\delta^{13}\text{C} = -23.8 \pm$

5.7‰) than total POC. Finally, we estimated the fluxes of POC, charcoal, and lignin from the Brazos River to the Gulf of Mexico. Examination of our dataset and existing data showed a weak correlation between the flux of POC, charcoal, or lignin and water or sediment discharge, suggesting the need to make measurements in different river systems to achieve a precise estimate of global river POC, charcoal and lignin fluxes.

4.1 Introduction

Rivers play an important role in the global carbon (C) cycle in that they continuously transport C from land to the ocean and the atmosphere. Conservative estimates by Cole et al. (2007) show that at least 0.9 Gt of terrestrial C, inorganic and organic, is delivered by rivers to the oceans annually, and the efflux of C-bearing gases (e.g. CO₂ and CH₄) from rivers to the atmosphere occurs at a rate of 0.75 Gt C yr⁻¹. These C fluxes are comparable to terrestrial net ecosystem productivity (NEP, ±2.0 Gt C yr⁻¹) (Randerson et al. 2002), and should be accounted for to better constrain the direction and magnitude of net land-atmosphere C exchange.

A thorough understanding of terrestrial C cycling in rivers, estuaries and the ocean requires characterization of river particulate organic carbon (POC). POC constitutes an important fraction of the total C (18%) and total organic carbon (OC, 40%) rivers export to the oceans (Hedges et al. 1997; Meybeck 1993). Although global river POC export (0.15-0.2 Gt C yr⁻¹) alone is adequate to account for all the OC buried in marine sediments (0.1-0.2 Gt C yr⁻¹), OC in marine sediments is predominantly composed of marine-derived materials (Beusen et al. 2005; Hedges and Keil 1995; Hedges et al. 1997). More than half of the terrestrial POC exported to the ocean is decomposed or transformed rapidly in the

ocean (Hedges et al. 1997; Burns et al. 2008), even though this POC was refractory on land. This points to the need to study the nature of riverine POC to understand susceptibility of terrestrial organic matter (OM) to degradation in the ocean.

Drainage basin properties and land use are two important controls on the sources and reactivity of riverine POC. For example, heavily-forested headwaters receive large amounts of land C in the form of litterfall (Selva et al. 2007). This litterfall-derived POC is labile and decomposition of this POC contributes to about 35% of the CO₂ outgassed from the Amazon River (Richey et al. 2002). Rivers in the Northeast U.S. draining OM-rich shales receive ancient OM from the watersheds, and the contribution of ancient OM to riverine POC is positively related to agricultural activities in the watersheds (Longworth et al. 2007; Raymond et al. 2004). Although this ancient OM is old in ¹⁴C age, a portion of it may be labile and susceptible to biological and chemical processes and may fuel part of the respiration of the Hudson River (Cole and Caraco 2001). In industrialized or urbanized watersheds, pollutants from industries and wastewater treatment plants are likely also an important source of riverine POC (Griffith et al. 2009; Krusche et al. 2002; Longworth et al. 2007).

Sinking POC, the operationally defined high-density fraction of POC, exported by rivers represents the terrestrial POC that is potentially buried in river deltas and removed from the fast portion of the global C cycle. However, the chemistry of riverine sinking POC remains almost unknown. A few studies have been conducted in the ocean to characterize sinking POC in the ocean column (Druffel et al. 1992; Hedges et al. 2001; Hwang and Druffel 2003; Hwang et al. 2006; Hwang et al. 2004). However, to date, only one study exists characterizing riverine sinking POC (Gao et al. 2007).

The Brazos River in Texas is of great interest in studying river C cycling and export for two reasons. First, the Brazos River has a river-dominated delta, and river-dominated continental margins are where most (>80%) of the OC burial occurs (Berner 1982, 1989; Hedges and Keil 1995) and where terrestrial OC constitutes a significant portion of the OC buried (Wakeham et al. 2009). Second, OC burial and preservation are positively correlated with total sedimentation rate (Berner 1989; Burdige 2007). Although the watershed area of the Brazos River is only ~3% of that of the Mississippi River, the sediment discharge of the Brazos River is as much as 8% of that of the Mississippi River (Milliman and Syvitski 1992). Yet, there is little data about the OM within the Brazos River or exported by the Brazos River to the Gulf of Mexico.

C isotopes (^{14}C and ^{13}C) and molar C/N ratio, either separately or combined, have been widely used to study sources and cycling of particulate organic matter (POM) (Hein et al. 2003; Lamb et al. 2006; Mayorga et al. 2005; Meyers 1994; Yu et al. 2010). $\Delta^{14}\text{C}$ and $\delta^{13}\text{C}$ values can provide source and age information of riverine C. For example, the longitudinal trends of increasing $\Delta^{14}\text{C}$ values and decreasing $\delta^{13}\text{C}$ values of fine POC along the Amazon River reveal that the old fine POC originating from the Andes is almost completely decomposed and replaced by the young fine POC from the lowland ecosystems downstream (Mayorga et al. 2005).

The C/N ratio of POM is an indicator of sources of POM. Terrestrial plants (C3 and C4) generally have very high C/N ratios (averaged 32) (Elser et al. 2000), and soil organic matter (SOM) generally has C/N ratios above 10 (Lamb et al. 2006; Meyers 1994). The lowest C/N ratios in terrestrial OM are found in agricultural soils, but these values are still above 8 (Yu et al. 2010). In contrast, freshwater phytoplankton and bacteria generally have

low C/N ratios, averaged 7 and 4, respectively (Elser et al. 2000; Lamb et al. 2006; Meyers 1994).

Solid-state ^{13}C nuclear magnetic resonance (NMR) spectroscopy is a potentially powerful technique to use in tracking sources and reactivity of riverine POC. This technique has been extensively used to characterize the chemical structure of SOM because of its advantages compared to other spectroscopic and characterization techniques (e.g. chromatography). First, solid-state ^{13}C NMR is non-destructive, and both soluble and insoluble fractions of OM can be examined (Salati et al. 2008). Second, solid-state ^{13}C NMR can detect not only the free forms of OM, but also the shielded forms of OM (Hedges et al. 2001). Third, solid-state ^{13}C NMR is potentially quantitative, and it can provide complete and unbiased average chemical structures of OM (Piccolo and Conte 1998; Smernik et al. 2002). Solid-state ^{13}C NMR has been used to characterize ocean POC and has provided valuable information on the metabolism and cycling of POC in the ocean (Baldock et al. 2004; Hedges et al. 2001; Nelson and Baldock 2005; Sannigrahi et al. 2005). However, to our knowledge this study is the first application of this technique to riverine POC.

In this study we combined the above three approaches to characterize riverine POM in the Brazos River. We determined isotopic (^{13}C and ^{14}C) composition of both total and sinking POM, and chemical (carbohydrate, protein, lignin, lipid, carbonyl and charcoal) and elemental (%C, %N, and C/N) composition of sinking POM along the main stem of the Brazos River. From these measurements, we (1) identify the sources of riverine POM; (2) explore the effects of drainage basin properties and land use on the sources and chemical composition of riverine POM; and (3) provide the first measurements of annual POC,

charcoal, and lignin export by the Brazos River to the Gulf of Mexico.

4.2 Study area

The Brazos River ranks first in Texas rivers in both length (1,680 km) and water discharge ($249 \text{ m}^3 \text{ s}^{-1}$) (Benke and Cushing 2005). It is formed by the confluence of its two tributaries (the Salt Fork and the Double Mountain Fork) about 110 km upstream of Seymour, TX, and it drains into the Gulf of Mexico near Freeport, TX (Fig. 4-1). The Brazos River watershed is low in relief, with a channel gradient of less than 0.67 m km^{-1} (Stricklin 1961). We refer to the river segment between Graham and Waco, TX as the middle Brazos, and the river segment downstream of Waco to the river mouth as the lower Brazos (Fig. 4-1).

We collected samples from six sites in the main stem of the middle and lower Brazos River (Fig. 4-1). Sites 1 and 2 are located in urban areas where the middle Brazos River runs through cities Granbury and Waco, respectively. The Brazos River is dammed only a few kilometers downstream of sites 1 and 2, respectively, forming Lake Granbury at site 1 and a town-lake at site 2. Sites 3-6 are in rural areas in the lower Brazos. There are no dams in the main stem of the lower Brazos.

The geology of the Brazos River watershed has been described in detail in Zeng et al. (2010) (see Chapter 3). There is some old OM-bearing bedrock present in the Brazos River watershed. Bedrock containing bituminous coal outcrops about 60 km upstream of site 1 (Hackley et al. 2009; Moore and Plummer 1922) (Fig. 4-1). Lignite outcrops in two belts parallel to the Gulf coast: an ~20 km wide one between sites 2 and 3, and an ~7 km wide one slightly downstream of site 3 (Ruppert et al. 2002) (Fig. 4-1). The predominant

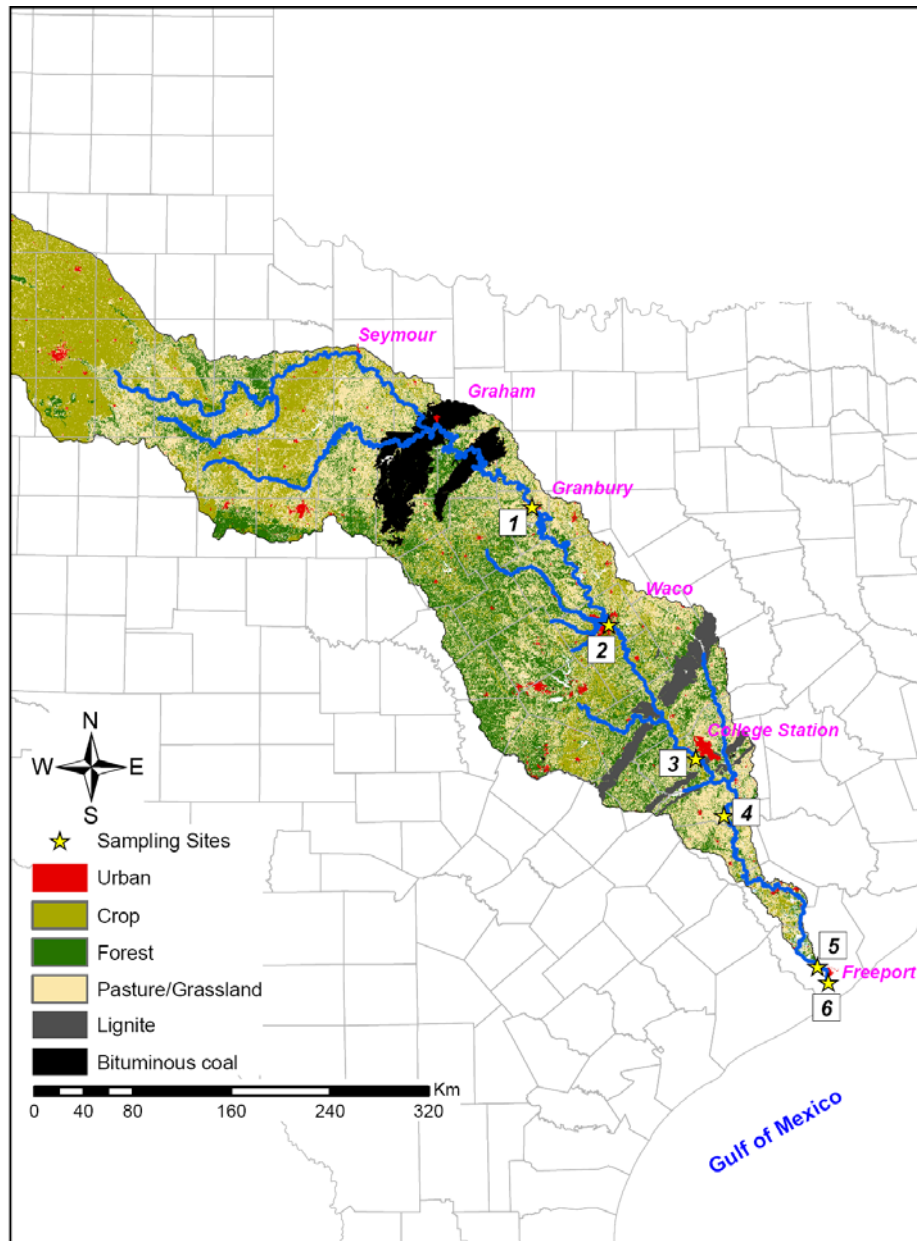


Figure 4-1. Land use and surface geologic map of the Brazos River watershed made according to the digital maps by Stoesser et al (2005), Tewalt et al (2008), and National Center for Earth Resources Observation and Science and U.S. Geological Survey (2005). Cities are labeled in pink. There are 6 sampling sites numbered in the boxes. Sites 1 and 2 are dammed several kilometers downstream. Dams cannot be seen because they are masked by sampling site symbols (yellow stars).

lithology is resistant limestone and red beds of Pennsylvanian and Cretaceous age in the middle Brazos, and sand, silt and clay deposits of Eocene, Miocene and Pleistocene age in the lower Brazos (Cronin et al. 1963; Moore and Plummer 1922; Stricklin 1961).

Land use shows different patterns between the middle and lower Brazos River watershed (Fig. 4-1). In the middle Brazos River watershed, forest and pasture dominate. In the lower Brazos River watershed, cropland and forests cover most of the watershed between sites 2 and 3, and pasture is the single dominant land use downstream of site 3 to the river mouth.

4.3 Methods

4.3.1 Sample collection

We used a submersible pump (SHURflo 9325-043-101) deployed from bridges to collect all the samples directly from the middle of the river at depths between 10 and 30 cm.

All the glassware used for sample collection and pre-treatment for C isotope analysis was pre-cleaned (soapy water, deionized water and Milli-Q water) and pre-combusted (500°C for 2 h). For each total POC sample, we collected 4 L of water in an amber glass bottle. The water was stored at 0°C for ~5 h during transport to the lab, and then was filtered through pre-combusted (500°C for 2 h) 47-mm diameter quartz fiber filters (Millipore, AQFA04700). We recorded the volume of water passing through each filter to calculate total POC concentration (POC_{TOT}). The filters were then frozen at -20°C until pre-treatment for ^{13}C and ^{14}C analysis.

For each sample for NMR analysis, we collected ~120 L (V , in L) of water into six

20-L acid-washed fluorinated high-density polyethylene (HDPE) containers. After overnight storage at 4°C to let the particles settle, the supernatant was removed by siphoning and the bottom water with river sediment was transferred to a clean glass container. We then centrifuged and freeze-dried the sediment in a pre-weighed 50 mL centrifuge tube (W_{S1}) to obtain a sinking POC sample. The tube with the dried sample was weighed (W_{S2}) and the concentration of sinking particulate matter (PM_{sink} , in $mg\ L^{-1}$) was calculated from $(W_{S2} - W_{S1})/V$.

To determine the concentration of total particulate matter (PM_{TOT} , in mg/L), we filtered 500 mL of well mixed river water through a dried and pre-weighed glass fiber filter (1 μm nominal pore size, 47 mm in diameter). The filter was dried at 50°C and weighed to calculate PM_{TOT} . Four replicates were obtained for each sample and the average PM_{TOT} value was calculated.

In the text below, sinking POC, sinking POM and sinking PM are used for the same sample depending on the analysis made to the sample. “Sinking POC” is for C isotope and NMR analysis; “sinking POM” is for C and N content analysis; and “sinking PM” is for total sample mass analysis.

4.3.2 Sample pre-treatment

4.3.2.1 For C isotope analysis

Before C isotope analysis, we removed carbonate from the total POC samples following the HCl_{vap} method in Komada et al. (2008). This method can remove carbonate efficiently while yielding accurate %OC, $\delta^{13}C$ and $\Delta^{14}C$ values (Komada et al. 2008). Briefly, total POC samples were thawed at room temperature and placed in a 250 mm ID

glass desiccator along with 60 mL concentrated HCl (12N, Fisher Scientific NF/FCC). The desiccator was soaked with 10% HCl for 24 h before use. The samples were fumigated in HCl vapor for 6 h. Upon completion, the HCl vapor in the desiccator was vented for 6 h and the samples were dried in an oven at 50°C.

Sinking POC samples for C isotope analysis were acidified with 1N HCl to remove carbonate. For each sample, a small aliquot was transferred to a pre-cleaned and pre-combusted glass vial. Milli-Q water was added just enough to moisten the sample, followed by 1N HCl until no bubbling was observed. The samples were then dried at 50°C. Samples were not rinsed prior to isotopic analysis.

4.3.2.2 For NMR analysis

We performed an HCl/HF demineralization on the sinking POC sample collected at site 5 (sample 5) to concentrate the OC and reduce the paramagnetic impurities in the sample, because an NMR spectrum could not be obtained for this sample due to its low OC and/or high paramagnetic impurity (e.g. Fe) content. To examine the effect of demineralization treatment on the chemical composition of sample 5, we performed the same treatment on two other samples. The size of these two samples is large enough for demineralization treatment, and good quality spectra of their untreated samples can be obtained. The demineralization procedure we followed was developed and described in detail by Gelinas et al. (2001), including HCl demineralization, HCl/HF demineralization, and recovery of acid-soluble OC.

HCl demineralization. In this step, HCl solution was added to the samples to remove salt, carbonate and sesquioxide coatings. The residue was separated from the supernatant

by centrifugation and the supernatant was saved for OC recovery.

HCl/HF demineralization. The residue was further demineralized using a 1N HCl and 10% (v/v) HF solution. After shaking for 12 h, the residue was separated from the supernatant by centrifugation and the supernatant was saved for OC recovery. The HCl/HF demineralization was repeated for a second time.

Recovery of acid-soluble OC. Concentrated HF was added to the HCl demineralization supernatants to precipitate Ca^{2+} as CaF_2 and OC-free CaCO_3 powder was added to the HCl/HF demineralization supernatants to precipitate F^- as CaF_2 . All the supernatants were adjusted to a final pH of ~ 7 with NaOH solution before NaHS solution was added in an N_2 -flushed glove bag to precipitate dissolved metals as sulfides. We discarded the CaF_2 and sulfide precipitates and extracted the acid-soluble OC in the supernatants using C_{18} disks (3M; Empore, St. Paul, MN). The OC on the C_{18} was then extracted using methanol. After removal of most of the methanol by blowing air on the surface of the methanol, we transferred the methanol containing the extracted OC to the residue. The mixture was then dried at 60°C in the oven to remove the rest of the methanol and homogenized before NMR analysis.

4.3.3 Sample measurements

4.3.3.1 C isotope analysis

We made ^{13}C and ^{14}C measurements of total and sinking POC samples at the W.M. Keck Carbon Cycle Accelerator Mass Spectrometry (AMS) Laboratory at the University of California, Irvine. The samples, with CuO and silver wire added, were combusted at 900°C in evacuated sealed quartz tubes for 3 h to convert POC to CO_2 . The CO_2 generated

was purified cryogenically and measured. We used the amount of CO₂ generated and the volume of water filtered through to calculate POC_{TOT} (in mg L⁻¹). A small aliquot of the CO₂ was taken for ¹³C analysis on a continuous flow stable isotope ratio mass spectrometer (Delta-Plus CFIRMS). The rest of the CO₂ was reduced to graphite in a reactor at 550°C with hydrogen and iron powder catalyst. The C isotope composition of the graphite was measured by AMS for Δ¹⁴C values.

4.3.3.2 ¹³C CP-MAS NMR analysis

¹³C NMR spectroscopy is a technique that identifies OC in different functional groups of a sample, e.g. alkyl C, O-alkyl C and aromatic C, etc (Baldock and Skjemstad 2000). For a review of the uses of NMR in biogeochemistry, see Hockaday and Masiello (in preparation). With the determined distribution of OC in the functional groups, a mixing model can be used to calculate the molecular composition of the sample, i.e. proportions of carbohydrate, protein, lignin, lipid, carbonyl, and charcoal (Baldock et al. 2004; Nelson and Baldock 2005; Nelson et al. 1999).

We conducted ¹³C CP-MAS (cross polarization-magic angle spinning) NMR experiments on a 200 MHz Bruker Avance spectrometer with a solid-state 4 mm dual frequency MAS probe. River sinking POC samples of known mass (approximately 80-120 mg) were packed in a 4 mm (outside diameter) NMR rotor with a Kel-F cap, and spun at a frequency of 5 kHz or 7 kHz.

The OC functional group distribution was measured by a CP pulse sequence with a contact time of 1 ms, an acquisition time of 18.5 ms, and a recycle delay time of 2.5 s. The number of acquisitions (scans) to obtain spectra ranged from 16,000-25,000. The data

collected were Fourier-transformed with 50 Hz line broadening to obtain a spectrum to which we applied manual phase and baseline corrections. We integrated the peak areas according to spectral regions specified in Baldock et al. (2004): alkyl (0-45 ppm), N-alkyl/methoxyl (45-60 ppm), O-alkyl (60-95 ppm), O₂-alkyl (95-110 ppm), aromatic (110-145 ppm), phenolic (145-165 ppm), and amide/carboxyl (165-215 ppm).

To determine the percentage of C observed (detected) by NMR, we compared the C-normalized signal intensity detected for each sample to the C-normalized signal intensity of an external standard, which is a mixture of 52.4% cellulose and 47.6% glycine. This procedure is known as spin counting (Smernik and Oades 2000). The following equation was used to calculate the percentage of C in the rotor that was observed (C_{obs}) in the NMR spectrum (Hockaday et al. 2009; Smernik and Oades 2000):

$$C_{\text{obs}} (\%) = 100 \times \frac{\text{signal intensity per unit C for sample}}{\text{signal intensity per unit C for standard}} \quad (1)$$

4.3.3.3 Molecular mixing models

We applied the molecular mixing model (MMM) developed by Baldock et al. (2004) to our NMR spectra to determine the molecular composition of the samples. For a detailed description of the MMM, see Baldock et al. (2004) and Nelson and Baldock (2005). Briefly, this model is based on two assumptions: (1) natural OM is assumed to be represented by a mixture of six organic components: carbohydrate, protein, lignin, lipid, carbonyl and charcoal; and (2) each of these organic components has a representative distribution of ¹³C-NMR signal intensities (Baldock et al. 2004). The input data to the model is the amount of ¹³C NMR signal intensity for each of the spectral regions. Input of the molar N/C ratio of

the sample can further constrain the model and provide an independent test of the model, but it is not required (Baldock et al. 2004). The output is the percentage of the six organic components in the sample. We call this model the terrestrial MMM because it is optimized to analyze terrestrial samples (Baldock et al. 2004; Nelson and Baldock 2005). For samples potentially comprising significant amount of phytoplankton materials, we modified the terrestrial MMM to obtain the aquatic MMM by replacing lignin with nucleic acid in the model.

4.3.3.4 Chemical composition of sinking POC

The integrated peak areas from ^{13}C CP-MAS NMR analysis were corrected for spinning side bands (SSB) of aromatic, phenolic and amide/carboxyl C. The corrected peak areas, as well as the molar N/C ratio determined by catalytic combustion with a model ESC4010 elemental analyzer (EA, Costech Analytical Technologies Inc., Valencia, CA), were then plugged into the terrestrial or aquatic MMM to calculate the percentage of carbohydrate, protein, lignin/nucleic acid, lipid, carbonyl, and charcoal in the sample. Whether the terrestrial or aquatic MMM was used for a specific sample is discussed in detail in the “Results” section.

4.3.3.5 Fraction of sinking POC in total POC

We analyzed a small aliquot of each sinking POM sample on the EA to obtain %OC, %N, and the molar C/N ratio (although the MMMs used N/C ratios, we work here with C/N ratios to conform with conventional use of C/N ratios as an indicator of OC sources). The percentage of sinking POC among total POC ($\text{POC}_{\text{sink}}/\text{POC}_{\text{TOT}}$, in %) was determined by

$$\text{POC}_{\text{sink}}/\text{POC}_{\text{TOT}} (\%) = (\text{PM}_{\text{sink}} \times \% \text{OC}_{\text{PMsink}}) \div \text{POC}_{\text{TOT}} \times 100\% \quad (2)$$

in which $\% \text{OC}_{\text{PMsink}}$ is the percentage of OC in sinking POM measured on the EA, and the unit of PM_{sink} and POC_{TOT} is mg L^{-1} .

4.3.3.6 OC recovery of demineralization

Not all acid-soluble OC lost to the supernatants was recovered by the C_{18} disks. Therefore, we measured the OC content of the untreated ($\% \text{OC}_{\text{before}}$) and demineralized ($\% \text{OC}_{\text{after}}$) sample using the EA and combined the sample mass before (M_{before}) and after (M_{after}) to determine the OC recovery of the demineralization process.

4.3.3.7 Statistical analysis

We applied Student's t -test to determine if there was significant difference in concentration and isotopic signatures of POC between the middle and lower Brazos, and between the total and sinking POC. A p value less than or equal to 0.05 suggests a significant difference, and a p value lower than 0.01 suggests a very significant difference.

4.4 Results

4.4.1 Concentration and isotopic composition of total and sinking POC

Total POC showed distinctive patterns along the Brazos River in both concentration and isotopic composition. POC_{TOT} was significantly ($p = 0.0044$) higher in the lower Brazos ($5.04 \pm 3.38 \text{ mg L}^{-1}$) than the middle Brazos ($1.20 \pm 0.34 \text{ mg L}^{-1}$) (Table 4-1, Fig.

Site	Site-mouth (km)	Date sampled	T (°C)	POC _{TOT}			POC _{sink}		DIC*
				mg C L ⁻¹	Δ ¹⁴ C (‰)	δ ¹³ C (‰)	Δ ¹⁴ C (‰)	δ ¹³ C (‰)	Δ ¹⁴ C (‰)
<i>The middle Brazos</i>									
1	460	3/5/2009	15.6	1.12	-45	-32.5	-3	-27.8	+10
		7/23/2009	27.3	1.94	-65	-30.9	+9	-27.0	-10
		10/8/2009	22.8	1.44	-50	-30.0	-17	-26.9	nd
		1/17/2010	7.2	1.30	-62	-33.4	nd	nd	nd
		<i>Mean ± SD</i>		1.45 ± 0.35	-55 ± 9	-31.7 ± 1.5	-4 ± 13	-27.2 ± 0.5	
2	344	1/6/2008	12.6	0.74	+2	-31.9	nd	nd	+73
		6/5/2008	23.5	1.12	+71	-26.8	nd	nd	nd
		7/3/2008	27.5	0.88	+119	-34.6	nd	nd	+162
		10/30/2008	18.7	1.13	+62	-33.3	+54	-27.5	+96
		7/23/2009	28.9	1.13	+62	-31.1	+66	-25.9	+179
		<i>Mean ± SD</i>		1.00 ± 0.18	+63 ± 41	-31.5 ± 3.0	+60 ± 9	-26.7 ± 1.1	
1-2		<i>Mean ± SD</i>		1.20 ± 0.34	+10 ± 69	-31.6 ± 2.3	+22 ± 36	-27.0 ± 0.7	
<i>The lower Brazos</i>									
3	230	3/5/2009	21.1	2.03	-86	-33.7	-69	-27.8	-84
4	160	6/13/2007	nd	5.90	-458	-28.2	nd	nd	-220
5	20	11/28/2007	16.6	8.30	-378	-27.6	nd	nd	-194
		11/19/2008	17.4	8.00	-457	-28.2	-94	-19.8	-192
		<i>Mean ± SD</i>		8.15 ± 0.21	-417 ± 56	-27.9 ± 0.4			
6	0	11/28/2007	15.8	0.98	-396	-28.0	nd	nd	-94
3-6		<i>Mean ± SD</i>		5.04 ± 3.38	-355 ± 155	-29.1 ± 2.6	-82 ± 18	-23.8 ± 5.7	

Site-mouth: distance from the site to the river mouth.

nd: no data

Table 4-1. Measured concentration and isotopic signatures of total POC, sinking POC and DIC in the Brazos River. *: Δ¹⁴C values of DIC are from Zeng et al. (2010).

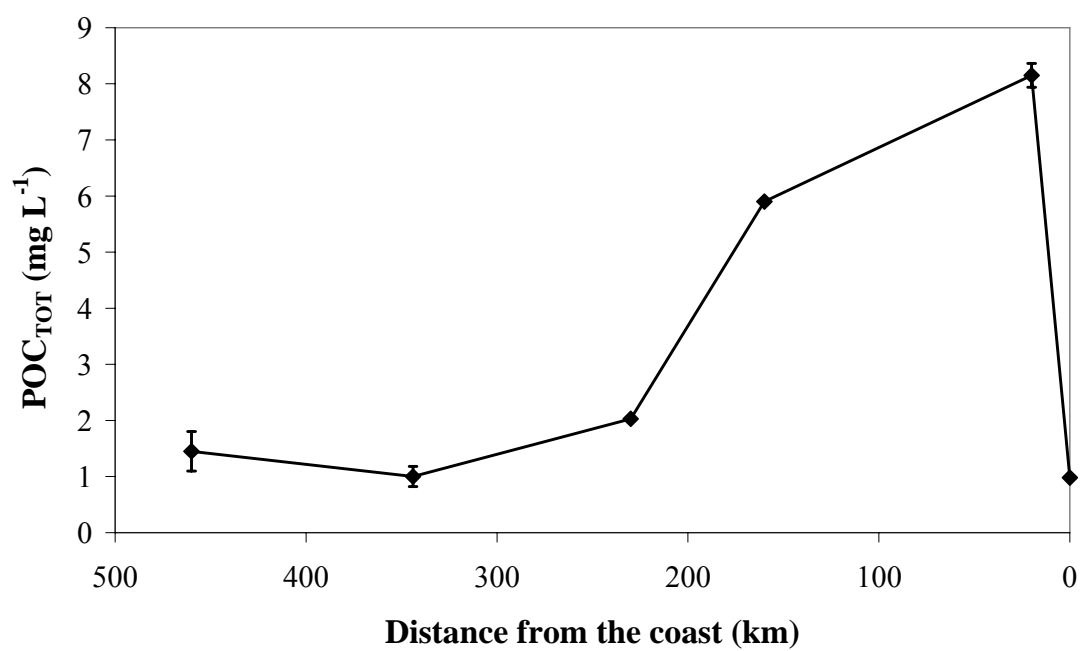


Figure 4-2. Longitudinal variations in the concentration of total POC. Vertical bars represent the standard deviation of all the data for the site.

4-2). Total POC in the middle Brazos ($\Delta^{14}\text{C} = +10 \pm 69\text{‰}$, $\delta^{13}\text{C} = -31.6 \pm 2.3\text{‰}$) was significantly more enriched in ^{14}C ($p < 0.0001$) and generally more depleted in ^{13}C than total POC in the lower Brazos ($\Delta^{14}\text{C} = -355 \pm 155\text{‰}$, $\delta^{13}\text{C} = -29.1 \pm 2.6\text{‰}$) (Table 4-1, Fig. 4-3). $\delta^{13}\text{C}$ values of total POC at sites 4-6 were generally higher than those of sites 1-3 (Table 4-1), probably due to a higher contribution of C4 plant-derived OM downstream of site 3 where pasture is the dominant land use.

In the middle Brazos, concentration of total POC was significantly ($p = 0.0412$) higher at site 1 than at site 2 (Table 4-1, Fig. 4-2). Total POC was more ^{14}C -depleted at site 1 than at site 2 (Table 4-1, Fig. 4-3). According to the $\Delta^{14}\text{C}$ values of the atmospheric CO_2 in 2004 (+55 to +66‰) (Hsueh et al. 2007) and a decreasing rate of 6‰ per year (Trumbore et al. 2006), the $\Delta^{14}\text{C}$ values of the atmospheric CO_2 in the years 2007-2010 are in the range of +19 to +48‰. All the $\Delta^{14}\text{C}$ values of POC at site 1 were lower than those of the atmospheric CO_2 . In contrast, the POC at site 2 was generally more ^{14}C -enriched than the atmospheric CO_2 .

Total POC in the lower Brazos was generally high in concentration and highly depleted in ^{14}C (Table 4-1), suggesting a significant input of old C in the lower Brazos. Total POC concentration dropped from 8.30 mg L^{-1} about 20 km upstream of the river mouth (site 5) to 0.98 mg L^{-1} at the mouth (site 6), while the $\Delta^{14}\text{C}$ value of POC remained almost the same, suggesting dilution at the mouth by the Gulf of Mexico water which has a low POC concentration (Bianchi et al. 1997).

Sinking POC showed a similar pattern: significantly ($p = 0.0141$) more enriched in ^{14}C in the middle Brazos ($\Delta^{14}\text{C} = +22 \pm 36\text{‰}$) than in the lower Brazos ($\Delta^{14}\text{C} = -82 \pm 18\text{‰}$), with no significant ($p = 0.20$) difference in $\delta^{13}\text{C}$ values between the middle and lower

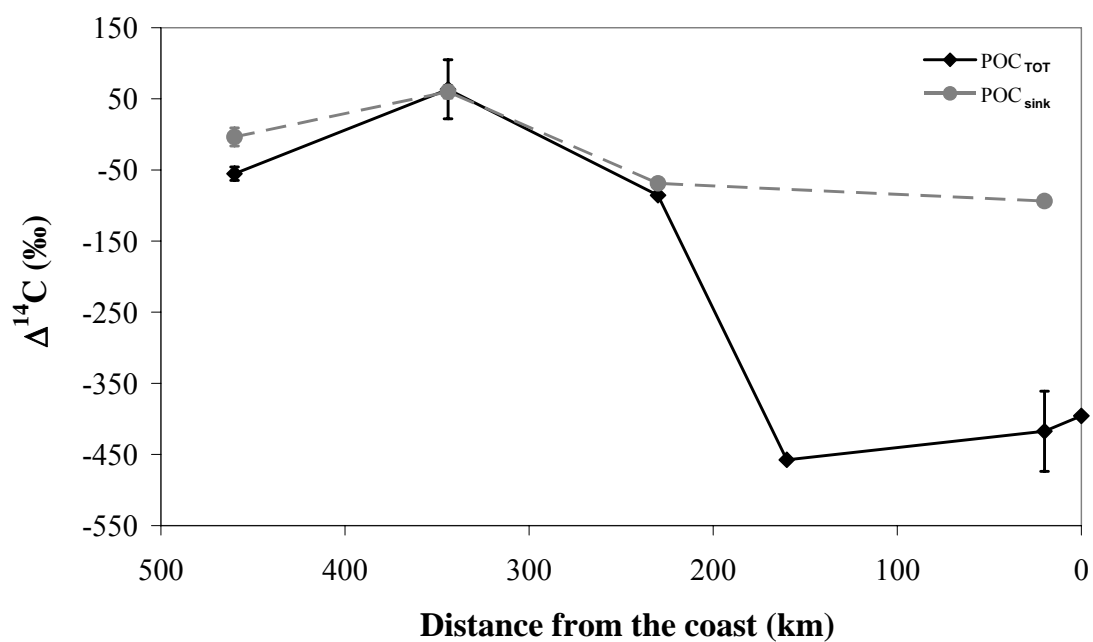


Figure 4-3. Longitudinal variations in the $\Delta^{14}\text{C}$ of total (solid line) and sinking (dotted line) POC. Vertical bars represent the standard deviation of all the data for the site.

Brazos (Table 4-1, Fig. 4-3). For each site, sinking POC was generally younger and significantly more ^{13}C -enriched ($p < 0.001$) compared to total POC.

Compared to longitudinal variations, temporal variations in concentration and C isotopic values were small for both total and sinking POC (Table 4-1). Our focus in this paper is therefore on the implications of the longitudinal variations in the concentration and C isotopic composition of total and sinking POC.

4.4.2 C and N concentration of sinking POM

Sinking POC comprised a small fraction of total POC in the middle Brazos. The percentage of sinking POC in total POC was measured for two samples collected at site 1, and was 19% for sample 1c and 6% for sample 1d (Table 4-2). Sinking PM comprised a higher portion (20-30%) of the total PM in river water (Table 4-2).

%OC, %N values and C/N ratios of untreated samples varied both spatially and temporally (Table 4-3, Fig. 4-4a and 4-4b). We grouped the samples according to their %OC, %N and C/N ratios: group I (samples 1a, 2a-b), group II (samples 1b-d), group III (sample 3), and group IV (sample 5). %OC values of group I-III samples were consistent, generally lower than 10%. However, %N values and C/N ratios varied largely among groups. Group II samples had the highest %N values (1.11-2.75%) and the lowest C/N ratios ($\text{C/N} = 6.67\text{-}8.32$); group III sample had low %N (0.47%) and the highest C/N ratio (21.19), and %N values (0.58-0.71) and C/N ratios (12.17-13.58) of group I samples were intermediate between those of group II and III samples. Sample 1b in group II differed from all other samples in that its %OC and %N values were the highest and C/N ratio was the lowest. Sample 5 in group IV had very low %OC (1.00%) and %N (0.11%) values,

Site	Date sampled	Sample name	PM_{sink} (mg L^{-1})	$\% \text{OC}_{\text{PM}_{\text{sink}}}$	POC_{TOT} (mg C L^{-1})	PM_{TOT} (mg L^{-1})	$\text{POC}_{\text{sink}}/\text{POC}_{\text{TOT}}$ (%)	$\text{PM}_{\text{sink}}/\text{PM}_{\text{TOT}}$ (%)
1	10/8/2009	1c	3.32	8.23	1.44	11.45	18.95	28.96
1	1/17/2010	1d	1.02	7.73	1.30	4.75	6.04	21.38

POC_{TOT} values here are from Table 4-1.

$\text{POC}_{\text{sink}}/\text{POC}_{\text{TOT}}$ (%) = $(\text{PM}_{\text{sink}} \times \% \text{OC}_{\text{PM}_{\text{sink}}})/\text{POC}_{\text{TOT}} \times 100\%$.

Table 4-2. Percentage of sinking POC in total POC.

Site	Date sampled	Sample name	Group	%OC	%N	Molar C/N	%C _{obs}	Alkyl/O-alkyl
1	3/5/2009	1a	I	8.14	0.70	13.58	51.85	0.58
	7/23/2009	1b	II	15.73	2.75	6.67	52.93	1.49
	10/8/2009	1c	II	8.23	1.15	8.32	43.27	1.06
	1/17/2010	1d	II	7.73	1.11	8.11	26.54	1.69
2	10/30/2008	2a	I	7.98	0.71	13.03	42.40	0.63
	7/23/2009	2b	I	6.08	0.58	12.17	35.20	0.86
3	3/5/2009	3	III	8.59	0.47	21.19	28.17	0.81
5	11/19/2008	5	IV	1.00	0.11	10.63	35.09	1.49

C in the molar C/N ratios is OC.

Table 4-3. %OC, %N, and molar C/N ratios of untreated sinking POM, the percentage of C in sinking POM detected by NMR, and the alkyl/O-alkyl ratio of sinking POM.

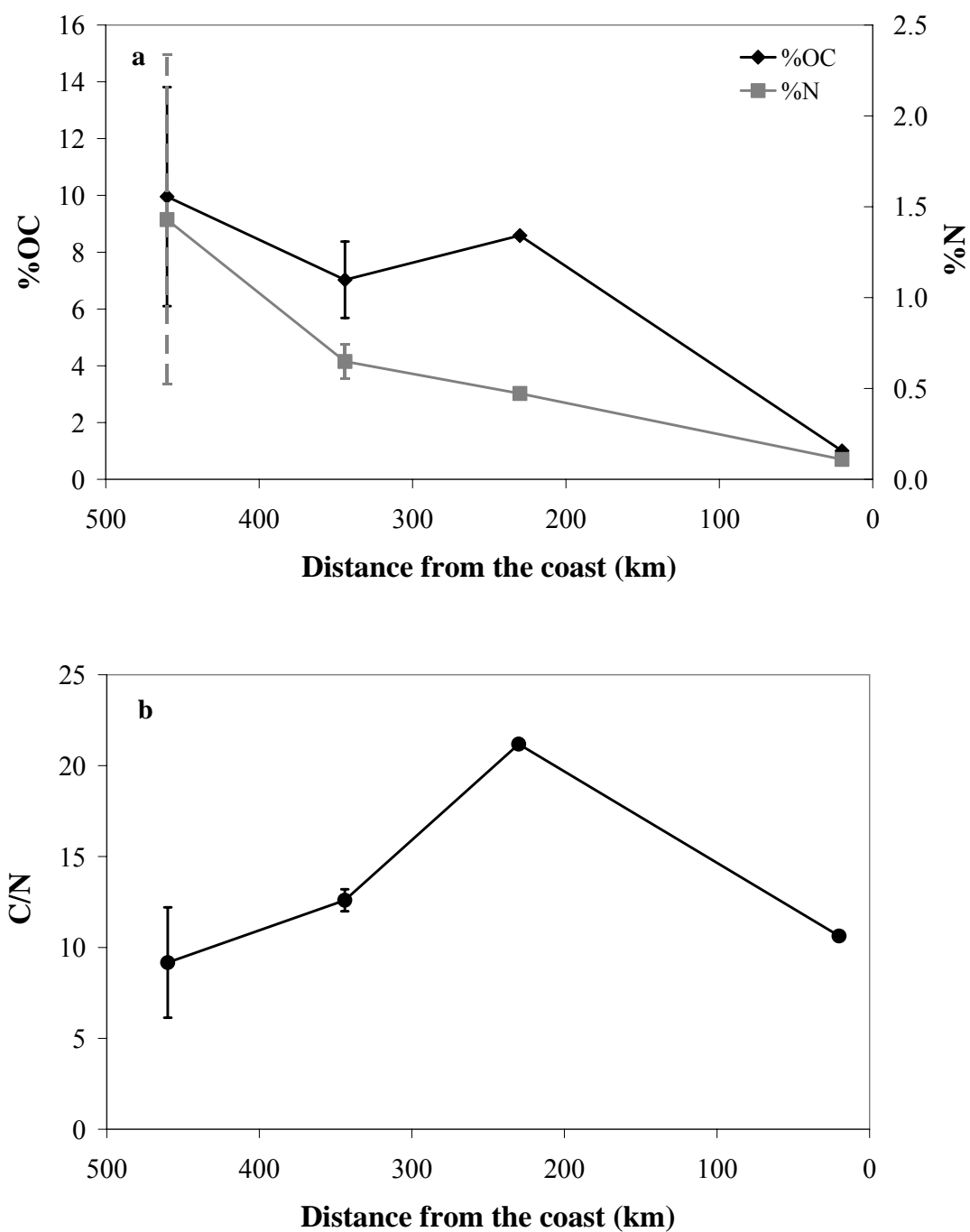


Figure 4-4. Longitudinal variations in %OC, %N and molar C/N ratios of natural sinking POM. Vertical bars represent the standard deviation of all the data for the site.

indicating the dilution effect of minerals from soils. Therefore, demineralization of sample 5 was required to obtain an NMR spectrum.

4.4.3 Selection of the MMMs for sinking POC samples

POC in rivers is a mixture of allochthonous (originating from terrestrial sources, e.g. soil) and autochthonous (originating from aquatic sources, e.g. phytoplankton) materials. Currently there is no MMM that works for such mixed systems. However, we can assign the aquatic or terrestrial MMM to a particular sample, depending on whether autochthonous or allochthonous POC dominates in the sample. We used the four criteria described below to determine whether autochthonous or allochthonous POC dominates and hence whether the aquatic or terrestrial MMM should be used for a particular sample.

The first criterion is the C/N ratio of the sample. The low C/N ratios (6.67-8.32, Table 4-3) of group II samples suggest a high contribution of phytoplankton materials to these samples. In contrast, the high C/N ratios (10.63-21.19, Table 4-3) of group I, III and IV samples suggest that terrestrial OM dominates in these samples.

The second is the similarity between the molecular composition of group II samples and that of phytoplankton. Phytoplankton has higher protein and lipid content and lower carbohydrate content compared to terrestrial OM (Burdige 2007; Fahnenstiel et al. 1989; Hedges and Oades 1997). Therefore, the high lipid and protein content of group II samples predicted by both the aquatic and the terrestrial MMMs (Table 4-5), and the similarity of the spectra of these samples (Fig. 4-5c, 4-5d and 4-5e) to those of phytoplankton (Hedges et al. 2002; Krull et al. 2009) imply that phytoplankton materials comprise a major fraction of these samples.

Site	Date sampled	Sample name	Group		Percentage of C resonating in spectral regions							Error	MMM chosen
					0-45	45-60	60-95	95-110	110-145	145-165	165-215		
1	3/5/2009	1a	I	<i>Measured</i>	<i>21.1</i>	<i>8.0</i>	<i>36.5</i>	<i>8.0</i>	<i>11.7</i>	<i>4.9</i>	<i>9.8</i>		
				Predicted by MMM _{Aq}	21.8	6.8	37.4	7.7	13.1	2.8	10.5	9.4	N
				Predicted by MMM_{Te}	21.0	8.7	36.5	8.0	11.8	4.1	9.8	1.0	Y
	7/23/2009	1b	II	<i>Measured</i>	<i>34.6</i>	<i>10.7</i>	<i>23.2</i>	<i>4.1</i>	<i>8.1</i>	<i>2.9</i>	<i>16.4</i>		
				Predicted by MMM _{Aq}	34.6	10.9	23.3	3.7	8.0	3.2	16.4	0.3	Y
				Predicted by MMM _{Te}	34.0	13.3	22.8	4.0	7.8	1.3	16.8	9.8	N
	10/8/2009	1c	II	<i>Measured</i>	<i>27.8</i>	<i>9.8</i>	<i>26.3</i>	<i>6.1</i>	<i>13.7</i>	<i>5.2</i>	<i>11.1</i>		
				Predicted by MMM _{Aq}	28.3	9.0	27.0	5.2	14.5	4.2	11.8	4.3	Y
				Predicted by MMM _{Te}	27.1	11.1	26.0	5.4	13.5	2.9	13.9	15.8	N
	1/17/2010	1d	II	<i>Measured</i>	<i>35.4</i>	<i>10.7</i>	<i>20.9</i>	<i>4.3</i>	<i>10.3</i>	<i>3.3</i>	<i>15.0</i>		
				Predicted by MMM _{Aq}	35.6	10.4	21.3	3.8	10.8	2.8	15.3	1.2	Y
				Predicted by MMM _{Te}	35.3	11.8	21.0	4.0	10.5	2.4	15.0	2.3	N
2	10/30/2008	2a	I	<i>Measured</i>	<i>21.3</i>	<i>8.9</i>	<i>33.6</i>	<i>7.4</i>	<i>13.6</i>	<i>5.0</i>	<i>10.3</i>		
				Predicted by MMM _{Aq}	22.0	7.3	34.5	7.2	15.0	3.0	11.0	10.2	N
				Predicted by MMM_{Te}	21.3	9.1	33.5	7.6	13.6	4.6	10.3	0.2	Y
	7/23/2009	2b	I	<i>Measured</i>	<i>27.1</i>	<i>9.4</i>	<i>31.7</i>	<i>6.3</i>	<i>9.4</i>	<i>4.9</i>	<i>11.3</i>		
				Predicted by MMM _{Aq}	28.0	7.7	32.6	6.4	10.9	2.3	12.1	13.9	N
				Predicted by MMM_{Te}	27.0	10.0	31.5	6.8	9.4	4.0	11.2	1.4	Y
3	3/5/2009	3	III	<i>Measured</i>	<i>23.3</i>	<i>10.1</i>	<i>28.8</i>	<i>6.6</i>	<i>14.3</i>	<i>5.6</i>	<i>11.3</i>		
				Predicted by MMM _{Aq}	25.0	5.3	30.5	6.5	16.7	3.4	12.7	40.7	N
				Predicted by MMM_{Te}	23.4	8.8	28.6	7.3	14.1	6.6	11.3	3.2	Y
5	11/19/2008	5	IV	<i>Measured</i>	<i>25.1</i>	<i>8.5</i>	<i>16.9</i>	<i>5.7</i>	<i>21.4</i>	<i>9.4</i>	<i>13.0</i>		
				Predicted by MMM_{Te}	24.9	10.7	17.0	5.1	21.7	7.5	13.0	9.1	Y

Table 4-4. Measured ¹³C NMR spectral distributions and predicted ¹³C NMR spectral distributions from aquatic and terrestrial MMMs (MMM_{Aq} and MMM_{Te}, respectively). All results are for untreated samples except sample 5. Error is the sum of squares of the differences between the predicted and measured spectral intensities. Measured values are in italic. The results from the MMM chosen are in bold.

Site	Date sampled	Sample name	Group	MMM type	Carbohydrate	Protein	Nucleic acids or lignin	Lipid	Carbonyl	Charcoal	MMM chosen*
1	3/5/2009	1a	I	Aquatic	48.7	21.8	1.5	13.3	3.1	11.7	N
				Terrestrial	47.2	23.4	12.4	10.6	0.8	5.6	Y
	7/23/2009	1b	II	Aquatic	21.5	37.1	13.2	20.9	4.7	2.6	Y
				Terrestrial	29.7	50.9	0	16.6	0	2.8	N
	10/8/2009	1c	II	Aquatic	29.7	30.5	10.3	17.5	0	12.0	Y
				Terrestrial	34.5	40.0	2.5	12.6	0	10.3	N
	1/17/2010	1d	II	Aquatic	23.3	36.3	5.7	23.9	3.6	7.2	Y
				Terrestrial	26.2	42.3	3.3	21.8	0.6	5.9	N
2	10/30/2008	2a	I	Aquatic	46.1	24.4	0	12.7	2.7	14	N
				Terrestrial	43.1	24.7	13.6	10.4	1.0	7.3	Y
	7/23/2009	2b	I	Aquatic	42.1	25.1	1.2	18.8	3.9	8.8	N
				Terrestrial	39.6	26.6	15.5	15.8	1.4	1.1	Y
3	3/5/2009	3	III	Aquatic	38.8	14.6	0	19.5	10.7	16.5	N
				Terrestrial	32.9	14.9	26.1	15.0	7.5	3.5	Y
5	11/19/2008	5	IV	Terrestrial	17.6	26.5	22.8	14.0	4.7	14.4	Y

* MMM chosen for each sample is the same as that in Table 4-4.

Table 4-5. Percentage of six chemical components in the sinking POM samples calculated from NMR data using terrestrial and aquatic MMMs. All results are for untreated samples except sample 5. The results from the MMM chosen are in bold.

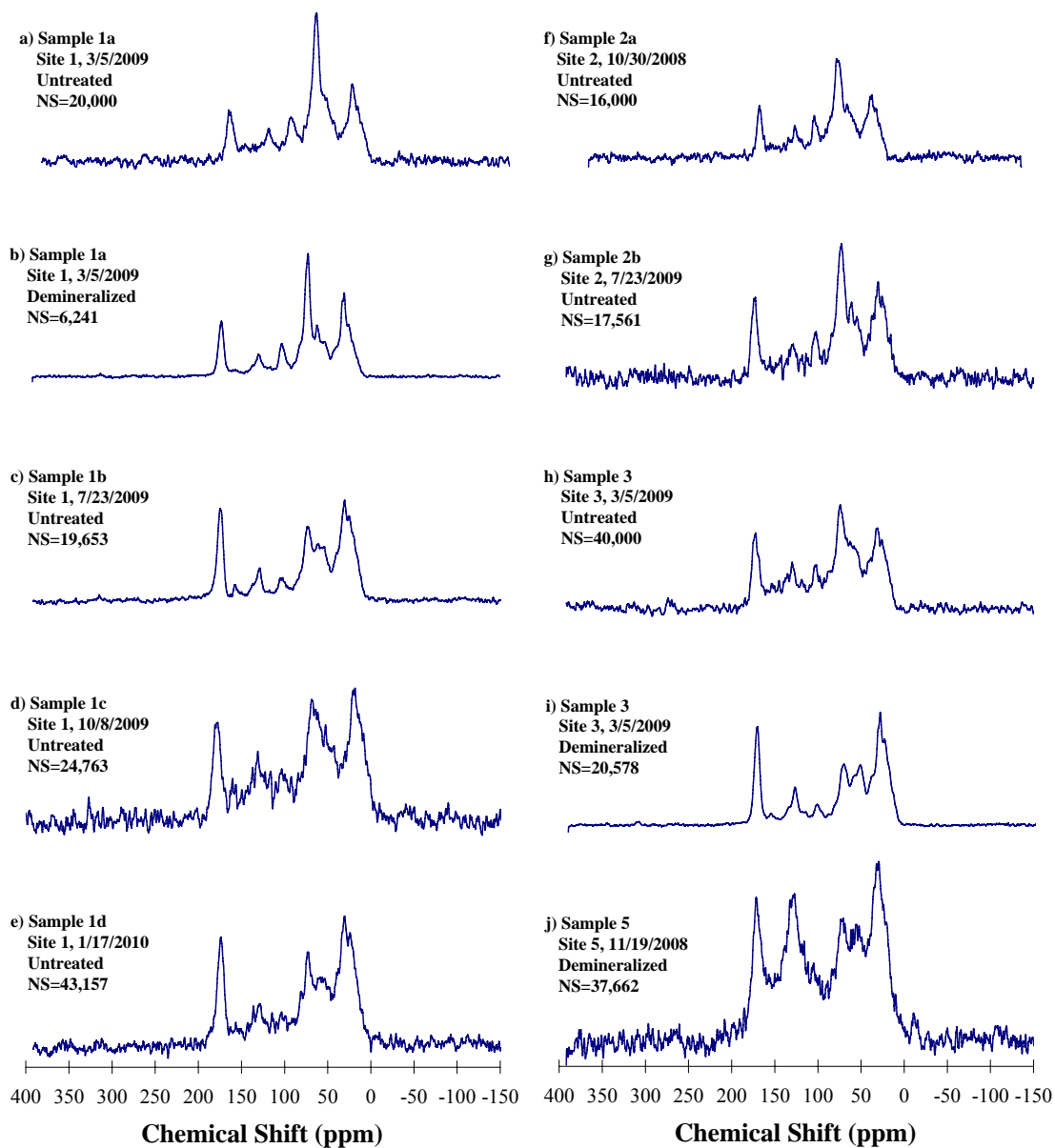


Figure 4-5. CP/MAS ^{13}C NMR spectra of sinking POM in the Brazos River. Vertical scales are equivalent for all samples. NS, number of scans acquired for each spectrum. Line broadening is 50 for all spectra.

The third is the overall goodness of fit of the models. The overall goodness of fit (error) is measured by the sum of squares of the differences between the predicted and measured spectral intensities. For group II samples, the errors associated with the aquatic MMM are much lower than the errors associated with the terrestrial MMM, while for group I and III samples the case is opposite (Table 4-4).

The last criterion is the nucleic acid/lignin content predicted by the models. When using the terrestrial MMM, it is assumed that there is a considerable amount of lignin in the sample. Therefore, a very low lignin content (0-3.3%, Table 4-5) predicted by the terrestrial MMM suggests that the terrestrial MMM is not appropriate for group II samples and the aquatic MMM should be used instead. Similarly, the very low nucleic acid content (0-1.5%, Table 4-5) predicted from the aquatic MMM indicates that the terrestrial MMM fits group I and III samples better. Although this criterion is limited because some fungi (e.g. white-rot fungus) preferentially degrade lignin (Baldock et al. 2004) and make low lignin content of terrestrial OM possible, we can still use this criterion here as a supplement to the above three criteria to support our selection of the MMMs for the samples.

According to these four criteria, we applied the aquatic MMM to group II samples and the terrestrial MMM to the rest (groups I, III and IV) (Table 4-5) to determine chemical composition of the sinking POC samples. For the group IV sample we didn't try the aquatic MMM because $\Delta^{14}\text{C}$ values of both total and sinking POC at site 5 (-457‰ and -94‰, respectively, Table 4-1) clearly pointed to its terrestrial origin.

4.4.4 Chemical composition of sinking POC

During OM decomposition, O-alkyl C is preferentially degraded, leading to a decrease

in the content of O-alkyl C and an increase in the content of alkyl C (Baldock et al. 1997). Therefore, the alkyl/O-alkyl ratio can be used to assess the extent of OM decomposition (Baldock et al. 1997). However, this application is restricted to samples with a common origin (Baldock et al. 1997). We therefore interpret the alkyl/O-alkyl ratios of our samples separately. The high alkyl/O-alkyl ratios of group II samples (Table 4-3), which have an aquatic origin, are likely due to the high contribution of phytoplankton materials to these samples. For the rest samples of a terrestrial origin, the high alkyl/O-alkyl ratio of group IV sample compared to those of group I and III samples (Table 4-3) is an evidence of input of degraded SOM to the lower Brazos River.

The amount of C observed by NMR analysis (%C_{obs}) ranged from 26 to 53% of total sinking POC (Table 4-3). The rest (47 to 74%) was not detected by NMR.

During demineralization, carbohydrate, lignin and carbonyl were preferentially lost to the supernatants, leading to relatively enrichment of protein and lipid in the residue (Table 4-6). The change in the relative content of protein and lignin was particularly remarkable (Table 4-6). Charcoal content decreased in sample 1a and increased in sample 3, but the changes were relatively small (1.8-2.4%, Table 4-6). If sample 5 responded to demineralization in the same way as samples 1a and 3, the chemical composition of the untreated sample 5 should be: carbohydrate > 17.6%, protein << 26.5%, lignin >> 22.8%, lipid <14%, carbonyl > 4.7%, and charcoal ≈ 14.4%.

Of the sinking POC detected by NMR, carbohydrate and protein were the two most important components except in sample 5, accounting for 44-71% of the sinking POC, followed by lipid (11-24%) (Fig. 4-6). Charcoal content varied from 1% to 14%. Carbonyl made the smallest contribution to the OC pool in most samples.

Site	Date sampled	Sample name	Treatment	%OC	%N	Molar C/N	%C _{obs}	Carbohydrate	Protein	Lignin	Lipid	Carbonyl	Charcoal	Alkyl/O-Alkyl
1	3/5/2009	1a	Untreated	8.14	0.70	13.58	51.85	47.2	23.4	12.4	10.6	0.8	5.6	0.58
			<i>Demineralized</i>	<i>26.93</i>	<i>3.10</i>	<i>10.13</i>	<i>79.41</i>	<i>45.0</i>	<i>32.0</i>	<i>3.6</i>	<i>16.2</i>	<i>0</i>	<i>3.2</i>	<i>0.84</i>
3	3/5/2009	3	Untreated	8.59	0.47	21.19	28.17	32.9	14.9	26.1	15.0	7.5	3.5	0.81
			<i>Demineralized</i>	<i>26.54</i>	<i>4.45</i>	<i>6.97</i>	<i>76.15</i>	<i>25.0</i>	<i>49.7</i>	<i>0.6</i>	<i>19.3</i>	<i>0</i>	<i>5.3</i>	<i>1.80</i>
5	11/19/2008	5	Untreated	1.00	0.11	10.63	NA	NA	NA	NA	NA	NA	NA	NA
			<i>Demineralized</i>	<i>8.66</i>	<i>0.79</i>	<i>12.87</i>	<i>35.09</i>	<i>17.6</i>	<i>26.5</i>	<i>22.8</i>	<i>14.0</i>	<i>4.7</i>	<i>14.4</i>	<i>1.49</i>

Table 4-6. Comparison of %OC, %N, molar C/N ratio, %C_{obs}, Alkyl/O-Alkyl and distribution of the six components before and after demineralization calculated from the terrestrial MMM. Data of demineralized samples are in italic.

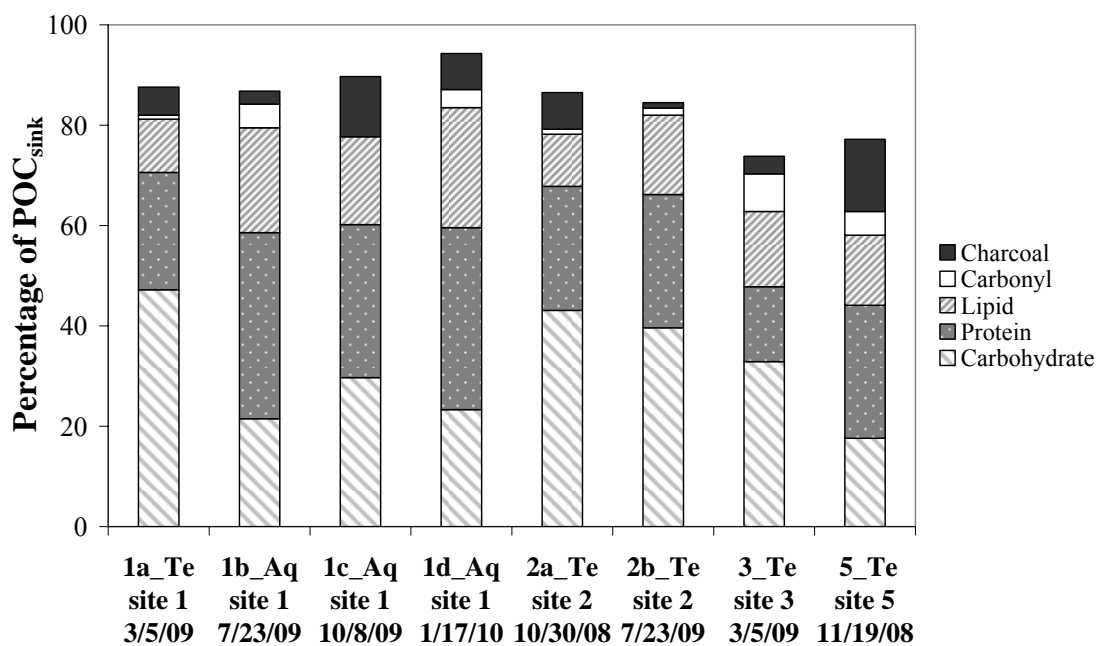


Figure 4-6. Chemical composition of sinking POC in the Brazos River. Only sample 5 was demineralized. Aq (aquatic) and Te (terrestrial) after sample names reflect the MMM model used for the sample.

There was no longitudinal trend in any of the 5 components: carbohydrate, protein, lipid, carbonyl or charcoal (Fig. 4-6). High carbohydrate content was observed in samples 1a, 2a and 2b, and 3. Sample 5 had higher lignin and charcoal and lower carbohydrate contents compared to other samples, indicating a higher contribution of degraded terrestrial OM. Relatively high charcoal contents were also observed in the samples collected at site 1 and site 2 (12% and 7%).

4.5 Discussion

4.5.1 Sources and chemical composition of total and sinking POC

4.5.1.1 Site 1 in the middle Brazos: urban wastewater input and river damming

Total POC at site 1 had $\Delta^{14}\text{C}$ values ranging from -65 to -45‰ (corresponding to radiocarbon ages of 540-370 years), suggesting an input of old terrestrial OC. Sources of old POC could be SOM, coal-bearing bedrock, and POC in wastewater treatment plant (WWTP) effluent and on-site wastewater treatment leakage. However, as discussed below, WWTP effluent and on-site wastewater treatment leakage may be the major source of the old riverine POC.

SOM is only a minor source of old riverine POC because transport of SOM to site 1 is limited. Although crop and pasture cover about one third of the area within a two-mile radius of Lake Granbury where site 1 is located (BRA 2010c), SOM input to site 1 at the center of the lake is likely limited due to the long distance between the inflow of the Brazos River above the lake and site 1 (~15 km). There are several creeks feeding the lake. However, these creeks drain into canals which do not mix with the main body of the lake (BRA 2010c), limiting their contribution of SOM to site 1. Erosion of soils in the river

banks is a more feasible way to contribute SOM to site 1. However, transport of SOM to site 1 is also limited because site 1 is ~200 m away from each side of the river banks.

Radiocarbon data suggest that coal-bearing bedrock is not an important source of old POC at site 1. Sinking POC ($\Delta^{14}\text{C} = -4 \pm 13\text{‰}$) was much more ^{14}C -enriched than total POC ($\Delta^{14}\text{C} = -55 \pm 9\text{‰}$) at site 1, implying that the old POC did not sink to the bottom of the lake but was carried by water downstream. The ^{14}C -enriched POC at site 2 indicates that the old POC from site 1 is completely decomposed over the 116 km reach of the Brazos River between sites 1 and 2. The labile nature of the old POC at site 1 thus rules out the coal-bearing bedrock as a source of the old POC at site 1, because coal-derived OC has significant aromatic character (Lett and Ruppel 2004) and is resistant to decomposition in natural environments.

POC from WWTPs and on-site wastewater treatment systems is likely the major source of the old POC at site 1 and the reason for the higher POC concentration at site 1 compared to site 2 (Table 4-1). POC in WWTP effluent is generally old due to the presence of fossil C contained in petroleum products (e.g. surfactants). $\Delta^{14}\text{C}$ values of POC in the effluent of twelve WWTPs in the Hudson and Connecticut River watersheds, which are representative of U.S. WWTPs, can be as low as -653‰, with an average of -103‰ and a median of -84‰ (Griffith et al. 2009). The predominant land use is residential (43%) within a one-mile radius around Lake Granbury (BRA 2010c). There are seven WWTPs in the watershed of Lake Granbury and many on-site wastewater treatment systems near the coves of the lake in the rapidly growing residential areas (Riebschleager and Karthikeyan 2008). These facilities discharge large amounts of treated wastewater into Lake Granbury (BRA 2010c; Riebschleager and Karthikeyan 2008). Surfactants and other petrochemical

products in the treated wastewater might have contributed to the old POC in the lake. Federle and Pastwa (1988) documented that although the majority of surfactants are removed during sewage treatment, a significant fraction escape degradation and are released into the environments. These surfactants can be decomposed within days in the natural environments (Federle and Pastwa 1988), and were likely removed during transit before they reached site 2.

Because phytoplankton materials are more aliphatic (Hedges and Oades 1997), the high lipid and protein content and the high alkyl/O-alkyl ratios of sinking POC at site 1 suggest that phytoplankton materials made up a considerable portion of POC at this site. This is supported by the relatively high productivity at site 1 (chlorophyll *a* = 20-30 $\mu\text{g L}^{-1}$) (TCEQ 2010), which is favored by the long residence time of water in the lake formed by river damming and the nutrients input from WWTPs and on-site sewage facilities around the lake (Riebschleager and Karthikeyan 2008). The $\Delta^{14}\text{C}$ values of phytoplankton, which are the same as the dissolved inorganic carbon (DIC) in the water (-10 to +10‰) (Zeng et al. 2010), were obscured by the very negative $\Delta^{14}\text{C}$ values of old POC and therefore were not reflected in the $\Delta^{14}\text{C}$ values of total POC.

The $\Delta^{14}\text{C}$ values of sinking POC at site 1 ($-4 \pm 13\text{‰}$) were close to those of phytoplankton, suggesting that phytoplankton materials constitute most of sinking POC. De Junet et al. (2009) also observed that phytoplankton and bacterioplankton comprised most of setting material in the reservoir formed by river damming. The high %OC and %N contents and low C/N ratio of sample 1b may indicate a higher phytoplankton growth rate on July 23, 2009 than on other sampling dates.

Charcoal was 2.6-12.0% of the sinking POC at site 1. Since SOM contributed little to

riverine POC, potential sources of charcoal at site 1 include combustion of biomass and fossil fuel. However, the $\Delta^{14}\text{C}$ values of sinking POC ($-4 \pm 13\text{‰}$) suggest that combustion of biomass is the dominant source of the charcoal at site 1, because charcoal from biomass combustion would have $\Delta^{14}\text{C}$ values reflecting those of the atmospheric CO_2 (+19 to +36‰ in 2009-2010) (Hsueh et al. 2007; Trumbore et al. 2006) while charcoal from fossil fuel burning has $\Delta^{14}\text{C}$ values of -1000‰. The charcoal content of sinking POC at sites 1 was generally higher in fall and winter than in spring and summer (Fig. 4-6), probably due to more biomass burning after harvest seasons.

4.5.1.2 Site 2 in the middle Brazos: shallow soil input

OM from shallow soil is the major source of POC at site 2. Total POC at site 2 was enriched in ^{14}C in all dates sampled ($\Delta^{14}\text{C} = +2$ to +119‰). The change from old POC at site 1 to ^{14}C -enriched POC at site 2 suggests decomposition of old POC and replacement by ^{14}C -enriched POC in the river segment between sites 1 and 2. Deposition of old POC in the riverbed is an unlikely explanation because sinking POC was young at site 1 (Table 4-1). Since only OM fixed between 1950 and 2004 would produce these $\Delta^{14}\text{C}$ values (Burchuladze et al. 1989), total POC at site 2 is mainly composed of decades-old OM from shallow soils.

The contribution of phytoplankton detritus to POC is smaller at this site than at site 1, as shown by the high carbohydrate content of sinking POC (Fig. 4-6). This is consistent with the lower nutrient and chlorophyll *a* content at site 2 compared to site 1 (BRA 2010a).

Similar to site 1, combustion of biomass is the major source of charcoal in the sinking POC at site 2. Some of this charcoal may have been stored in shallow soils for a few years

before it was exported to the Brazos River with other SOM.

4.5.1.3 Sites 3-6 in the lower Brazos: deep erosion of old soil

Old POC is generally found in high to medium relief rivers (Gao et al. 2007; Masiello and Druffel 2001; Mayorga et al. 2005) and rivers with OM-rich sedimentary rock outcrops in their watersheds (Raymond et al. 2004). However, we also observed old POC in the lower Brazos where the watershed is flat. Although there are small areas of lignite-bearing bedrock in the lower Brazos watershed, our data suggest that lignite contributed little to the old POC in the river. This lignite-bearing bedrock outcrops mostly upstream of site 3. If there were a significant lignite input to the river, we would expect high charcoal content and highly ^{14}C -depleted POC at site 3, which we did not observe (charcoal content was 3.5% and $\Delta^{14}\text{C}$ value of POC was -86‰ at site 3, Table 4-1). Instead, sites 4-6 had much higher charcoal content and older POC than site 3 (Table 4-1, Fig. 4-6), suggesting that most of the charcoal and old POC were added to the river downstream of site 3.

The much higher concentration, lower $\Delta^{14}\text{C}$ and higher $\delta^{13}\text{C}$ values of total POC at sites 4-6 compared to sites 1-3 (Table 4-1) suggest a large input of old SOM downstream of site 3 (Fig. 4-1). Soil (including modern soils and paleosols) erosion rates are significantly higher in the lower Brazos than in the middle Brazos as indicated by the total suspended solid (TSS) data. TSS averaged 247 mg L^{-1} 50 km downstream of site 3, 197 mg L^{-1} at site 4 and 130 mg L^{-1} near site 6, much higher than 24 and 40 mg L^{-1} at sites 1 and 2, respectively (BRA 2010a).

The much higher TSS in the lower Brazos compared to the middle Brazos is due to the soft river banks and bed, agricultural land use, and high precipitation in the lower Brazos

River watershed. In the lower Brazos the river banks and bed are soft alluvium which is more susceptible to erosion, while in the middle Brazos the river banks and bed are resistant Pennsylvanian and Cretaceous limestone bedrock (Stricklin 1961). Alfisols and Vertisols are the dominant soil orders in both the middle and the lower Brazos River watershed. However, land use is different between the middle and lower Brazos River watersheds. In the middle Brazos River watershed, the primary land use is forest and agricultural pasture, with sparse urban areas at sites 1 and 2, while in the lower Brazos River watershed, the primary land use is agricultural cropland and pasture. From site 2 to site 3, the land adjacent to the Brazos River is covered by cropland with little or no riparian borders. Downstream of site 3, pasture covers most of the watershed. Precipitation is higher in the lower Brazos than in the middle Brazos. Mean annual precipitation varies from 880 mm (34.7 in) in the middle Brazos River watershed to 1200 mm (47.2 in) in the lower Brazos River watershed (Mishra and Singh 2010).

Since the predominant source of POC in the lower Brazos is SOM, we would expect that sinking POC is older than total POC, as observed for soils (Trumbore 2000) and a subtropical river in China (Gao et al. 2007). However, we observed the opposite: sinking POC was generally younger and more ^{13}C -enriched than total POC. This pattern indicates that the high-density fraction of riverine POC in the lower Brazos contained more young terrestrial materials, probably derived from C4 plants, than the low-density fraction of riverine POC.

4.5.1.4 Linking total POC data in this study to published DIC data for the Brazos River

The $\Delta^{14}\text{C}$ values of riverine total POC are positively related to the $\Delta^{14}\text{C}$ values of

riverine DIC collected on the same date (data from Zeng et al. 2010) ($r^2 = 0.87$, Fig. 4-7), revealing the interconversion between riverine POC and DIC via respiration and photosynthesis. POC was always more ^{14}C -depleted than DIC (Table 4-1). More ^{14}C -depleted POC than DIC has been observed in most rivers that have radiocarbon data for paired POC and DIC samples (Raymond and Bauer 2001; Raymond et al. 2004). The relative ^{14}C -enrichment of DIC relative to POC is due to (1) preferential respiration of the relatively young fraction of POC and/or (2) input of POC which is more depleted in ^{14}C (e.g. soil) than phytoplankton. In the lower Brazos, CO_2 supersaturation (~ 3 times the atmospheric CO_2 concentration) and $\Delta^{14}\text{C}$ values of DIC (-193 to -194‰ , Table 4-1) (Zeng et al. 2010) suggest decomposition of 1700-year-old riverine POC, the younger fraction of the 4300-year-old bulk POC ($\Delta^{14}\text{C} = -417\text{‰}$), in the water column.

4.5.2 Implications for the marine C cycle

The focus of this work was a longitudinal survey of the organic geochemistry of the Brazos River. We have only 1-2 data points at the river mouth, prohibiting a full scale-up to investigate the marine C cycle implications of our results. Nevertheless, we can bound some processes with the data we have. In the following paragraphs we estimate the fluxes of POC, charcoal and lignin from the Brazos River to the Gulf of Mexico.

4.5.2.1 The Brazos River POC export

Existing estimates of global river POC export are generally based on the world's large rivers. However, small rivers can have higher concentrations of POC than large rivers, e.g. $8.0\text{--}8.3\text{ mg L}^{-1}$ in the Brazos River compared to $0.61\text{--}2.78\text{ mg L}^{-1}$ in the Mississippi River

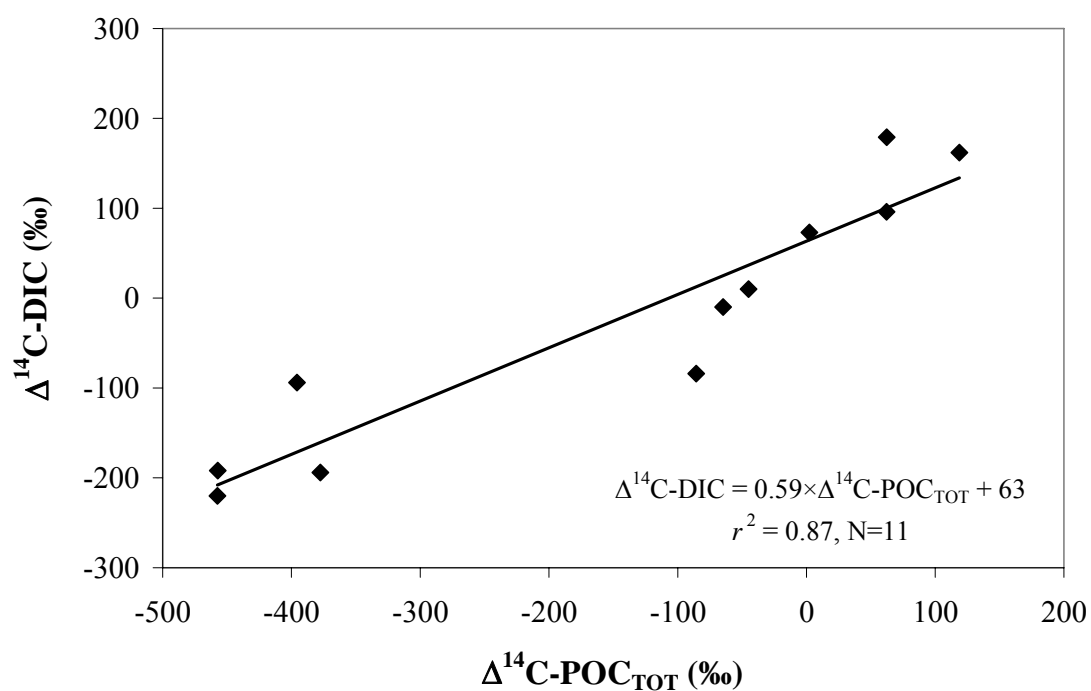


Figure 4-7. Correlation between $\Delta^{14}\text{C-DIC}$ and $\Delta^{14}\text{C-POC}_{\text{TOT}}$ of the Brazos River. Each pair of riverine DIC and POC samples was collected on the same date. $\Delta^{14}\text{C-DIC}$ values of the Brazos River are from Zeng et al. (2010).

(Bianchi et al. 2007). Together, global small river POC export may account for a significant fraction of total POC delivered by rivers to the ocean (Wheatcroft et al. 2010).

Our two measurements of POC concentration at site 5 (Table 4-1), which is close (20 km) to the mouth of the Brazos River but not affected by the Gulf of Mexico water as suggested by the C isotope data, are consistent despite the large variation in river water discharge on the two dates sampled ($149 \text{ m}^3 \text{ s}^{-1}$ on Nov 28, 2007 and $39 \text{ m}^3 \text{ s}^{-1}$ on Nov 19, 2008, data from the U.S. Geological Survey). Therefore, we used the average of these two measurements (8.15 mg L^{-1}) as the annual mean POC concentration at this site, recognizing that the number of measurements is too low for a fully representative scale-up. Based on the annual mean river water discharge of $274 \text{ m}^3 \text{ s}^{-1}$ (data from the U.S. Geological Survey), we estimated the Brazos River POC export to be $7.0 \times 10^4 \text{ t C yr}^{-1}$.

4.5.2.2 The Brazos River charcoal export

Estimating river export of charcoal is important because charcoal preferentially accumulates in marine sediments compared to other C sources (Masiello and Druffel 1998, 2003; Middelburg et al. 1999) owing to the resistance of charcoal to biological attack (Baldock and Smernik 2002) and chemical degradation (Hedges and Keil 1995; Middelburg et al. 1999). However, studies on river export of particulate charcoal are rare, existing in only a few rivers (Masiello and Druffel 2001; Mitra et al. 2002), limiting our understanding of rivers' role as a carrier of charcoal to the ocean.

Here we scaled up our measurements to the annual sinking charcoal export of the Brazos River, defined as the amount of charcoal that is exported with sinking PM by the Brazos River per year, using the following equation:

$$\text{Charcoal export} = \text{sediment discharge} \times \frac{\text{PM}_{\text{sink}}}{\text{PM}_{\text{TOT}}} \times \frac{\text{OC}}{\text{PM}_{\text{sink}}} \times \frac{\text{charcoal}}{\text{OC}} \quad (3)$$

We used values at site 5 in the scale-up calculation whenever possible. Due to the low number of measurements in this study, we made the following three assumptions in the calculation. First, we assumed that site 5 has the same percentage of sinking PM in total PM ($\frac{\text{PM}_{\text{sink}}}{\text{PM}_{\text{TOT}}}$) as site 1, which is the only site where $\frac{\text{PM}_{\text{sink}}}{\text{PM}_{\text{TOT}}}$ was measured. Second, we assumed that CP NMR spectroscopy can detect all the charcoal in the sinking POM samples. Third, we assumed that all the measured values of $\frac{\text{PM}_{\text{sink}}}{\text{PM}_{\text{TOT}}}$, OC content in the sinking PM ($\frac{\text{OC}}{\text{PM}_{\text{sink}}}$), and the charcoal content of sinking POC ($\frac{\text{charcoal}}{\text{OC}}$) are representative of their annual mean values.

Using the average TSS, 130 mg L⁻¹ (BRA 2010a), and the mean annual water discharge, 274 m³ s⁻¹ (U.S. Geological Survey), near the mouth, we calculated the Brazos River sediment discharge to be 1.12 × 10⁶ t yr⁻¹. This is only ~10% of the sediment discharge (11-16 × 10⁶ t yr⁻¹) published for the Brazos River (Bianchi et al. 1999; Meade and Parker 1985; Milliman and Syvitski 1992). The reason for the discrepancy is that the old data, 11-16 × 10⁶ t yr⁻¹, were obtained before 1964 (Milliman and Syvitski 1992). Since then, two of the three major dams in the Brazos River have been built (in 1969 and 1978, respectively, Brazos River Authority, www.brazos.org). These dams reduced the sediment load of the Brazos River. To be conservative, we used the 1.12 × 10⁶ t yr⁻¹ as the sediment

discharge value in our calculation. The $\frac{PM_{\text{sink}}}{PM_{\text{TOT}}}$ values measured at site 1 have an average of 25% (Table 4-2). The $\frac{OC}{PM_{\text{sink}}}$ value at site 5 is 1% (Table 4-3), and the $\frac{\text{charcoal}}{OC}$ value at site 5 is 14.4% (Table 4-5). With these values, we estimated that the charcoal delivered with sinking PM by the Brazos River is $0.4 \times 10^3 \text{ t yr}^{-1}$.

It should be noted that our estimate of the Brazos River annual sinking charcoal export, $0.4 \times 10^3 \text{ t yr}^{-1}$, represents a very conservative value. First, the $\frac{PM_{\text{sink}}}{PM_{\text{TOT}}}$ value at site 5 is likely much higher than that of site 1 used in the calculation, because soil materials with a density higher than phytoplankton constituted a much higher fraction of total PM at site 5 than at site 1. An increase in $\frac{PM_{\text{sink}}}{PM_{\text{TOT}}}$ would increase the estimate of charcoal export. Second, previous studies show that the our measurement technique, which relies on CP NMR spectroscopy, underestimates charcoal content by a factor of 2 to 3 (Hockaday et al. 2009; Nelson and Baldock 2005; Skjemstad et al. 1999). To be conservative, we used the charcoal content from the CP NMR measurements in the calculation without making any correction. It should be also noted that the calculated Brazos River annual sinking charcoal export here is only for the portion of charcoal associated with sinking PM. If the charcoal contained in suspended PM is included, the Brazos River exports more than $0.4 \times 10^3 \text{ t yr}^{-1}$ of charcoal to the Gulf of Mexico.

4.5.2.3 The Brazos River lignin export

Lignin, which only exists in terrestrial high plants, is another component of POM that

is relatively resistant to degradation. Because of this, lignin and lignin-derived phenols are extensively used as a tracer of terrestrial OM in the ocean.

We estimated the Brazos River export of sinking lignin to the Gulf of Mexico in the same way we did for the sinking charcoal export. Due to loss of lignin during demineralization (Table 4-6), as well as the likely higher $\frac{PM_{\text{sink}}}{PM_{\text{TOT}}}$ value at site 5 compared to site 1 as discussed above, our estimate $0.64 \times 10^3 \text{ t yr}^{-1}$ using the lignin content (22.8%, Table 4-5) of the demineralized sample 5 and the $\frac{PM_{\text{sink}}}{PM_{\text{TOT}}}$ value at site 1 reflects the lower bound of the Brazos River annual sinking lignin export. The total particulate lignin export of the Brazos River is higher than $0.64 \times 10^3 \text{ t yr}^{-1}$ when the lignin in suspended PM is included.

4.5.2.4 Linking river POC, charcoal and lignin fluxes to water and sediment discharge

Another issue that must be considered in global scale-ups of geochemical fluxes of POC, charcoal, and lignin is whether the size of the flux is related to water or sediment discharge (e.g. more mass is delivered when water or sediment discharge increases). Accurate global extrapolation depends on the assumption of a strong correlation between flux magnitude and water or sediment discharge. Here we compiled our data for the Brazos River and the data published for other rivers from the literature to examine if such correlations exist.

River POC, charcoal and lignin fluxes vary significantly among rivers (Table 4-7). We only found a moderate correlation ($r^2 = 0.66$, $N = 20$) between POC export and sediment discharge, while all other pairs (POC or charcoal or lignin versus water discharge, and

River	Water discharge (m ³ s ⁻¹)	Sediment discharge (×10 ⁶ t yr ⁻¹)	POC export (×10 ⁵ t C yr ⁻¹)	Charcoal export (×10 ⁴ t C yr ⁻¹)	Lignin export (×10 ³ t C yr ⁻¹)	Reference
Brazos	274	1.12	0.7	>0.04	>0.64	This study
Santa Clara	34	59	3.6	5.9	nd	Masiello and Druffel 2001
Mississippi	15,000	132	28.8	48 ± 22	nd	Mitra et al. 2002
	17,345	61.3	9.3	nd	0.12	Bianchi et al. GCA 2007
	14,385	80.3	7.9	nd	nd	Duan and Bianchi 2006
	nd	17.7 (sand)	3.4 ± 0.9 (sand)	nd	1.22 ± 0.94 (sand)	Bianchi et al. Estuarine 2007
		103.4 (mud)	3.3 (mud)		0.31 ± 0.25 (mud)	
Atchafalaya	nd	11.2 (sand)	1.3 ± 0.7 (sand)	nd	1.24 ± 1.21 (sand)	Bianchi et al. Estuarine 2007
Ob	12,811	nd	3.6	1.8	nd	Elmquist et al. 2008
Yenisey	19,660	nd	1.7	1	nd	Elmquist et al. 2008
	18,043	17.1	1.71	nd	1.8	Lobbess et al. 2000
Lena	16,584	nd	12	3.6	nd	Elmquist et al. 2008
	16,616	10.8	4.62	nd	2.3	Lobbess et al. 2000
Indigirka	1,719	nd	1.7	1.3	nd	Elmquist et al. 2008
	1,570	8.4	1.74	nd	0.08	Lobbess et al. 2000
Kolyma	3,869	nd	3.1	2.4	nd	Elmquist et al. 2008
	3,111	14.9	3.1	nd	0.10	Lobbess et al. 2000
Yukon	6,342	nd	0.12	0.11	nd	Elmquist et al. 2008
Mackenzie	10,464	nd	21	9.9	nd	Elmquist et al. 2008
Mezen	650	4.3	0.37	nd	0.11	Lobbess et al. 2000
Vizhas	2	0.011	0.0004	nd	0.0001	Lobbess et al. 2000
Vaskina	2	0.0073	0.0005	nd	0.0001	Lobbess et al. 2000
Velikaja	1	0.0035	0.0002	nd	0.00003	Lobbess et al. 2000
Moroyyakha	2	0.0051	0.0006	nd	0.0001	Lobbess et al. 2000
Olenek	999	0.96	0.26	nd	0.11	Lobbess et al. 2000
Omoloy	35	0.0064	0.011	nd	0.003	Lobbess et al. 2000
Yana	980	2.2	0.49	nd	0.20	Lobbess et al. 2000

nd: no data.

Table 4-7. River POC, particulate charcoal and lignin export from this study and the literature. Different water and sediment discharge data for the same river are for different periods when the measurements were made.

charcoal or lignin versus sediment discharge) showed very weak correlations ($r^2 < 0.35$). The poor correlations between these parameters suggest significant spatial geochemical heterogeneity in world rivers. Therefore, for a better constraint on global river POC, charcoal and lignin fluxes, measurements are needed in river systems under various ecosystem, climate and land use conditions.

4.6 Conclusions

The isotopic and chemical composition of total and sinking POC in the Brazos River was mainly controlled by land use and by the climate in the watershed. There was little or no effect of ancient OM, which is present in the Brazos River watershed, on riverine POC. Petroleum products (e.g. surfactants) that survived passage through WWTPs and on-site sewage facilities in urban areas might be added to the middle Brazos and draw the $\Delta^{14}\text{C}$ of total POC to negative values. Phytoplankton, the growth of which is facilitated by the relatively long hydraulic residence time of the lake formed by river damming and the nutrients from urban WWTPs and on-site sewage facilities, also comprised a considerable fraction of riverine POC in the middle Brazos, particularly for the sinking POC. Decades-old OM in shallow soil is another source of riverine POC in the middle Brazos. In contrast, millennia-old SOM from erosion of deep soil is the predominant source of riverine POC in the lower Brazos. The severe soil erosion in the lower Brazos is due to the non-resistant river banks and bed, agricultural land use, and high precipitation. Sinking POC comprised more young, probably C4 plant-derived, OM than total POC in the lower Brazos. Charcoal in the middle Brazos is mainly from recent biomass burning, whereas charcoal in the lower Brazos is from deep soil erosion.

The Brazos River discharges 7×10^4 t of POC, of which at least 0.4×10^3 t is charcoal and at least 0.64×10^3 t is lignin, to the Gulf of Mexico annually. The lack of a strong correlation between POC, charcoal, or lignin export and water or sediment discharge across rivers suggest that rivers behave differently and scaling up to global river POC, charcoal, and lignin fluxes requires a higher spatial and temporal resolution of measurements than presented here.

4.7 Acknowledgements

This work was funded by the Texas Water Resources Institute, the U.S. Geological Survey, and the National Institutes for Water Research. Many thanks to John Southon, Guaciara dos Santos Winston, Xiaomei Xu, Will Beaumont, Ellen R.M. Druffel, Sheila Griffin, Robert Beverly, and Claudia Czimczik at the W.M. Keck Carbon Cycle Accelerator Mass Spectrometry Laboratory at the University of California, Irvine for their assistance with carbon isotope analyses. FWZ is grateful to John B. Anderson, Fred M. Weaver, Xinfeng Shi, LaQuanti Calligan, Kaijian Liu, Krystle Hodge, Yongbo Zhai, Morgan Gallagher, Wei Chen, Yuan Li and Yinbin Ma for their assistance in sample collection.

CHAPTER 5

Conclusions

I measured $p\text{CO}_2$, the concentration and C isotopic composition ($\delta^{13}\text{C}$ and $\Delta^{14}\text{C}$) of DIC and POC, and the chemical composition of bulk and sinking POC in two small humid subtropical rivers (Buffalo Bayou and Spring Creek) and a midsized subtropical river (the Brazos River) in Texas. Based on the results from these measurements, I conclude that:

1. The small humid subtropical rivers studied here were highly supersaturated with CO_2 throughout the year, suggesting that humid subtropical rivers are likely a significant source of atmospheric CO_2 globally. CO_2 concentrations in the Buffalo Bayou and Spring Creek were 7-10 times that of the atmosphere, comparable to those of tropical rivers and much higher than those of temperate rivers. My conservative calculation reveals that Buffalo Bayou and Spring Creek release CO_2 to the atmosphere at a rate per unit water surface area intermediate between those of tropical and temperate rivers.
2. Land use and human activities are an important control on the sources and cycling of riverine C in the Brazos and Buffalo Bayou.
 - a) By enhancing air-water CO_2 exchange and stimulating growth of phytoplankton, river damming and nutrient addition from urban treated wastewater discharge led to low CO_2 concentrations (close to that of the atmosphere) and to high $\delta^{13}\text{C}$ values of DIC in the middle Brazos. Phytoplankton detritus and OM from

shallow soil and urban treated wastewater were the sources of riverine POC in the middle Brazos.

- b) Agricultural land use and high precipitation enhanced erosion of deep soils in the lower Brazos. As a result, millennial-aged SOM was lost to the river and added to the old POC pool in the lower Brazos. Decomposition of this old SOM contributed to the CO₂ evaded from the lower Brazos.
 - c) Crushed limestone/dolomite minerals and oyster shells used in road construction is being dissolved and slowly drained into the highly urbanized Buffalo Bayou and the lower Brazos, and may be a source of the old CO₂ released to the atmosphere.
3. Basin lithology is not an important control on the sources of C in the middle Brazos. Limestone bedrock contributed little or nothing to riverine DIC, although it outcrops in large areas in the middle Brazos. Similarly, little coal or lignite is detected in the riverine POC in the Brazos. However, the high erodibility of alluvium in the river banks and bed of the lower Brazos has enhanced the input of old SOM to the riverine POC pool.
 4. Radiocarbon data of DIC in the relatively undeveloped Spring Creek and at one site of the middle Brazos suggest that the ecosystem residence time in the subtropical Texas is years to decades.
 5. Precipitation is another important control on CO₂ concentration in the rivers I studied. It affected the daytime and seasonal variations in river CO₂ concentration in Buffalo Bayou and Spring Creek. The relatively low precipitation in the Brazos River watershed might be a reason for the much lower pCO₂ in the Brazos compared to

Buffalo Bayou and Spring Creek and other subtropical rivers.

REFERENCES

- Abril G, Guerin F, Richard S, Delmas R, Galy-Lacaux C, Gosse P, Tremblay A, Varfalvy L, Dos Santos MA, Matvienko B (2005) Carbon dioxide and methane emissions and the carbon budget of a 10-year old tropical reservoir (Petit Saut, French Guiana). *Glob. Biogeochem. Cycle* 19: 16
- Alin SR, Aalto R, Goni MA, Richey JE, Dietrich WE (2008) Biogeochemical characterization of carbon sources in the strickland and fly rivers, Papua New Guinea. *J. Geophys. Res.-Earth Surf.* 113: 21
- Aulenbach BT, Hooper RP, Bricker OP (1996) Trends in the chemistry of precipitation and surface water in a national network of small watersheds. *Hydrol. Process.* 10: 151-181
- Baker A, Cumberland S, Hudson N (2008) Dissolved and total organic and inorganic carbon in some British rivers. *Area* 40: 117-127
- Baldock JA, Masiello CA, Gelinas Y, Hedges JI (2004) Cycling and composition of organic matter in terrestrial and marine ecosystems. *Mar. Chem.* 92: 39-64
- Baldock JA, Oades JM, Nelson PN, Skene TM, Golchin A, Clarke P (1997) Assessing the extent of decomposition of natural organic materials using solid-state C-13 NMR spectroscopy. *Aust. J. Soil Res.* 35: 1061-1083
- Baldock JA, Skjemstad JO (2000) Role of the soil matrix and minerals in protecting natural organic materials against biological attack. *Organic Geochemistry* 31:

- 697-710
- Baldock JA, Smernik RJ (2002) Chemical composition and bioavailability of thermally, altered *Pinus resinosa* (Red Pine) wood. *Organic Geochemistry* 33: 1093-1109
- Barnes RT, Raymond PA (2009) The contribution of agricultural and urban activities to inorganic carbon fluxes within temperate watersheds. *Chem. Geol.* 266: 327-336
- Barth JAC, Cronin AA, Dunlop J, Kalin RM (2003) Influence of carbonates on the riverine carbon cycle in an anthropogenically dominated catchment basin: evidence from major elements and stable carbon isotopes in the Lagan River (N. Ireland). *Chem. Geol.* 200: 203-216
- Benke AC, Cushing CE (Eds) (2005) *Rivers of North America*. Elsevier Academic Press.
- Berner RA (1982) Burial of organic carbon and pyrite sulfur in the modern ocean: its geochemical and environmental significance *Am. J. Sci.* 282: 451-473
- Berner RA (1989) Biogeochemical cycles of carbon and sulfur and their effect on atmospheric oxygen over Phanerozoic time. *Glob. Planet. Change* 75: 97-122
- Beusen AHW, Dekkers ALM, Bouwman AF, Ludwig W, Harrison J (2005) Estimation of global river transport of sediments and associated particulate C, N and P. *Glob. Biogeochem. Cycle* 19, GB4S05, DOI 10.1029/2005GB002453
- Bianchi TS, Lambert CD, Santschi PH, Guo LD (1997) Sources and transport of land-derived particulate and dissolved organic matter in the Gulf of Mexico (Texas shelf/slope): The use of lignin-phenols and loliolides as biomarkers. *Organic Geochemistry* 27: 65-78

- Bianchi TS, Pennock JR, Twilley RR (Eds) (1999) *Biogeochemistry of Gulf of Mexico Estuaries*. John Wiley & Sons, Inc.
- Bianchi TS, Wysocki LA, Stewart M, Filley TR, McKee BA (2007) Temporal variability in terrestrially-derived sources of particulate organic carbon in the lower Mississippi River and its upper tributaries. *Geochimica et Cosmochimica Acta* 71: 4425-4437
- Boer SI, Arnosti C, van Beusekom JEE, Boetius A (2009) Temporal variations in microbial activities and carbon turnover in subtidal sandy sediments. *Biogeosciences* 6: 1149-1165
- Bouillon S, Abril G, Borges AV, Dehairs F, Govers G, Hughes HJ, Merckx R, Meysman FJR, Nyunja J, Osburn C, Middelburg JJ (2009) Distribution, origin and cycling of carbon in the Tana River (Kenya): a dry season basin-scale survey from headwaters to the delta. *Biogeosciences* 6: 2475-2493
- BRA (2009) Brazos River Watershed Information Center, Brazos River Authority. <http://crpdata.brazos.org/>. Cited 20 Aug, 2009.
- BRA (2010a) Basin Summary Report 2007 by Brazos River Authority. http://www.brazos.org/BasinSummary_2007.asp. Assess 12 Oct 2010.
- BRA (2010b) Brazos River Authority, Van M. Walker, GIS Coordinator, personal communication, 13 Jan, 2010.
- BRA (2010c) Lake Granbury Watershed Protection Plan by Brazos River Authority and Espey Consultants, Inc. http://www.brazos.org/gbWPP_Reports.asp. Assessed 12 Oct 2010

- Burdige DJ (2007) Preservation of organic matter in marine sediments: controls, mechanisms, and an imbalance in sediment organic carbon budgets? *Chem. Rev.* 107: 467-485
- Burns KA, Hernes PJ, Brinkman D, Poulsen A, Benner R (2008) Dispersion and cycling of organic matter from the Sepik River outflow to the Papua New Guinea coast as determined from biomarkers. *Organic Geochemistry* 39: 1747-1764
- Bricker OP, Rice KC (1993) Acid-rain. *Annu. Rev. Earth Planet. Sci.* 21: 151-174
- Broecker WS, Walton A (1959) Radiocarbon from Nuclear Tests. *Science* 130: 309-314
- Brunet F, Dubois K, Veizer J, Ndondo GRN, Ngoupayou JRN, Boeglin JL, Probst JL (2009) Terrestrial and fluvial carbon fluxes in a tropical watershed: Nyong basin, Cameroon. *Chem. Geol.* 265: 563-572
- Brunet F, Gaiero D, Probst JL, Depetris PJ, Lafaye FG, Stille P (2005) $\delta^{13}\text{C}$ tracing of dissolved inorganic carbon sources in Patagonian rivers (Argentina). *Hydrol. Process.* 19: 3321-3344
- Burchuladze AA, Chudy M, Eristavi IV, Pagava SV, Povinec P, Sivo A, Togonidze GI (1989) Anthropogenic ^{14}C variations in atmospheric CO_2 and wines. *Radiocarbon* 31: 771-776
- Burkhardt S, Amoroso G, Riebesell U, Sultemeyer D (2001) CO_2 and HCO_3^- uptake in marine diatoms acclimated to different CO_2 concentrations. *Limnol. Oceanogr.* 46: 1378-1391
- Cai WJ, Wang Y (1998) The chemistry, fluxes, and sources of carbon dioxide in the

- estuarine waters of the Satilla and Altamaha Rivers, Georgia. *Limnol. Oceanogr.* 43: 657-668
- Chakrapani GJ, Veizer J (2005) Dissolved inorganic carbon isotopic compositions in the Upstream Ganga river in the Himalayas. *Curr. Sci.* 89: 553-556
- Cole JJ, Caraco NF (2001) Carbon in catchments: connecting terrestrial carbon losses with aquatic metabolism. *Mar. Freshw. Res.* 52: 101-110
- Cole JJ, Caraco NF, Peierls BL (1992) Can phytoplankton maintain a positive carbon balance in a turbid, fresh-water, tidal estuary. *Limnol. Oceanogr.* 37: 1608-1617
- Cole JJ, Prairie YT, Caraco NF, McDowell WH, Tranvik LJ, Striegl RG, Duarte CM, Kortelainen P, Downing JA, Middelburg JJ, Melack J (2007) Plumbing the global carbon cycle: Integrating inland waters into the terrestrial carbon budget. *Ecosystems* 10: 171-184
- Cronin JG, Follett CR, Shafer GH, Rettman PL (1963) Reconnaissance Investigation of the Ground-Water Resources of the Brazos River Basin, Texas. Texas Water Commission Bulletin 6310.
- Dauwe B, Middelburg JJ, Herman PMJ, Heip CHR (1999) Linking diagenetic alteration of amino acids and bulk organic matter reactivity. *Limnol. Oceanogr.* 44: 1809-1814
- De Junet A, Abril G, Guerin F, Billy I, De Wit R (2009) A multi-tracers analysis of sources and transfers of particulate organic matter in a tropical reservoir (Petit Saut, French Guiana). *River Res. Appl.* 25: 253-271
- Doran E (1965) Shell roads in Texas. *Geogr. Rev.* 55: 223-240

- Douglas R, Staines-Urias F (2007) Dimorphism, shell Mg/Ca ratios and stable isotope content in species of *Bolivina* (benthic foraminifera) in the Gulf of California, Mexico. *J. Foraminifer. Res.* 37: 189-203
- Druffel ERM, Williams PM, Bauer JE, Ertel JR (1992) Cycling of dissolved and particulate organic matter in the open ocean. *J. Geophys. Res.-Oceans* 97: 15639-15659
- Duan SW, Bianchi TS (2006) Seasonal changes in the abundance and composition of plant pigments in particulate organic carbon in the lower Mississippi and Pearl Rivers. *Estuaries Coasts* 29: 427-442
- Elmquist M, Semiletov I, Guo LD, Gustafsson O (2008) Pan-Arctic patterns in black carbon sources and fluvial discharge deduced from radiocarbon and PAH source appointment markers in estuarine surface sediments. *Glob. Biogeochem. Cycle* 22: 13
- Elser JJ, Fagan WF, Denno RF, Dobberfuhl DR, Folarin A, Huberty A, Interlandi S, Kilham SS, McCauley E, Schulz KL, Siemann EH, Sterner RW (2000) Nutritional constraints in terrestrial and freshwater food webs. *Nature* 408: 578-580
- EPA (2001) Ambient water quality criteria recommendations. Information supporting the development of state and tribal nutrient criteria. Rivers and streams in nutrient ecoregion X: p20
- Fahnenstiel GL, Chandler JF, Carrick HJ, Scavia D (1989) Photosynthetic characteristics of phytoplankton communities in lakes Huron and Michigan: P-I parameters and end-products. *J. Great Lakes Res.* 15: 394-407

- Federle TW, Pastwa GM (1988) Biodegradation of surfactants in saturated subsurface sediments: a field study. *Ground Water* 26: 761-770
- Finlay JC (2003) Controls of streamwater dissolved inorganic carbon dynamics in a forested watershed. *Biogeochemistry* 62: 231-252
- Fisher WL (1982) Geologic Atlas of Texas, Houston Sheet. Bureau of Economic Geology, The University of Texas at Austin,
- Gao QZ, Tao Z, Yao GR, Ding J, Liu ZF, Liu KX (2007) Elemental and isotopic signatures of particulate organic carbon in the Zengjiang River, southern China. *Hydrol. Process.* 21: 1318-1327
- Garrels RM, Mackenzie FT (1971) *Evolution of Sedimentary Rocks*. W.W. Norton, New York.
- Gatz DF (1991) Urban precipitation chemistry-A review and synthesis. *Atmospheric Environment Part B-Urban Atmosphere* 25: 1-15
- Gelinas Y, Baldock JA, Hedges JI (2001) Demineralization of marine and freshwater sediments for CP/MAS ^{13}C NMR analysis. *Organic Geochemistry* 32: 677-693
- Gentry DK, Sosdian S, Grossman EL, Rosenthal Y, Hicks D, Lear CH (2008) Stable isotope and Sr/Ca profiles from the marine gastropod *Conus ermineus*: Testing a multiproxy approach for inferring paleotemperature and paleosalinity. *Palaios* 23: 195-209
- Grace J, Malhi Y (2002) Global change - Carbon dioxide goes with the flow. *Nature* 416: 594-595

- Green RE, Bianchi TS, Dagg MJ, Walker ND, Breed GA (2006) An organic carbon budget for the Mississippi River turbidity plume and plume contributions to air-sea CO₂ fluxes and bottom water hypoxia. *Estuaries Coasts* 29: 579-597
- Griffith DR, Barnes RT, Raymond PA (2009) Inputs of Fossil Carbon from Wastewater Treatment Plants to US Rivers and Oceans. *Environ. Sci. Technol.* 43: 5647-5651
- Gu B, Schelske CL, Hodell DA (2004) Extreme ¹³C enrichments in a shallow hypereutrophic lake: Implications for carbon cycling. *Limnol. Oceanogr.* 49: 1152-1159
- Hackley PC, Guevara EH, Hentz TF, Hook RW (2009) Thermal maturity and organic composition of Pennsylvanian coals and carbonaceous shales, north-central Texas: Implications for coalbed gas potential. *Int. J. Coal Geol.* 77: 294-309
- Hedges JJ, Baldock JA, Gelinas Y, Lee C, Peterson M, Wakeham SG (2001) Evidence for non-selective preservation of organic matter in sinking marine particles. *Nature* 409: 801-804
- Hedges JJ, Baldock JA, Gelinas Y, Lee C, Peterson ML, Wakeham SG (2002) The biochemical and elemental compositions of marine plankton: A NMR perspective. *Mar. Chem.* 78: 47-63
- Hedges JJ, Keil RG (1995) Sedimentary organic matter preservation: an assessment and speculative synthesis. *Mar. Chem.* 49: 81-115
- Hedges JJ, Keil RG, Benner R (1997) What happens to terrestrial organic matter in the ocean? *Organic Geochemistry* 27: 195-212

- Hedges JJ, Oades JM (1997) Comparative organic geochemistries of soils and marine sediments. *Organic Geochemistry* 27: 319-361
- Hein T, Baranyi C, Herndl GJ, Wanek W, Schiemer F (2003) Allochthonous and autochthonous particulate organic matter in floodplains of the River Danube: the importance of hydrological connectivity. *Freshw. Biol.* 48: 220-232
- Helie JF, Hillaire-Marcel C, Rondeau B (2002) Seasonal changes in the sources and fluxes of dissolved inorganic carbon through the St. Lawrence River - isotopic and chemical constraint. *Chem. Geol.* 186: 117-138
- Hemond HF, Fechner-Levy EJ (2000) Chemical fate and transport in the environment. Academic Press, San Diego
- Herczeg AL, Broecker WS, Anderson RF, Schiff SL, Schindler DW (1985) A new method for monitoring temporal trends in the acidity of fresh waters. *Nature* 315: 133-135
- Ho DT, Bliven LF, Wanninkhof R, Schlosser P (1997) The effect of rain on air-water gas exchange. *Tellus Ser. B-Chem. Phys. Meteorol.* 49: 149-158
- Hockaday WC, Masiello CA. Basic solid state ^{13}C nuclear magnetic resonance in the biogeosciences. In preparation for *Biogeochemistry*.
- Hockaday WC, Masiello CA, Randerson JT, Smernik RJ, Baldock JA, Chadwick OA, Harden JW (2009) Measurement of soil carbon oxidation state and oxidative ratio by ^{13}C nuclear magnetic resonance. *J. Geophys. Res.-Biogeosci.* 114: 14
- Houghton RA (2003) Why are estimates of the terrestrial carbon balance so different? *Glob. Change Biol.* 9: 500-509

- Hsueh DY, Krakauer NY, Randerson JT, Xu XM, Trumbore SE, Southon JR (2007) Regional patterns of radiocarbon and fossil fuel-derived CO₂ in surface air across North America. *Geophys. Res. Lett.* 34: 6
- Hwang J, Druffel ERM (2003) Lipid-like material as the source of the uncharacterized organic carbon in the ocean? *Science* 299: 881-884
- Hwang J, Druffel ERM, Eglinton TI, Repeta DJ (2006) Source(s) and cycling of the nonhydrolyzable organic fraction of oceanic particles. *Geochimica et Cosmochimica Acta* 70: 5162-5168
- Hwang J, Druffel ERM, Griffin S, Smith KL, Baldwin RJ, Bauer JE (2004) Temporal variability of $\Delta^{14}\text{C}$, $\delta^{13}\text{C}$, and C/N in sinking particulate organic matter at a deep time series station in the northeast Pacific Ocean. *Glob. Biogeochem. Cycle* 18: 10
- Iwata T, Takahashi T, Kazama F, Hiraga Y, Fukuda N, Honda M, Kimura Y, Kota K, Kubota D, Nakagawa S, Nakamura T, Shimura M, Yanagida S, Xeu L, Fukasawa E, Hiratsuka Y, Ikebe T, Ikeno N, Kohno A, Kubota K, Kuwata K, Misonou T, Osada Y, Sato Y, Shimizu R, Shindo K (2007) Metabolic balance of streams draining urban and agricultural watersheds in central Japan. *Limnology* 8: 243-250
- Jahne B, Heinz G, Dietrich W (1987) Measurement of the diffusion-coefficients of sparingly soluble gases in water. *J. Geophys. Res.-Oceans* 92: 10767-10776
- Jones CA (2009) Texas A&M University - Lake Granbury and Bosque River Assessment, Final Scientific/Technical Report. Texas Water Resources Institute Technical Report, TR-350 (April 2009)

- Kanduc T, Ogrinc N, Mrak T (2007a) Characteristics of suspended matter in the River Sava watershed, Slovenia. *Isot. Environ. Health Stud.* 43: 369-386
- Kanduc T, Szramek K, Ogrinc N, Walter LM (2007b) Origin and cycling of riverine inorganic carbon in the Sava River watershed (Slovenia) inferred from major solutes and stable carbon isotopes. *Biogeochemistry* 86: 137-154
- Karim A, Veizer J (2000) Weathering processes in the Indus River Basin: implications from riverine carbon, sulfur, oxygen, and strontium isotopes. *Chem. Geol.* 170: 153-177
- Keller N, Del-Piero D, Longinelli A (2002) Isotopic composition, growth rates and biological behaviour of *Chamelea gallina* and *Callista chione* from the Gulf of Trieste (Italy). *Marine Biology* 140: 9-15
- Kibler KW (1999) Radiocarbon dating of *Rangia cuneata*: Correction factors and calibrations for the Galveston Bay area. *Texas Archaeological Society Publication* 70: 457-466
- Komada T, Anderson MR, Dorfmeier CL (2008) Carbonate removal from coastal sediments for the determination of organic carbon and its isotopic signatures, $\delta^{13}\text{C}$ and $\Delta^{14}\text{C}$: comparison of fumigation and direct acidification by hydrochloric acid. *Limnol. Oceanogr.: Methods* 6: 254-262
- Krull E, Haynes D, Lamontagne S, Gell P, McKirdy D, Hancock G, McGowan J, Smernik R (2009) Changes in the chemistry of sedimentary organic matter within the Coorong over space and time. *Biogeochemistry* 92: 9-25

- Krusche AV, Martinelli LA, Victoria RL, Bernardes M, de Camargo PB, Ballester MV, Trumbore SE (2002) Composition of particulate and dissolved organic matter in a disturbed watershed of southeast Brazil (Piracicaba River basin). *Water Res.* 36: 2743-2752
- Lal R (2003) Soil erosion and the global carbon budget. *Environ. International* 29: 437-450
- Lamb AL, Wilson GP, Leng MJ (2006) A review of coastal palaeoclimate and relative sea-level reconstructions using $\delta^{13}\text{C}$ and C/N ratios in organic material. *Earth-Sci. Rev.* 75: 29-57
- Lambs L, Brunet F, Probst JL (2009) Isotopic characteristics of the Garonne River and its tributaries. *Rapid Commun. Mass Spectrom.* 23: 2543-2550
- Lett RG, Ruppel TC (2004) Coal, Chemical and Physical Properties. *Encyclopedia of Energy* 1: 411-423
- Levin I, Kromer B, Wagenback D, Minnich KO (1987) Carbon isotope measurements of atmospheric CO_2 at a coastal station in Antarctica. *Tellus* 39B: 89-95
- Livingstone DA (1963) Chemical composition of rivers and lakes. U.S. Geol. Survey Prof Paper: 44-G
- Lobbes JM, Fitznar HP, Kattner G (2000) Biogeochemical characteristics of dissolved and particulate organic matter in Russian rivers entering the Arctic Ocean. *Geochimica et Cosmochimica Acta* 64: 2973-2983
- Lohrenz SE, Cai WJ (2006) Satellite ocean color assessment of air-sea fluxes of CO_2 in a

- river-dominated coastal margin. *Geophysical Research Letters* 33: 4
- Longworth BE, Petsch ST, Raymond PA, Bauer JE (2007) Linking lithology and land use to sources of dissolved and particulate organic matter in headwaters of a temperate, passive-margin river system. *Geochimica et Cosmochimica Acta* 71: 4233-4250
- Masiello CA, Druffel ERM (1998) Black carbon in deep-sea sediments. *Science* 280: 1911-1913
- Masiello CA, Druffel ERM (2001) Carbon isotope geochemistry of the Santa Clara River. *Glob. Biogeochem. Cycle* 15: 407-416
- Masiello CA, Druffel ERM (2003) Organic and black carbon ^{13}C and ^{14}C through the Santa Monica Basin sediment oxic-anoxic transition. *Geophysical Research Letters* 30: 4
- Matson GC, Hopkins OB (1917) The Corsicana oil and gas field Texas. Contribution to economic geology, Part II. *Bulletin* 661-F: 211-252
- Mayorga E, Aufdenkampe AK, Masiello CA, Krusche AV, Hedges JI, Quay PD, Richey JE, Brown TA (2005) Young organic matter as a source of carbon dioxide outgassing from Amazonian rivers. *Nature* 436: 538-541
- McConnaughey TA, Gillikin DP (2008) Carbon isotopes in mollusk shell carbonates. *Geo-Marine Letters* 28: 287-299
- McFarland A, Kiesling R, Pearson C (2001) Characterization of a Central Texas Reservoir with Emphasis on Factors Influencing Algal Growth. Texas Institute for Applied Environmental Research, Tarleton State University, Stephenville, Texas,

TR0104 (April 2001)

McFarland AMS, Hauck LM (2001) Determining nutrient export coefficients and source loading uncertainty using in-stream monitoring data. *J. Am. Water Resour. Assoc.* 37: 223-236

McNichol AP, Jones GA, Hutton DL, Gagnon AR, Key RM (1994) The rapid preparation of seawater sigma- CO_2 for radiocarbon analysis at the National Ocean Sciences AMS facility. *Radiocarbon* 36: 237-246

Meade RH, Parker R (1985) Sediment in rivers of the United States. In: National water summary 1984: U.S. Geological Survey Water Supply Paper 2275: 49-60.

Melching CS, Flores HE (1999) Reaeration equations derived from US geological survey database. *J. Environ. Eng.-ASCE* 125: 407-414

Meybeck M (1993) Riverine transport of atmospheric carbon - sources, global typology and budget. *Water Air Soil Pollut.* 70: 443-463

Meyers PA (1994) Preservation of elemental and isotopic source identification of sedimentary organic matter. *Chem. Geol.* 114: 289-302

Middelburg JJ, Nieuwenhuize J, van Breugel P (1999) Black carbon in marine sediments. *Mar. Chem.* 65: 245-252

Milliman JD, Syvitski JPM (1992) Geomorphic/tectonic control of sediment discharge to the ocean: the importance of small mountainous rivers. *J. Geol.* 100: 525-544

Mishra AK, Singh VP (2010) Changes in extreme precipitation in Texas. *J. Geophys. Res.-Atmos.* 115: 29

- Mitra S, Bianchi TS, McKee BA, Sutula M (2002) Black carbon from the Mississippi River: Quantities, sources, and potential implications for the global carbon cycle. *Environ. Sci. Technol.* 36: 2296-2302
- Mook WG, Bommerso.Jc, Staverma.Wh (1974) Carbon isotope fractionation between dissolved bicarbonate and gaseous carbon-dioxide. *Earth Planet. Sci. Lett.* 22: 169-176
- Moore RC, Plummer FB (1922) Pennsylvanian stratigraphy of north central Texas. *J. Geol.* 30: 18-42
- National Center for Earth Resources Observation and Science and U.S. Geological Survey (2005) Conterminous United States Land Cover 1992 - 200-Meter Resolution, available online at <http://nationalatlas.gov/atlasftp.html>
- Nelson PN, Baldock JA (2005) Estimating the molecular composition of a diverse range of natural organic materials from solid-state ^{13}C NMR and elemental analyses. *Biogeochemistry* 72: 1-34
- Nelson PN, Baldock JA, Clarke P, Oades JM, Churchman GJ (1999) Dispersed clay and organic matter in soil: their nature and associations. *Aust. J. Soil Res.* 37: 289-315
- NOAA (2009a) National Climatic Data Center. <http://www.ncdc.noaa.gov>. Cited 20 Aug, 2009
- NOAA (2009b) National Weather Service, Southern Region Headquarters. <http://www.srh.weather.gov>. Cited 26 May 2009
- Nordt L, Orosz M, Driese S, Tubbs J (2006) Vertisol Carbonate Properties in Relation to

- Mean Annual Precipitation: Implications for Paleoprecipitation Estimates. *The Journal of Geology* 114: 501-510
- Nordt LC, Hallmark CT, Wilding LP, Boutton TW (1998) Quantifying pedogenic carbonate accumulations using stable carbon isotopes. *Geoderma* 82: 115-136
- Oh NH, Raymond PA (2006) Contribution of agricultural liming to riverine bicarbonate export and CO₂ sequestration in the Ohio River basin. *Glob. Biogeochem. Cycle* 20: 17
- Oren A, Gurevich P, Anati DA, Barkan E, Luz B (1995) A bloom of *Dunaliella parva* in the Dead Sea in 1992: Biological and biogeochemical aspects. *Hydrobiologia* 297: 173-185
- Paquay FS, Mackenzie FT, Borges AV (2007) Carbon dioxide dynamics in rivers and coastal waters of the "Big Island" of Hawaii, USA, during baseline and heavy rain conditions. *Aquat. Geochem.* 13: 1-18
- Phillips JD (2007) Geomorphic context, constraints, and change in the lower Brazos and Navasota Rivers, Texas. Phase 2 of the project "Field data collection in support of geomorphic classification of the lower Brazos and Navasota Rivers", Texas Water Development Board report
- Piccolo A, Conte P (1998) Advances in NMR and IR spectroscopies of soil organic particles. In: Huang, P.M., Senesi, N., Buffle, J. (Eds.), *Structure and Surface Reactions of Soil Particles*. John Wiley & Sons Ltd., Chichester, pp. 184-250.
- Randerson JT, Chapin FS, Harden JW, Neff JC, Harmon ME (2002) Net ecosystem

- production: A comprehensive measure of net carbon accumulation by ecosystems. *Ecol. Appl.* 12: 937-947
- Rasera M, Ballester MVR, Krusche AV, Salimon C, Montebelo LA, Alin SR, Victoria RL, Richey JE (2008) Small rivers in the southwestern Amazon and their role in CO₂ outgassing. *Earth Interact.* 12: 16
- Raymond PA, Bauer JE (2001a) DOC cycling in a temperate estuary: A mass balance approach using natural C-14 and C-13 isotopes. *Limnol. Oceanogr.* 46: 655-667
- Raymond PA, Bauer JE (2001b) Riverine export of aged terrestrial organic matter to the North Atlantic Ocean. *Nature* 409: 497-500
- Raymond PA, Bauer JE (2001c) Use of C-14 and C-13 natural abundances for evaluating riverine, estuarine, and coastal DOC and POC sources and cycling: a review and synthesis. *Organic Geochemistry* 32: 469-485
- Raymond PA, Bauer JE, Caraco NF, Cole JJ, Longworth B, Petsch ST (2004) Controls on the variability of organic matter and dissolved inorganic carbon ages in northeast US rivers. *Mar. Chem.* 92: 353-366
- Raymond PA, Bauer JE, Cole JJ (2000) Atmospheric CO₂ evasion, dissolved inorganic carbon production, and net heterotrophy in the York River estuary. *Limnol. Oceanogr.* 45: 1707-1717
- Raymond PA, Caraco NF, Cole JJ (1997) Carbon dioxide concentration and atmospheric flux in the Hudson River. *Estuaries* 20: 381-390
- Raymond PA, Cole JJ (2001) Gas exchange in rivers and estuaries: Choosing a gas

- transfer velocity. *Estuaries* 24: 312-317
- Raymond PA, Oh NH (2007) An empirical study of climatic controls on riverine C export from three major U.S. watersheds. *Glob. Biogeochem. Cycles* 21: GB2022. DOI 10.1029/2006GB002783
- Richey JE, Melack JM, Aufdenkampe AK, Ballester VM, Hess LL (2002) Outgassing from Amazonian rivers and wetlands as a large tropical source of atmospheric CO₂. *Nature* 416: 617-620
- Riebschleager KJ, Karthikeyan R (2008) Bacterial impairment assessment for Lake Granbury watershed. Report as of FY2007 for 2007TX266B
- Rightmire CT (1967) A radiocarbon study of the age and origin of caliche deposits. M.A. Thesis, Univ. Texas, Austin
- Roelke DL, Brooks BW, Grover JP (2007) Water quality program for Lake Granbury Texas, 4th quarter report. http://lakegranbury.tamu.edu/docs/projectupdate_2007-10-30_ga.pdf: Cited on August 10, 2009
- Rotatore C, Colman B, Kuzma M (1995) The active uptake of carbon dioxide by the marine diatoms *Phaeodactylum tricornutum* and *Cyclotella* sp. *Plant Cell Environ.* 18: 913-918
- Ruppert LF, Kirschbaum MA, Warwick PD, Flores RM, Affolter RH, Hatch JR (2002) The US Geological Survey's national coal resource assessment: the results. *Int. J. Coal Geol.* 50: 247-274
- Salati S, Adam F, Cosentino C, Torri G (2008) Studying soil organic matter using ¹³C

- CP-MAS NMR: The effect of soil chemical pre-treatments on spectra quality and representativity. *Chemosphere* 70: 2092-2098
- Sannigrahi P, Ingall ED, Benner R (2005) Cycling of dissolved and particulate organic matter at station Aloha: Insights from ^{13}C NMR spectroscopy coupled with elemental, isotopic and molecular analyses. *Deep-Sea Research Part I-Oceanographic Research Papers* 52: 1429-1444
- Sarmiento JL, Sundquist ET (1992) Revised budget for the oceanic uptake of anthropogenic carbon-dioxide. *Nature* 356: 589-593
- Selva EC, Couto EG, Johnson MS, Lehmann J (2007) Litterfall production and fluvial export in headwater catchments of the southern Amazon. *J. Trop. Ecol.* 23: 329-335
- Shah SD, Houston NA, Braun CL (2007) Hydrogeologic characterization of the Brazos River alluvium aquifer, Bosque County to Fort Bend County, Texas. U.S. Geological Survey
- Shelby CA, McGowen MK, Aronow S, Fisher WL, L. F. Brown J, McGowen JH, Groat CG, Barnes VE (1992) Geologic Atlas of Texas, Beaumont Sheet. In: Fisher WL (Ed). Bureau of Economic Geology, The University of Texas at Austin
- Sickman JO, DiGiorgio CL, Davisson ML, Lucero DM, Bergamaschi B (2010) Identifying sources of dissolved organic carbon in agriculturally dominated rivers using radiocarbon age dating: Sacramento-San Joaquin River Basin, California. *Biogeochemistry* 99: 79-96
- Sickman JO, Zanolli MJ, Mann HL (2007) Effects of urbanization on organic carbon loads

- in the Sacramento River, California. *Water Resour. Res.* 43: 15
- Skjemstad JO, Reicosky DC, Wilts AR, McGowan JA (2002) Charcoal carbon in US agricultural soils. *Soil Sci. Soc. Am. J.* 66: 1249-1255
- Skjemstad JO, Taylor JA, Smernik RJ (1999) Estimation of charcoal (char) in soils. *Commun. Soil Sci. Plant Anal.* 30: 2283-2298
- Smernik RJ, Baldock JA, Oades JM, Whittaker AK (2002) Determination of $T_1\rho H$ relaxation rates in charred and uncharred wood and consequences for NMR quantitation. *Solid State Nucl. Magn. Reson.* 22: 50-70
- Smernik RJ, Oades JM (2000) The use of spin counting for determining quantitation in solid state ^{13}C NMR spectra of natural organic matter 1. Model systems and the effects of paramagnetic impurities. *Geoderma* 96: 101-129
- Stauffer RE (1990) Electrode pH error, seasonal epilimnetic pCO_2 , and the recent acidification of the Maine lakes. *Water Air Soil Pollut.* 50: 123-148
- Stiller M, Magaritz M (1974) Carbon-13 enriched carbonate in interstitial waters of Lake Kinneret sediments. *Limnol. Oceanogr.* 19: 849-853
- Stiller M, Rounick JS, Shasha S (1985) Extreme carbon-isotope enrichments in evaporating brines. *Nature* 316: 434-443
- Stoeser DB, Shock N, Green GN, Dumonceaux GM & Heran WD (2005) Geologic Map Database of Texas: U.S. Geological Survey Open Data Series, available online at <http://pubs.usgs.gov/ds/2005/170>
- Stricklin FL (1961) Degradational stream deposits of the Brazos River, central Texas.

- Geological Society of America Bulletin 72: 19-36
- Stuiver M, Polach HA (1977) Discussion: Reporting of ^{14}C Data. Radiocarbon 19: 355-363
- Stumm W, Morgan JJ (1996) Aquatic chemistry: chemical equilibria and rates in natural waters. Wiley, New York
- TCEQ (2010) Surface water quality monitoring web reporting by Texas Commission on Environmental Quality. <http://www8.tceq.state.tx.us/SwqmisWeb/public/index.faces>. Assessed 12 Oct 2010
- Telmer K, Veizer J (1999) Carbon fluxes, pCO_2 and substrate weathering in a large northern river basin, Canada: carbon isotope perspectives. Chem. Geol. 159: 61-86
- Tewalt SJ, Kinney SA & Merrill MD (2008) GIS representation of coal-bearing areas in North, Central, and South America: U.S. Geological Survey Open-File Report 2008-1257, available online at <http://pubs.usgs.gov/of/2008/1257/>
- Titi H, Rasoulilian M, Martinez M, Becnel B, Keel G (2003) Long-term performance of stone interlayer pavement. J. Transp. Eng.-ASCE 129: 118-126
- Torgersen T, Branco B (2008) Carbon and oxygen fluxes from a small pond to the atmosphere: Temporal variability and the CO_2/O_2 imbalance. Water Resour. Res. 44: 14
- Trumbore S (2000) Age of soil organic matter and soil respiration: Radiocarbon constraints on belowground C dynamics. Ecol. Appl. 10: 399-411
- Trumbore S, Da Costa ES, Nepstad DC, De Camargo PB, Martinelli L, Ray D, Restom T,

- Silver W (2006) Dynamics of fine root carbon in Amazonian tropical ecosystems and the contribution of roots to soil respiration. *Global Change Biology* 12: 217-229
- USDA (2009) <http://websoilsurvey.nrcs.usda.gov>. Cited 11 July 2009.
- USGS (2007) 2006 Minerals Yearbook (Stone, Crushed). U.S. Department of the Interior, U.S. Geological Survey, Washington, DC
- USGS (2009) 2007 Minerals Yearbook (Stone, Crushed) [Advance Release]. U.S. Department of the Interior, U.S. Geological Survey, Washington, DC
- Valastro S, Davis EM, Rightmir.Ct (1968) University of Texas at Austin Radiocarbon Dates 6. *Radiocarbon* 10: 384-401
- Wachniew P (2006) Isotopic composition of dissolved inorganic carbon in a large polluted river: The Vistula, Poland. *Chem. Geol.* 233: 293-308
- Wachniew P, Rozanski K (1997) Carbon budget of a mid-latitude, groundwater-controlled lake: Isotopic evidence for the importance of dissolved inorganic carbon recycling. *Geochimica et Cosmochimica Acta* 61: 2453-2465
- Wakeham SG, Canuel EA, Lerberg EJ, Mason P, Sampere TP, Bianchi TS (2009) Partitioning of organic matter in continental margin sediments among density fractions. *Mar. Chem.* 115: 211-225
- Wang FS, Wang YC, Zhang J, Xu H, Wei XG (2007) Human impact on the historical change of CO₂ degassing flux in River Changjiang. *Geochem. Trans.* 8: 7
- Wanninkhof R (1992) Relationship between wind-speed and gas-exchange over the ocean. *J. Geophys. Res.-Oceans* 97: 7373-7382

- West TO, McBride AC (2005) The contribution of agricultural lime to carbon dioxide emissions in the United States: dissolution, transport, and net emissions. *Agriculture Ecosystem & Environment* 108: 145-154
- Wheatcroft RA, Goni MA, Hatten JA, Pasternack GB, Warrick JA (2010) The role of effective discharge in the ocean delivery of particulate organic carbon by small, mountainous river systems. *Limnol. Oceanogr.* 55: 161-171
- Wisshak M, Correa ML, Gofas S, Salas C, Taviani M, Jakobsen J, Freiwald A (2009) Shell architecture, element composition, and stable isotope signature of the giant deep-sea oyster *Neopycnodonte zibrowii* sp. n. from the NE Atlantic. *Deep-Sea Research Part I-Oceanographic Research Papers* 56: 374-407
- Yao GR, Gao QZ, Wang ZG, Huang XK, He T, Zhang YL, Jiao SL, Ding J (2007) Dynamics Of CO₂ partial pressure and CO₂ outgassing in the lower reaches of the Xijiang River, a subtropical monsoon river in China. *Sci. Total Environ.* 376: 255-266
- Yu FL, Zong YQ, Lloyd JM, Huang GQ, Leng MJ, Kendrick C, Lamb AL, Yim WWS (2010) Bulk organic $\delta^{13}\text{C}$ and C/N as indicators for sediment sources in the Pearl River delta and estuary, southern China. *Estuar. Coast. Shelf Sci.* 87: 618-630
- Zeng F-W, Masiello CA (2010) Sources of CO₂ evasion from two subtropical rivers in North America. *Biogeochemistry* 100: 211-225
- Zeng F-W, Masiello CA, Hockaday WC (2010) Controls on the origin and cycling of riverine dissolved inorganic carbon in the Brazos River, Texas. *Biogeochemistry* (in press). DOI 10.1007/s10533-010-9501-y.

- Zhang J, Quay PD, Wilbur DO (1995) Carbon-isotope fractionation during gas-water exchange and dissolution of CO₂. . *Geochimica et Cosmochimica Acta* 59: 107-114
- Zhang SR, Lu XX, Sun HG, Han JT, Higgitt DL (2009) Major ion chemistry and dissolved inorganic carbon cycling in a human-disturbed mountainous river (the Luodingjiang River) of the Zhujiang (Pearl River), China. *Sci. Total Environ.* 407: 2796-2807